FINAL REPORT 2

(SECOND CONTRACT YEAR)

Exploration and Evaluation of New Glasses in Fiber Form

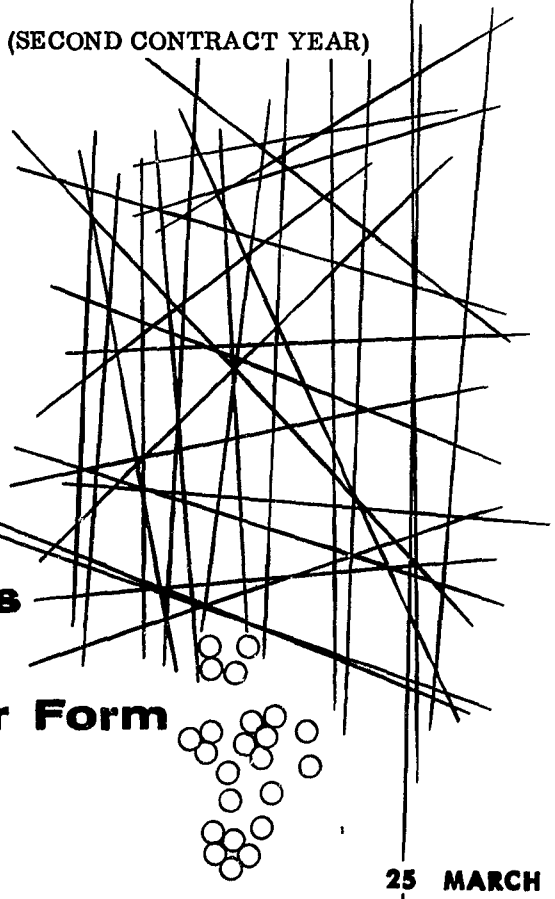

25 MARCH 1964

1 JANUARY 1963 through 31 DECEMBER 1963

[redacted]

U.S. Naval Research Laboratory
contract NONR 3654(00)(X)

PAGES _____

ARE

MISSING

IN

ORIGINAL

DOCUMENT

EXPLORATION AND EVALUATION OF NEW GLASSES IN FIBER FORM

Prepared under U. S. Naval Research Laboratory
Contract NONR 3654 (00) (X)

FINAL REPORT NO. 2

(Second Contract Year)
1 January 1963 through 31 December 1963

This report applies to work on:

NRL Project 62 R05 19A
Technical Memo 239

Issued: 25 March 1964

Prepared by: Gunther K. Schmitz
Senior Research Engineer

Approved by: A. G. Metcalfe
Associate Director,
Research Laboratories

John V. Long
Director of Research

SOLAR

A Division of International Harvester Company
2200 Pacific Highway, San Diego 12, California

FOREWORD

This report covers the work performed by Solar during the second contract year, 1 January through 31 December 1963, under the direction of J. A. Kies, Scientific Officer, Navel Research Laboratory on Contract NONR 3654(00) (X).

The work was performed by Gunther K. Schmitz as Principal Investigator, under the general guidance of John V. Long, Director, Research Laboratories and Arthur G. Metcalfe, Associate Director. Other Research personnel contributing to the work were Donald G. Clark, Senior Research Technician and Diether Roth, Research Technician (Experimental work); and Robert M. Gardner, Engineer (Computer Program).

ABSTRACT

The work performed during the second contract year was to establish the first year's findings on a firmer basis. This goal has been achieved by tensile strength measurements on Virgin E- and S-glass at approximately the same gage lengths previously used for fibers from E- and S-glass strands.

The resulting strength-length curves were similar in shape to the strand fiber curves indicating that mixed flaw populations were present also on freshly drawn fibers, but to varying degrees depending on drawing conditions. Analysis of the corresponding failure probability plots provided detailed information on the characteristics of the different types of flaws as well as on the proportional amounts present at the various fiber lengths. The existence of mixed flaw populations limits the application of single exponent failure probability functions, such as the Weibull, to certain gage lengths.

Resistance to mechanical damage was found to be similar for the two glasses and it was concluded that surface defects due to stranding were similar with respect to both severity and density.

TABLE OF CONTENTS

LIST OF ILLUSTRATIONS

LIST OF ILLUSTRATIONS (Cont)

I. INTRODUCTION

The proportion of the strength of virgin glass monofilaments that can be retained in a large pressure vessel, such as the Polaris first or second stage motor case, is approximately 50 percent. As the freshly drawn monofilament passes through the different production processes, progressive strength loss occurs. Such strength loss is demonstrated by the following typical data:

	Average Strength (psi)	Strength Loss (%)	Incremental Strength loss (%)
Virgin Fiber	665,000[1]	0	--
Forming Strand	545,000[1]	18	18
Six-inch Pressure Bottle	450,000	32	17
Polaris Motor Case	380,000	43	15

Two facts become apparent immediately. First, there is a size effect indicated for the different diameters of the pressure vessel. Second, the fiber experiences a substantial strength loss from its virgin state to the finished strand.

The size effect has not been studied in detail partly because the basic information on the effect of size on strength of monofilaments has not been available, although some preliminary work was done as discussed elsewhere.

Damage inflicted upon the virgin fiber by the first mechanical process, stranding, may be inevitable. However, the magnitude depends on the resistance to damage of the glass composition and on the stranding process including type and amount of finish applied. Control of the later, i.e., HTS finish versus A-1100 or 801, has already raised the percentage of strength retained. It appears that further improvement is possible if the characteristics of the defects can be determined and their effect on strength be demonstrated.

---

1. Owens-Corning (OCF) S-glass data, Polaris Meeting, January 1964.

The number of defects present on glass fibers increases with size, for instance with length. A study of the strength-length relationship, therefore, should provide information about the characteristics of defects. The present program was initiated to study this effect of length on the strength of fibers. The first year's work was mainly concerned with the length effect on the strength of fibers from strands, while the second year's work concentrated on virgin fibers and on damage problems. The objectives of the program are described in the following section.

II. PROGRAM OBJECTIVES

The prime objectives of the program may be stated as follows:

- The examination of strength properties of virgin and damaged glass fibers by means of the length effect
- The determination of the strongest fiber for particular applications

Further objectives are:

- The systematic study of failure distribution at different strength levels
- The effect of distribution variations of failure distributions on the strength-length relationship
- Correlation of single fiber strength with the strength of strands of the same glass formulation

These objectives were attained by tensile tests on monofilaments, both drawn at Solar and also those supplied by a commercial vendor, and on current production strands supplied by the same vendor.

A sizable portion of the program was accomplished in the first contract year, 1962, and is reviewed in Section IV. The tasks performed in 1963 were essentially a continuation and expansion of this work, based on some unexpected results.

III. THEORETICAL BACKGROUND

The theoretical strength of glass may be estimated in several ways. A mechanical model leads to a strength equal to one-tenth of the elastic modulus, and a chemical approach derives the strength from the bond energy. Both approaches lead to values above one million psi. To explain the observed lower values, Griffith (Ref. 1) introduced the concept that glass contains pre-existing flaws so that the fracture process is one of crack propagation rather than initiation. In agreement with this concept, Griffith found a size effect for glass of different diameters. Weibull (Ref. 2) proposed a statistical theory of failure based on randomly distributed flaws of random severity. The "weakest link" approach was adopted as a criterion of failure, or a brittle material fails when the stress at any one flaw becomes larger than the ability of the surrounding material to resist the local stresses. Weibull assumed a reasonable distribution function and derived the expression:

$$S = 1 - e^{-V\left(\frac{\sigma}{\sigma_o}\right)^m} \qquad (1)$$

where S = probability of failure

σ = applied stress to a volume of material, V

σ_o = upper limiting strength

m = index of relative number of flaws.

This relationship is deficient because the applied stress must approach infinity if the probability of failure is to approach unity (certainty of failure). Kies (Ref. 3) suggested that a simple solution to this problem would be to modify the Weibull relationship:

$$S = 1 \quad e^{-V\left(\frac{\sigma-\sigma_u}{\sigma_o-\sigma}\right)^a} \qquad (2)$$

where σ_u = lower limiting strength of glass (may be zero)

a = damage coefficient,

and the other variables have the same meaning as in the original Weibull expression.

Apart from the early work of Griffith on the effect of diameter, there have been few attempts to apply statistical theories to the failure of glass. Whereas Griffith found the strength of glass to decrease as the size increased, Thomas (Ref. 4) in a series of carefully controlled experiments found no effect over the diameter range 20×10^{-5} to 60×10^{-5} inch. Thomas attempted to compensate for the size change by variation in drawing speed, and adopted careful precautions to avoid damage after drawing. Variation of gage length, rather than diameter, to study the flaw distribution as in Reference 3, has the advantage that specimens can be taken from a single drawing of glass fibers so that the mixed flaw populations that result from the different drawing conditions necessary for different diameters are avoided. Also, the differences in drawing conditions for different diameters of filaments produce uncontrolled degrees of compaction so that aside from the flaws the glasses are physically different. Variation of gage length, therefore, has been used in the present work.

If further assumption is made that the loss of strength after drawing results from surface damage, then the volume term in the relationships advanced earlier may be replaced by area. For constant diameter fibers, the area may be replaced by the gage length. Virgin fiber strength must be reached by the damaged fibers at lengths free of defects causing premature failure. On the basis of these considerations, Figure 1 represents an early model of the expected relationship between logarithms of the appropriate strength function and the length. Examination of the model is an inherent part of this work.

IV. REVIEW OF PREVIOUS WORK

The length effect on fiber strength was studied for E-glass and 994-glass in the first year's work (Ref. 5). The fibers used were primarily from strands and the majority of tests were conducted with 994 fibers, first with experimental (X-994) and later in the year with semi-production (S-994) fibers. In addition, strand tests were performed on sections of the same strand from which single fibers had been separated. Test equipment was designed for single-fiber investigation of various gage lengths and equipment as well as test procedures were perfected so that reproducible results could be obtained for gage lengths from 30 cm to 0.025 cm, a range of three length decades.

4.1 SINGLE-FIBER TESTS

Tensile test results on fibers longer than 1.5 cm confirmed the linear log strength-log length relationship previously established by Kies and that fiber strength increased with shorter gage length. However, the strength-length plot did not continue linearly up to the virgin fiber strength as was proposed in the model shown in Figure 1, but a slope change occurred at a certain critical gage length. This is shown in Figure 2, which represents a summary of the single-fiber work on 994 glass.

The existence of the slope change led to the conclusion that at least two different types of surface defects were present on strand fibers; one severe type with large spacing that controls the strength of fibers above the critical gage length and another type, considerably less severe, with narrow spacing that controls failure at short gage lengths below the critical lengths. Analysis of the respective failure probability plots confirmed this conclusion; bi-modal failure distributions were found to exist at gage lengths near the slope change, while single-mode distributions occurred at gage lengths removed from the critical length, i.e., from the slope change. These findings served as a basis for an analytical method developed in this reporting period, and made it possible to characterize the different types of flaws present in mixed flaw populations.

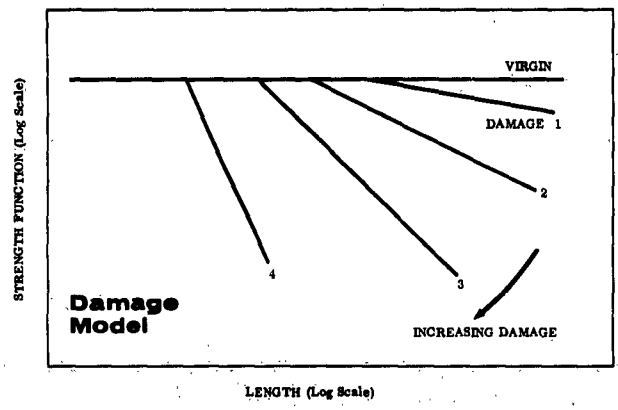

FIGURE 1. DAMAGE MODEL

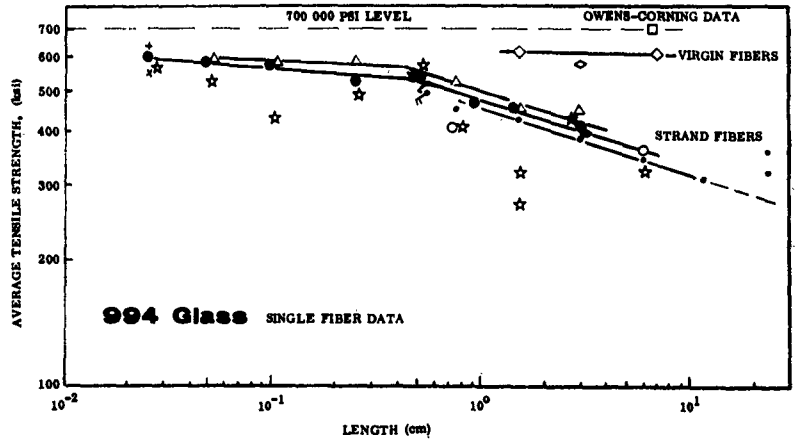

FIGURE 2. SINGLE-FIBER DATA; 994 Glass

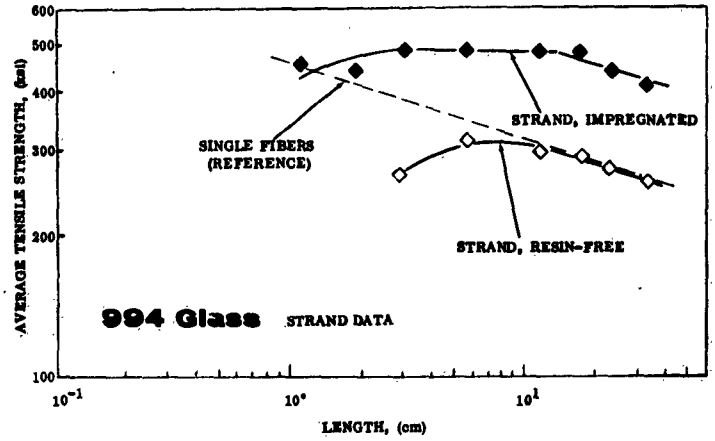

FIGURE 3. STRAND DATA: 994 Glass

4.2 STRAND TESTS

To provide a link between the strengths of single fibers and strands, the investigation of the length effect was extended to strands of the same spool from which fibers were separated for single-fiber tests. A strength reversal occurred at shorter test lengths as can be seen in Figure 3. The reversal could be related to the effect of poor fiber collimation evidenced by load-elongation curves. At longer gage lengths, where the collimation effect is small, the strength of resin-free strands equals that of single fibers. This points to the fact that gage length rather than accumulated fiber length (within a strand) is the criterion for the length effect. The shift of strength of resin impregnated strands (Fig. 3) to higher strength values supports the concept of strength enhancement through load transfer in a composite structure.

In summary, the results obtained during the first year showed that more than one type of surface defect controls the strength-length relationship of fibers separated from strands, and that different upper strength limits can be expected for very short fibers depending on damage characteristics. These results were made possible by development of a tensile test method capable of investigating fibers as short as 0.025 cm. The length effect on strands was found to be, in part, overridden by the effect of poor fiber collimation.

V. SCOPE OF CURRENT PROGRAM

The principal purpose of the work planned for 1963 was to establish the first year's findings on a firmer basis and to arrive at final conclusions on the problem of fiber damage. Most of the work was to be done on virgin fibers.

The following tasks were programmed:

Task I. Tensile strength measurements on freshly drawn fibers and on fibers with at least two degrees of controlled surface damage.

Gage lengths between 0.025 cm and 8 cm appeared sufficient to bracket the region of the anticipated slope changes. Both E-glass and S-glass were to be investigated; E-glass fibers were to be drawn at Solar whereas S-glass fibers were to be supplied by Owens-Corning or drawn at Solar pending negotiations with OCF.

These test series would allow a more precise determination of the effect of mixed flaw populations on the logarithmic strength-length curve than was possible from the uncontrolled damage of strand fibers.

Task II. Analysis of failure distribution plots, with respect to variations in type of defect.

Large sample sizes of approximately 100 fibers per gage length are necessary in order to arrive at statistically reliable distributions. These distributions were expected to provide thorough information about defects on freshly drawn fibers (E-glass) and virgin S-glass fibers. Comparison of plots from virgin and damaged fibers were expected to allow assessment of the additional damage in terms of differences in stress concentration effects.

Task III. Continuation of analysis of bi-modal failure distributions and correlation with strength-length curve characteristics.

This task was considered to be the final step in the progressive development of a reliable method for a comprehensive description of strength characteristics of glass fibers.

Two other tasks were planned at the beginning of this contract year, but their execution was to depend on time and man-hours available.

1. Examination of surface flaws on fibers by a sodium vapor decoration technique developed in England by J. E. Gordon (Ref. 6). Preliminary tests were conducted but results were negative and work was discontinued mainly because the anticipated man-hour and time effort was considered too large for this program.

2. Testing of a limited amount of fibers separated from strands of current production glasses, i.e., S- and E-glass and, testing of strands to study length and collimation effects. This task is similar to the strand work done during the first year. It was not pursued because of time limitations.

Development of a multiple-fiber tester, of a device for artificial fiber damage, and of single-bushing-fiber drawing equipment was an inherent part of Task I. The multiple tester was necessary to expedite testing of the large sample sizes anticipated.

VI. EXPERIMENTAL APPROACH

A wide range of gage lengths is necessary in order to investigate the length effect. It was desired to cover, among others, the previously unexplored range between 0.5 cm and approximately 0.015 cm for virgin fibers. Anderegg (Ref. 7) has performed conventional tensile tests from 100 to 0.5 cm, and the gage length of approximately 0.015 cm was obtained as the equivalent gage length (to uniaxial tension) in the loop test developed by Sinclair (Ref. 8). The complex bending stress condition in the loop test does not lead to completely unambiguous interpretation in terms of a tensile test because of the stress gradients.

Because this work has been performed with gage lengths one order of magnitude lower than those studied previously in tensile tests, it has been necessary to pay unusual attention to the experimental techniques. The most difficult problem has been the determination of the exact gage length below 1 mm.

6.1 MATERIALS TESTED

Two glasses, E- and S-glass, were investigated. Table I summarizes the materials tested and also includes other necessary information such as manufacturer and purpose of test. S-glass fibers were shipped by air from OCF, Granville, Ohio, in a special container, insulated to minimize temperature effects.

TABLE I

MATERIALS TESTED

Glass	Source	Test Series	Purpose of Test	Drawn or Received
E	Monofilaments, Solar-drawn from single bushing, OCF marbles	EM I	Preliminary damage.	March 1963
		EM II	Virgin, failure Probability plots.	May 1963
		EM III	Damage and control.	November 1963
S	Monofilaments, OCF-drawn from single bushing	SM I	Virgin baseline.	20 June 1963
		SM II	Damage and control.	15 September 1963

NOTE: No finish applied to fibers.

6.2 SAMPLING TECHNIQUES

Since glass fiber strength is derived from statistical measurements, the method of sampling will affect both average strength and failure distributions. It is desirable to achieve random sampling as closely as possible. Sampling procedures varied slightly for the different test series, depending upon purpose of tests (i.e., virgin only or virgin control and damage), sample sizes desired, and whether test specimens were sampled from Solar-drawn monofilaments or from fibers delivered by OCF.

6.2.1 Sampling of OCF-delivered Fibers

S-glass fibers had been mounted by OCF on Solar-supplied serrated frames in groups of five. Test lengths were assigned randomly to individual fibers.

Some of the 8-cm gage length frames were divided by a metal center strip to double the amount of test specimens for gage lengths below 2 cm. The purpose was not only to increase the total amount of test specimens, but for the damage program to have virgin control and damaged specimens available from the same fiber. In practice, one side of a divided frame was tested first and then the other after artificial damage had been applied. Extreme caution was observed to avoid additional damage.

6.2.2 Sampling From Solar-drawn E-glass Monofilaments

The monofilament length between bushing and drum (62 inches) was sufficient to provide up to 20 test specimens. For the damage program with smaller sample sizes (Series EM III), only one or two specimens were taken for each gage length for both damage and virgin control. This method ensures optimum random sampling since each monofilament is represented not only at each gage length, but also at each test condition.

The sampling procedure for Series EM II (large sample sizes, virgin only) differed from the above in that only three gage lengths out of the programmed nine were assigned to one monofilament, but three or four fibers were sampled for each gage length. This approach was necessary because of the time factor involved in testing large sample sizes, and the need to reduce the setup time for different gage lengths in the test equipment. Such changes are difficult below 0.25 cm where microscopic observation was required to adjust the gripping points to the desired gage lengths. A

certain bias was introduced by this sampling method because of strength variations between filaments that affect the three or four fibers at once. However, analysis revealed that bias is negligible for sample sizes between 70 to 100.

6.2.3 Sampling From Strands

Although no strand fibers were tested in this contract period, the description of the sampling procedure and fiber separation technique is repeated because of doubts expressed during the Polaris meeting, January 1964, about the validity of the strand fiber data reported last year (Ref. 5).

Assuming a desired sample size of 50 fibers for each of the nine different gage lengths tested, a sufficient length (three feet) of strand is taken from the spool. A bundle of approximately 65 fibers (to allow for fiber separation loss) out of 204 total in the strand is separated, cut into nine parts, and labeled in ascending order of the programmed gage lengths. Each part is subdivided into three groups from which individual fibers are separated. Thus, 50 fibers are obtained for each gage length from a population of 65. Separation of individual fibers is carried out in the following manner. One end of a bundle is taped to a holder (in front of a dark background for better visibility). A fiber is separated from the free end by means of a slender, sharply pointed needle. Fiber and remaining bundle are then slowly pulled apart by exerting a constant, gentle pull outward-downward on both ends. Separation takes place in short leaps depending on the amount or tenacity of finish. This particular mode of separation seems to indicate that a finish-finish separation took place rather than finish-glass.

In order to determine if the strength of the fibers was affected by the separation process, a comparison was made between the average strength of the first half of the population of 50 fibers and the second half. Table II shows that the average strength of the first 25 fibers separated is not significantly different from that of the second 25 fibers and no preferential orientation of plus or minus exists. The absence of differences indicates that there is no progressive damage introduced in separation.

FIGURE 4. SINGLE FIBER TESTER SET-UP FOR SHORT FIBER TESTING

FIGURE 5. MULTIPLE FIBER TESTER

TABLE II

EFFECT OF FIBER SEPARATION ON STRENGTH

Fiber	Test Length (cm)	Average Strength Total (ksi)	Average Strength First (ksi)	Average Strength Second (ksi)	Variation From Average Total First (%)	Variation From Average Total Second (%)
SS 1	0.75	455	462	447	+1.5	-1.7
	1.5	435	450	419	+3.5	-3.7
	3	388	380	396	-2.0	+2.0
	6	346	382	310	+10.1	-10.4
	12	310	323	292	+4.1	-4.5
	24	325	324	327	-0.3	+0.6
SS 2	0.5	526	542	511	+3.1	-2.8
	0.5	491	485	499	-1.2	+1.7

6.3 TEST EQUIPMENT

6.3.1 Tensile Testers

A single-fiber tester was built at Solar. It was based on a proven design by W. H. Otto (Ref. 9). Some modifications included: gripping wax carriers, type of wax, reduction gears for various fiber lengths, and arrangement on an optical bench to accommodate change in gage length.

Figure 4 shows the test apparatus in a setup for short gage length testing.[1] Here the gripping points (wax carriers 1/2 inch diameter) are in line-of-sight of the bifilar micrometer microscope at 20 magnification to determine the gage length. The dial indicator served as a crosshead zero position index as well as a head travel measuring device.

---

1. Load measuring components are:

   - Load sensor: Schaevitz LVDT; TDC-3, ±350 gr.
   - Differential transformer indicator: Daytronic 300B.
   - Load recorder: Texas Instrument Servo/riter, PSR, chart speed 1 in./10 sec.

   A Minlark 1/50 hp speed-controlled Bodin motor (240:1 ratio) operated the drive spindle through double-belt reduction gears.

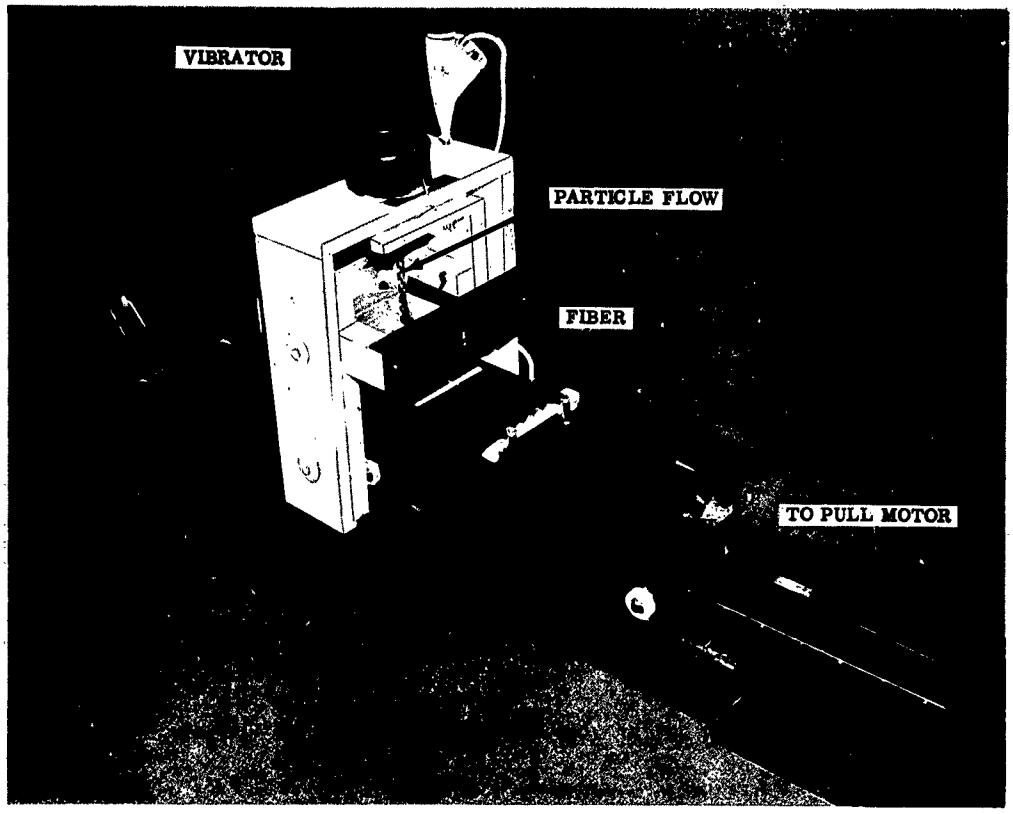

FIGURE 6. FIBER DAMAGE APPARATUS WITH SLED-MOUNTED FIBER AFTER DAMAGE

Magnification: 50X

FIGURE 7. GARNET GRAINS USED FOR ARTIFICIAL FIBER DAMAGE

The entire equipment was powered by a constant voltage source. Accuracy of the load recording was found to be ±1 percent; this included systems, calibration, and read-out error.

To handle large sample sizes, a multiple-fiber tester was designed to test four fibers simultaneously. Figure 5 shows this equipment. Load sensors are the same as used in the single-fiber tester. The load signals are recorded on four Varian Recorders via four Schaevitz LVDT regulator demodulators, DMPS-1 (right in Fig. 5). The lower gage length limit is 0.5 cm for multiple-fiber and 0.25 cm for single-fiber testing.

6.3.2 Fiber Damage Apparatus

The device, shown in Figure 6, is designed to allow variations of the two damage parameters, severity and density of defects.

Free-falling particles of approximately 200 to 300 μ diameter (versus 10 μ average fiber diameter) have been used for damage. One type is depicted in Figure 7. The particles stream out of the 0.05-inch orifice of the slightly vibrated funnel (located in the superstructure) at a constant rate. Adjustment of the free-falling height provides for the desired degree of damage. Immediately above the fiber is installed a 1-mm slot (two razor blades) to reduce the number of particles enough so that reasonable fiber velocities can be employed. The frame-mounted fiber is attached to the sled and pulled through the particle stream. A frame contains four fibers and each fiber is damaged individually. A speed-controlled motor (not shown) allows the fiber velocity to be adjusted to the programmed distribution of particle hits.

6.4 TESTING PROCEDURES

6.4.1 General Procedure

Tensile testing was conducted in a laboratory atmosphere of 77 ± 2 degrees F and of relative humidity between 40 and 50 percent. These conditions are generally regarded as satisfactory so long as fibers are tested within a few days. In this work, E-glass fibers were tested within 24 hours after drawing, i.e., a one-day supply of monofilaments was drawn in a given drawing operation. The first shipment of S-glass fibers was tested within five days after arrival, whereas testing of the second shipment was delayed for eight weeks because of difficulties with the fiber damage program.

Extreme care was taken in the handling of fibers. No contact was permitted with the center section of the fibers to be used as gage length. Frames were used to transfer fibers to the tensile machine and were not removed until the wax gripping medium had solidified. Horizontal and longitudinal alignment was ensured to avoid bending stresses at the point of fiber exit from the wax. It was found that the commonly used red sealing wax did not grip the fiber adequately. At short gage lengths, fiber slippage led to uncertainty in the exact length under stress. A search led to superior wax (Hi-Test Chemical Co. Wax No. 3066). This wax required the fiber to be exposed to 350 F for approximately 30 seconds; the absence of preferential failures at the fiber exit from the wax was taken to be proof that this exposure had no detrimental effect.

Tests were conducted at a strain rate of 0.06 to 0.07 per minute; this led to failure of virgin E- and S-glasses in the same time of about 45 seconds and ensured approximately equal exposures to the atmosphere during stressing.

Fiber diameters were measured with a Leitz microscope at 500 magnifications by means of a bifilar eyepiece with micrometer readout. The fiber was immersed in methylphenol ether (Anisole) with a refractive index of 1.518. The fibers had refractive indices in the range 1.49 to 1.55. Self-consistent diameter readings were obtained by limiting the readout to one operator. It is estimated that the average diameter error did not exceed ±1 percent of the fiber diameter of 40×10^{-5} inch. Since the purpose of this work was the comparison of strengths at different lengths, reproducibility was more important than absolute values. A comparison with another laboratory showed somewhat larger differences.[1]

Combination of the error due to diameter readout and the error due to load measurement leads to an overall maximum error in the stress of ±3.5 percent. This includes only self-consistency errors.

---

1. This comparison was made with Narmco Research and Development, San Diego, by arrangement with Mr. W. H. Otto. It was found that individual readout of the four participants was self-consistent (less than 1 percent), but actual values varied by up to 2.8 percent. This leads to a maximum strength difference of 5.6 percent due to diameter readout; this figure corresponds with an average difference of five percent in strength based on many years of observations by Mr. W. H. Otto (Ref. 9).

6.4.2 Determination of Gage Length

Gage length is an important variable in this study and must be known accurately. Above 0.25 cm, there appears to be no problem if the gage length is taken between the fiber exit points from the wax. Further support for this approach is provided by the small percentage of failures at the exit point or in the wax (less than seven percent).

For gage lengths below 0.25 cm, the number of failures at the exit point or in the wax increases slowly until reaching 15 percent at 0.05 cm, and then increases more rapidly to 25 percent at 0.025 cm. Such tests are rejected. In view of the large number of rejections at 0.05 cm and below, a study was made of the wax solidification process and its effect on gripping. The standard fiber mounting process included fan cooling to reduce the waiting time between tests. First, it was shown that stress buildup (to 10 percent of failure strength) in the fiber by contraction on cooling did not affect strength; continuous reduction of the stress during cooling had no effect. Second, the solidification pattern was changed by replacement of accelerated fan cooling by natural convective cooling. More uniform cooling resulted and much more effective gripping of the fiber was indicated by several factors, including the percentage of failures in the wax fell markedly; the elastic pullout of the wax was reduced; and load-elongation curves departed to a lesser extent from a straight line. The improvement was very marked at the 0.025 cm gage length, but the natural convective cooling time was 20 minutes so that the method was somewhat impractical. However, the interpretation of results that are presented later is not critically dependent on the strength values for the 0.025 cm gage length, so that limited determinations were made with this method of cooling. In the case of fibers separated from strands, it was found that these problems were less apparent, suggesting that the finish applied in stranding aids in wax gripping.

Fiber breakage within the wax makes the gage length indeterminate and, as discussed earlier, such failures are rejected. Other problems in the determination of gage length arise from slippage in the wax and wax pullout. Slippage implies separation at the fiber-wax interface so that the true gripping point (i.e., where stress attenuation begins) is within the wax, and the gage length is indeterminate. Such slippage is clearly indicated by a sawtooth pattern in the load-elongation diagram; the respective results were rejected and have been included in the rejection percentages

cited earlier. Some wax pullout is inevitable because the elastic modulus of the mounting medium is low, but such pullout indicates good adherence of the wax to the fiber. This was indicative of a good test and fracture within the pulled out wax cone occurred very infrequently. In these cases, the gage length was measured between the tips of the cones. The gage length measured immediately prior to fracture for good tests was approximately 0.005 to 0.008 cm longer than the originally set gage length. These dimensions include the elastic extensions of the glass which range from 0.0015 to 0.006 cm before fracture at the nominal gage lengths from 0.025 to 0.10 cm. It can be seen that the uncertainty is marked only in the case of the 0.025 cm nominal gage length.

6.4.3 Artificial Fiber Damage

A preliminary study was made early in the program to determine a suitable damage method. Free-falling glass spheres (300 μ) were used as well as a fluidized bed of these spheres and of irregular alumina particles (Al_2O_3, 150 μ average) into which the frame mounted fibers were dipped longitudinally (Ref. 10). The free-falling particle method was selected mainly because of the positive control of the damage process. The damage device, described before, was developed on this basis.

The damage procedure is simple. The fiber is pulled through a controlled particle stream at a velocity necessary to achieve the desired hit distribution. In order to guarantee reproducibility of results, a number of measurements and adjustments had to be made prior to the damage of test fibers.

- The flow rate of particles was measured at the funnel exit.
- The particle stream was centered on the 1 mm slot above the fiber.
- Some fibers mounted on special frames were damaged and the separation between hits was measured under a metallographic microscope (Leitz MM 5) in polarized light which gave a clear image of the impact marks.
- The flow pattern below the slot was "frozen" to an adhesive tape being pulled through the particle stream at the same speed as the fiber.
- The resulting swath path (1 cm wide) was preserved for comparison with later damage runs; it was found that visual comparison of swath paths aided best in flow pattern adjustment and gave good reproducibility of actual hit distributions.

The first particles used for the final portion of the damage program were the 300 μ glass spheres. Impact height was 20 cm and the hit density approximately 1 cm at a fiber velocity of 10 cm/sec. Results were unsatisfactory, however, and the smooth surfaced glass spheres were replaced by irregular-shaped Garnet grains. The following condition was selected:

Particles	- Garnet grain, irregular shape (Fig. 7)
Size	- Tyler Sieve, -48 +65; average smallest dimension 250 μ, largest 500 μ.
Specific weight	- 4.2 to 4.5 gr/cm^3
Impact height	- 25 cm
Fiber velocity	- 10 cm/sec
Average number of hits	- 3 to 4 per cm.

Virgin control samples were tested in each case to establish a baseline. For sampling procedures, refer to Section 6.2.

VII. EXPERIMENTAL RESULTS

Table III contains the total number of tests performed on various glasses at different gage lengths. Average strengths were calculated from the individual results and plotted against length on logarithmic paper.[1] Figures 8 and 9 show the results for virgin fibers from the two glass compositions.

A comparison of different failure distribution functions is made in Figure 10 for one gage length, while Gaussian distribution plots as related to various gage lengths are shown in Figures 11 through 13. In Figures 14 and 15, hypothetical strength-length curves are shown for some typical distributions of stress concentration factors.

TABLE III

SUMMARY OF SAMPLES SIZES AT DIFFERENT TEST LENGTHS

Length (cm)	EM I		EM II	EM III		SM I	SM II		Length (cm)
	V	D	V	V	D	V	V	D	
0.025	-	-	49	-	-	31	-	-	0.025
0.05	-	-	81	-	-	18	-	-	0.05
0.1	27	14	85	22	25	13	10	12	0.1
0.25	14	-	92	23	25	5	10	17	0.25
0.5	24	20	93	23	24	25	20	20	0.5
1.0	19	15	96	25	25	27	14	18	1.0
2	26	15	77	21	25	24	14	15	2
4	28	10	85	25	25	19	17	12	4
8	20	20	84	21	25	18	17	17	8
	158	94	742	160	174	200	102	111	

V - Virgin
D - Damaged

1741 valid tests
350 preliminary work and drawing performance checks

Total 2091

1. It will be shown later that more complex functions than log (average strength) may be appropriate, such as $\log \frac{\sigma-\sigma_u}{\sigma_o-\sigma}$ for the Kies distribution. However, such changes have no effect on the conclusions that will be drawn from these results in the succeeding paragraphs.

Figure 16 shows the predicted strength-length relationship for fiber lengths below those investigated. Strength loss of virgin fibers due to artificial damage is shown in the strength-length diagrams of Figure 17.

The method of analysis of failure probability plots is demonstrated in Figure 18 and analytical results of plots from several test series are presented in Figures 19 through 24.

Figure 25 compares the strength reduction of E- and S-glass as a result of both controlled artificial damage and stranding. Microphotographs in Figures 26 and 27 show the surface damage caused by the particles used for artificial damage.

Average test data are summarized in Tables A-I through A-V in Appendix A. Failure distributions, plotted on Gaussian probability paper, are presented in Appendix B.

VIII. DISCUSSION

8.1 CHARACTERISTICS OF DEFECTS IN GLASS FIBERS

The results presented in Figures 8 and 9 generally support the model advanced in Figure 1. One marked difference is that the strength at short gage lengths is not constant as proposed in the model. At longer gage lengths, the strength decrease is in general agreement with the model. Making the reasonable assumption that fibers from strands contain greater damage than virgin monofilaments, then:

1. Greater damage causes increasing loss of strength at long gage lengths (compare strand with virgin fiber data in Figures 8 and 9, respectively).
2. Greater damage may tend to increase the slope of the curve.
3. Greater damage tends to move the position of the slope change to shorter gage lengths.

Although there appears to be general agreement with the simple model proposed in Figure 1, more detailed examination shows that this model has certain limitations.

The general relationship between the probability of failure, S, and the applied stress, σ , is given by:

$$S = 1 - e^{-L\, f(\sigma)} \qquad (3)$$

where the f (σ) is chosen for the statistics selected. The function of stress must be one that will give close to a straight line on a log σ – log L plot.

For constant length L, it is possible to design graph paper such that a plot of S against σ gives a straight line. The Gaussian (normal) probability paper is the best known example, but for the purposes of this work, special paper was constructed for other functions. Scales were chosen so that a straight line would result if the distribution would follow the appropriate statistics.

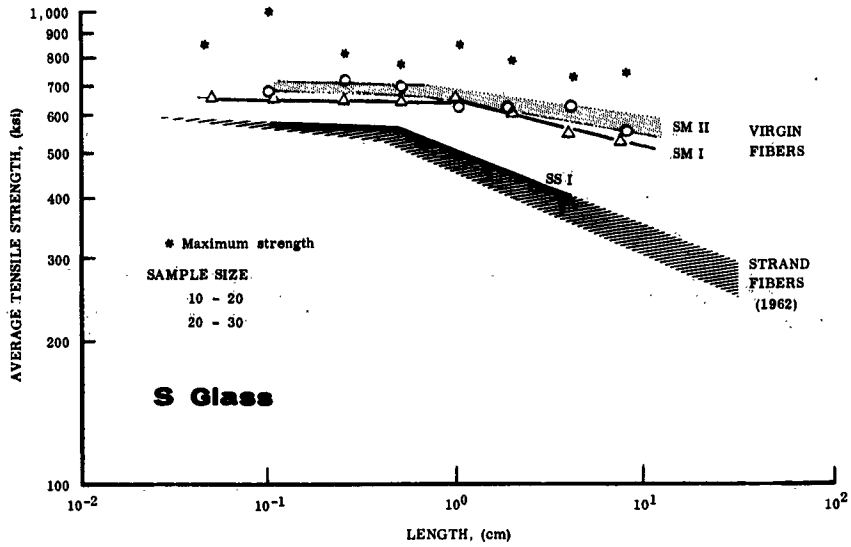

FIGURE 8. LENGTH EFFECT ON STRENGTH OF S-GLASS FIBERS

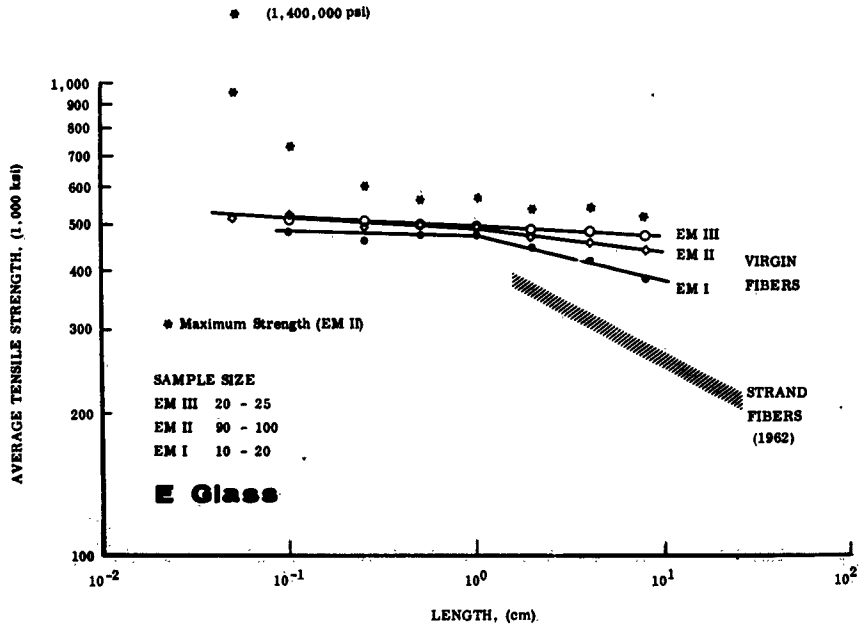

FIGURE 9. LENGTH EFFECT ON STRENGTH OF E-GLASS FIBERS

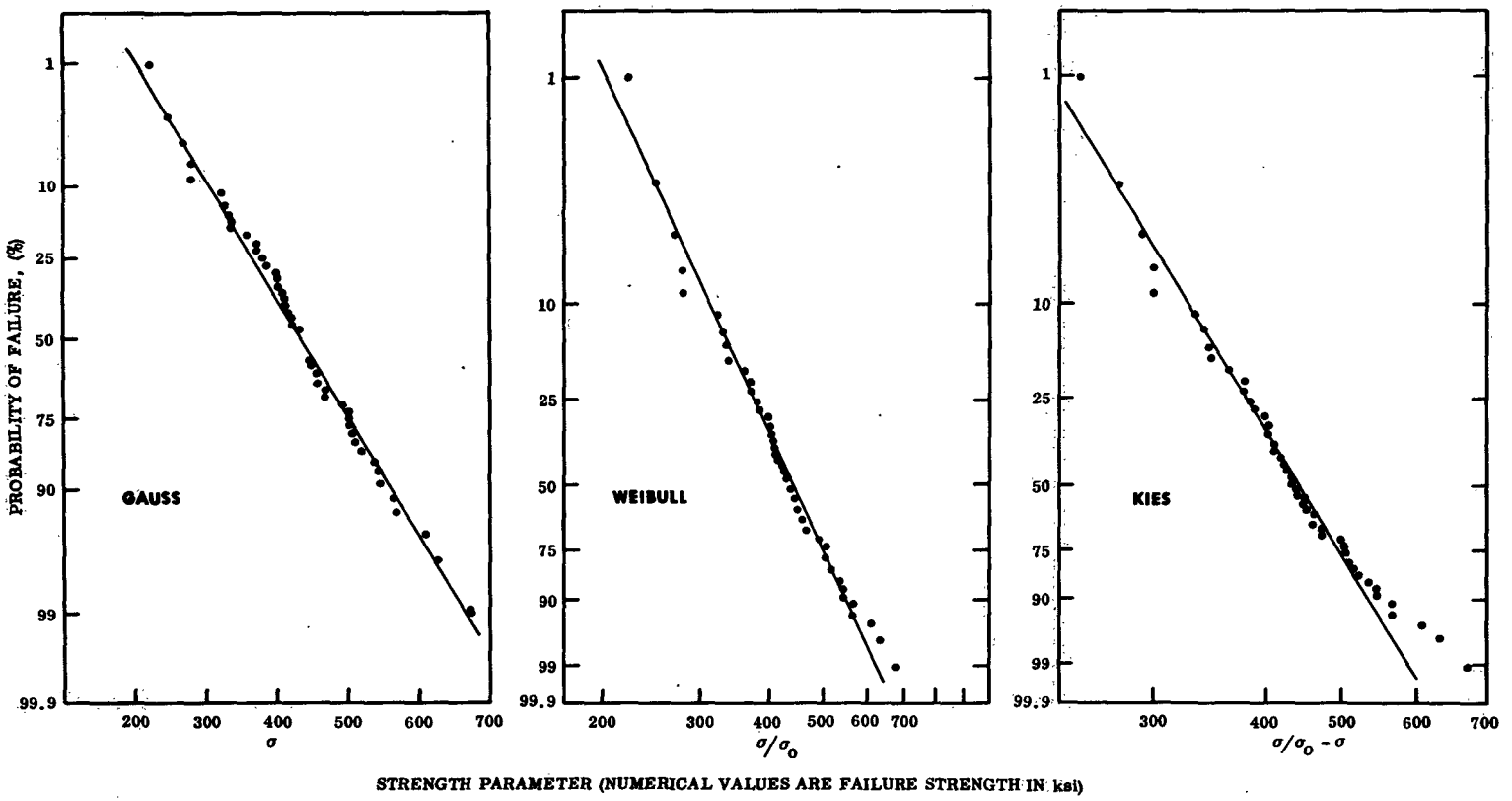

FIGURE 10. EFFECT OF DISTRIBUTION FUNCTIONS ON PROBABILITY PLOT

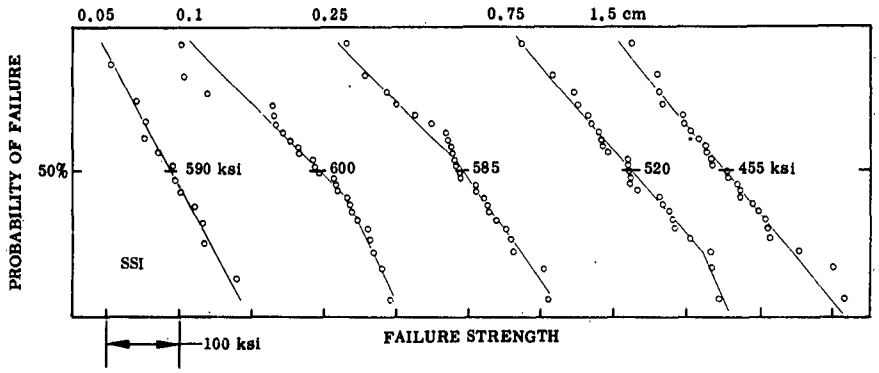

FIGURE 11. GAUSSIAN FAILURE DISTRIBUTIONS AT DIFFERENT GAGE LENGTHS

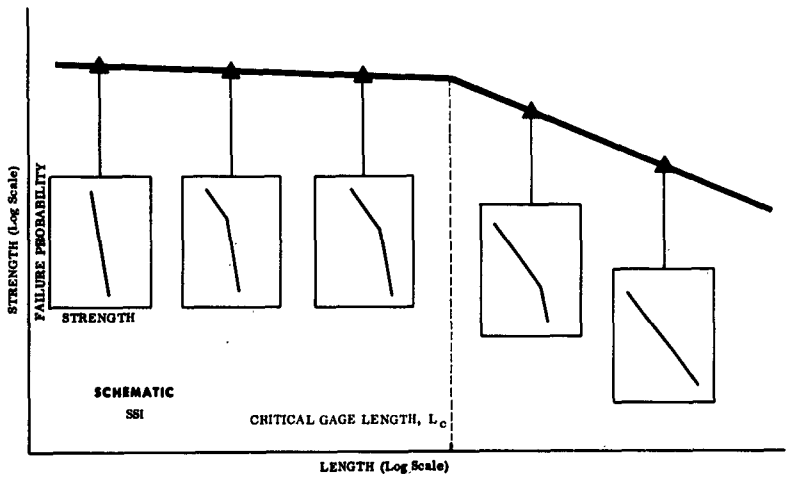

FIGURE 12. SYSTEMATIC CHANGE OF FAILURE DISTRIBUTION CURVES WITH GAGE LENGTH

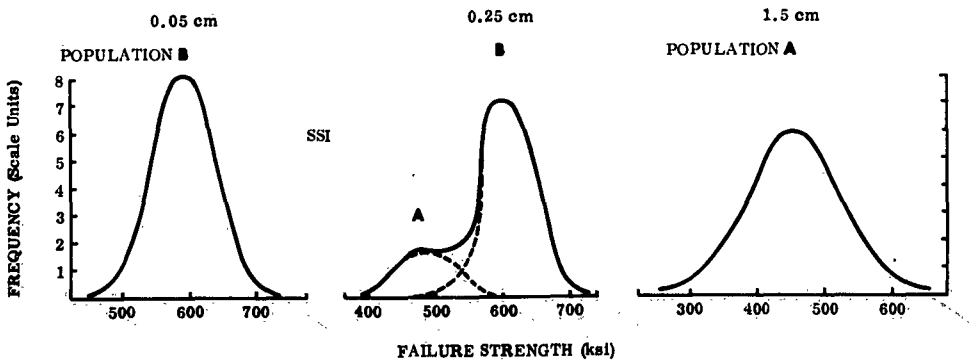

FIGURE 13. FREQUENCY DISTRIBUTION OF FAILURE STRENGTH AT DIFFERENT GAGE LENGTHS

Figure 10 compares a typical set of data on the Gaussian, Kies, and Weibull distributions. As a result of the examination of many sets of data (Ref. 5), it was found that the Gaussian distribution fitted the results best for gage lengths removed from the position of the slope change. Therefore, the Gaussian distribution was used in all subsequent work to examine the data obtained at each gage length.

Analysis of Gaussian distribution plots covering the range of gage lengths across the slope change revealed a systematic trend. Figure 11 shows the failure probability plots for test series SS I between 0.05 and 1.5 cm.[1] Reference to Figure 8 shows that the slope change occurs at 0.5 cm. In Figure 11, straight-line plots are obtained at lengths of 0.05 and 1.5 cm indicative of failure strengths following a Gaussian distribution, whereas increasing irregularity occurs at intermediate lengths. Figure 12 shows these failure probability plots superimposed on the logarithmic strength-length relationship. It is obvious that the failure strengths fall on a normal distribution at both short and long lengths, but on a mixed distribution at intermediate lengths. Comparison of the slopes of the failure probability versus strength curves in Figure 11 for 0.05 and 1.5 cm shows that the normal distribution is much wider, i.e., a wider dispersion at the longer, 1.5 cm length. Figure 13 presents these distributions in the more usual form and includes the bi-modal distribution curve for an intermediate length. The meaning of the slope change in logarithmic strength-length relationships shown in Figures 8 and 9 is now clear: it represents a transition from one distribution of strengths to another and is therefore not a sharp break, but a gradual change of slope.

A distribution of strengths can be represented equally by a distribution of stress concentrators that cause failure at the observed strength. A scratch or other surface damage on virgin glass with a stress concentration factor of 1.25 will reduce the failure stresses to 80 percent of that of virgin glass. The average strength of the S-glass strand fibers at 1.5 cm gage length was 455,000 psi (Fig. 8) so that the average stress concentration factor introduced by stranding is $\frac{650}{455}$ or 1.42.[2]

---

1. Strand fiber data have been selected for this discussion because the damage characteristics are well defined. Defects on virgin fibers are relatively mild and the resulting probability plots do not show the features discussed here quite as clearly.

2. At this time, S-glass was drawn on an experimental basis (X994) and the virgin fiber strength was 650,000 psi according to the manufacturer. Current values are 670,000 psi to 720,000 psi.

The wide dispersion of the strength distributions shown in Figure 13 indicates that the stress concentration factors of those defects causing failure must also have a wide dispersion. In other words, stranding causes surface damage that varies considerably in magnitude. The separation of these defects along the fiber must be of the order of 1 cm. This statement is based on the shape of the failure-probability versus strength plots in Figure 11 where it can be seen that near 0.5 cm, approximately half of the fibers do not contain these severe defects and fall on a strength distribution characteristic of very short lengths. Thus, it has been shown that the defects controlling failure at long gage lengths for fibers from strands have the following characteristics:

1. A wide range of stress concentration factors. Typical values for 10 cm length are 1.2 to 5.4 for 99 percent and 1 percent probability, respectively.

2. Wide separation between flaws in the order of 1 cm as mentioned before.

Using the same arguments, it can be shown that the flaws controlling failure at short gage lengths have the following characteristics:

1. A narrow range of stress concentration factors with typical values between 1.0 and 1.5 for 99 percent and 1 percent probability at 0.025 cm length.

2. Narrow separation of flaws, probably less than 0.1 cm apart.

The characteristics of flaws in both E- and S-glasses are remarkably similar (Fig. 8 and 9). This similarity extends to both monofilaments and fibers from strands, and to commercially produced as well as laboratory samples. Conclusions are possible as to the influence of drawing and stranding processes on flaw and damage formation. This will be discussed later in connection with artificial fiber damage.

8.2 DAMAGE MODEL FOR GLASS FIBERS.

It has been shown that two distributions are required to describe damage to glass fibers. One is the distribution of severities of defects than can be described in terms of a distribution of stress concentrators. The other is a distribution of spacings between the defects. More than one type of damage has been identified by analysis of the length effect and described qualitatively.

A most significant conclusion from this result is that the single exponent, e.g., the m in the Weibull relation, is inadequate to describe the strength of glass fibers. This can be seen readily by applying one of the failure probability functions to the results for the length of fibers at the slope change in Figure 12. The Weibull equation,

$$S_1 = 1 - e^{-L\left(\frac{\sigma}{\sigma_o}\right)^{m_1}} \text{ with } m_1 \approx 100$$

will describe the straight line for short gage lengths, and

$$S_2 = 1 - e^{-L\left(\frac{\sigma}{\sigma_o}\right)^{m_2}} \text{ with } m_2 \approx 6.4$$

will describe the straight line for long gage lengths. The exponent m in each case describes the slope, because

$$\ln L = m \ln\left(\frac{\sigma}{\sigma_o}\right) - \ln(\ln 1/2)$$

for the plotted strength where the failure probability is equal to 0.5.

However, at the length, L_c, where the slope change occurs, the strengths are equal for the two failure distributions. This requires m_1 to be equal to m_2, which is clearly not the case, or for σ_o to have different values for each part of the curve, which makes σ_o descriptive of the damage rather than a material constant. It follows therefore that single exponent distributions such as the Weibull are empirical simplifications that can be applied to a single population of defects, but do not describe the population fully.

The need for two variables, namely severity of defect and separation, to be defined in order to describe a population of defects can be made apparent from the following hypothetical cases.

Figure 14 shows the effect of a narrow distribution of flaw severities plotted in terms of frequency versus stress concentration factor (Insert A). The corresponding failure probability versus applied stress plot in Insert B is steep because the stress concentration factors vary but little (Insert A), and the plot is at high applied stress because the average stress concentration factor is very low. Insert C shows the effect of different frequency-flaw separation curves on the slope of the logarithmic strength-length plot.

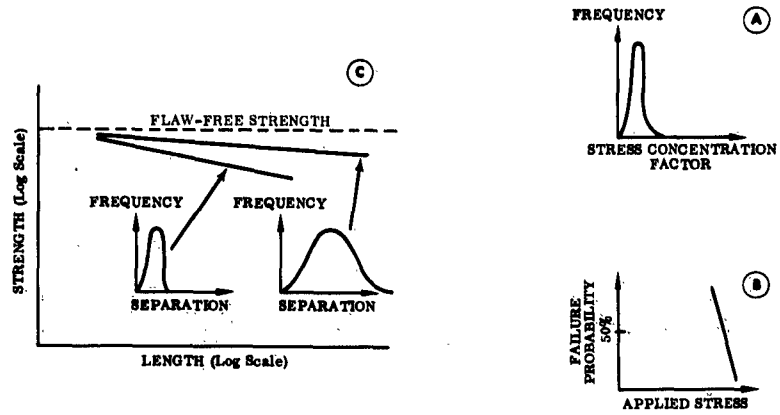

FIGURE 14. EFFECT OF NARROW DISTRIBUTION OF STRESS CONCENTRATION FACTORS ON STRENGTH-LENGTH PLOT.

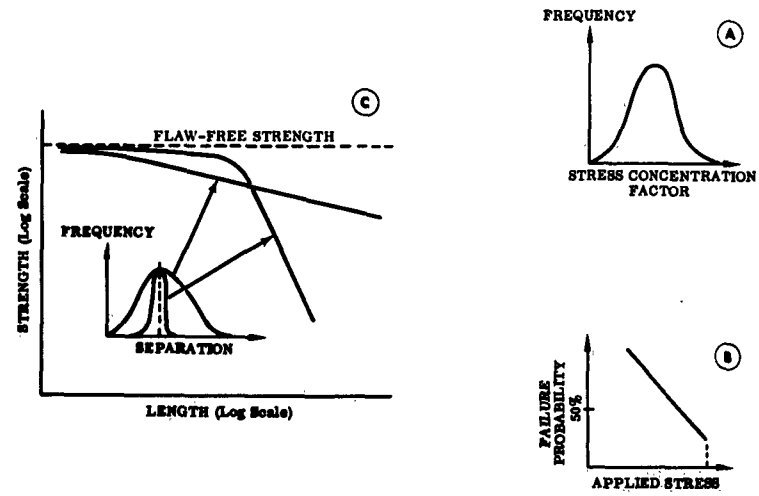

FIGURE 15. EFFECT OF WIDE DISTRIBUTION OF STRESS CONCENTRATION FACTORS ON STRENGTH-LENGTH PLOT.

Figure 15 shows the effect of keeping the average separation of defects constant, but changing the width of this distribution. More severe flaws with a wider distribution are used in this example (Insert A) and the corresponding failure probability curve is shown in Insert B. Insert C shows the result. Because the probability of finding faults decreases rapidly at short gage lengths for the narrow distribution of flaw separations, the average strength will be comprised of an increasing percentage of high values equal to the flaw-free strength. Thus, the curve will show a slope change and approach the theoretical strength asymptotically.

Consideration of these hypothetical curves shows that the downward turn of the logarithmic strength-length plot above the critical gage length, L_c, (Fig. 12) is dependent on appropriate values of the two factors describing the flaws; severity and separation. However, the change of slope need not be an increase (down turn) as the gage length increases (or, in reversed order, a decrease with decreasing gage length).

Indeed, recent evidence for lengths shorter than 0.1 cm shows that the opposite type of slope may occur below 0.025 cm. Data for both E- and S-glasses show an increasing number of high-strength fibers, as the gage length decreases, with values as high as 1,400,000 psi (Fig. 8 and 9). These can be fitted to the curve only by an upturn in the logarithmic strength-length plot at still shorter gage lengths such as advanced in Figure 16.[1] The "flaw-free" strength in Figure 15 could be that of fibers without surface damage and the higher-strength fibers can then be explained as increasing freedom from internal (structural) defects. The latter explanation seems appropriate as strengths of 1,500,000 to 2,000,000 psi are equal to the theoretical strength.

---

1. The extrapolated average strength curve was computed from percent σ max = 1,500,000 psi as noted, and an average strength of 525,000 psi. The latter is the average strength value of fibers containing mild flaws typical for short gage lengths. The curve is conservative because no allowance is made for either the strength values above 1.5 million psi nor for the progressive increase of the number of intermediate values, between 525,000 psi and 1.5 to 2 million psi on the probability plot.

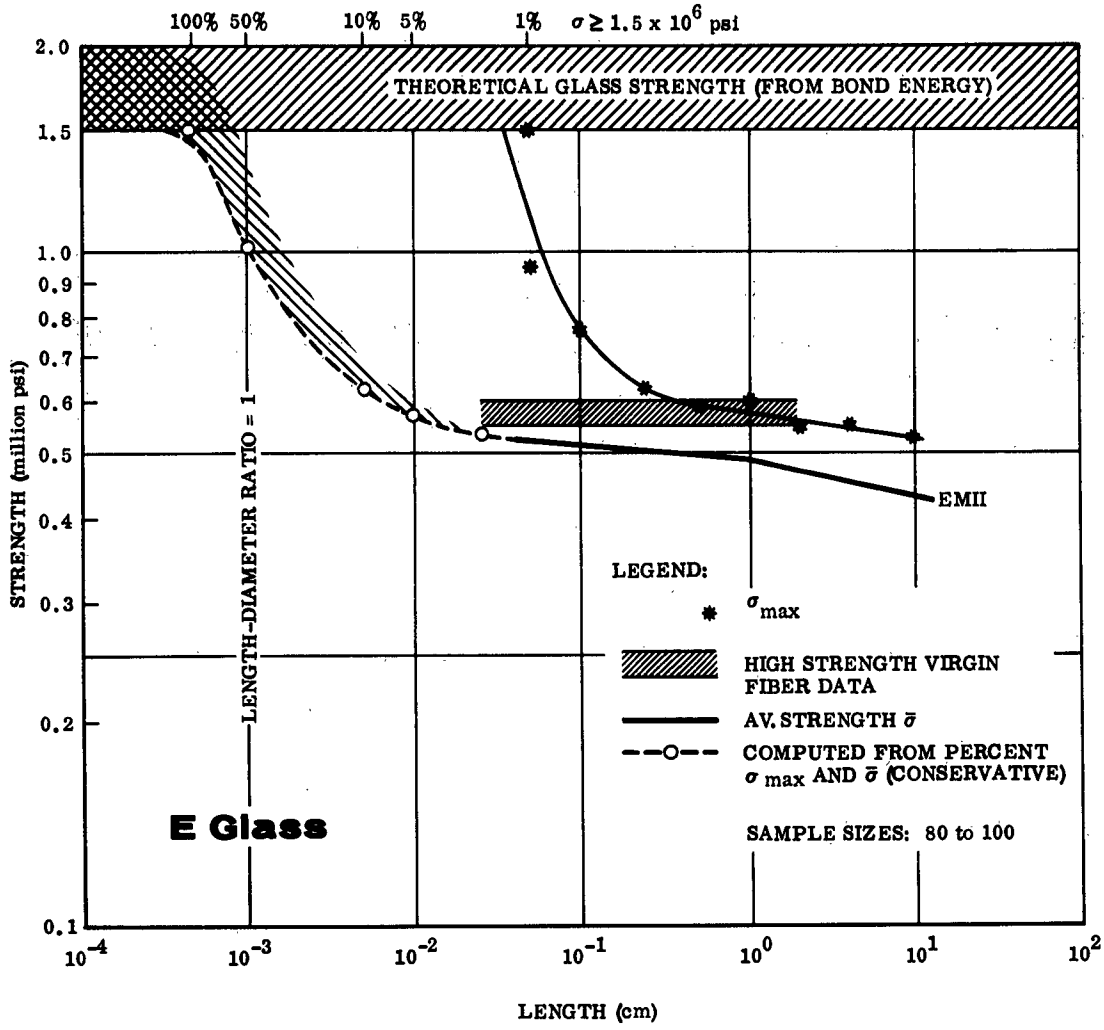

FIGURE 16. PREDICTED STRENGTH-LENGTH RELATION FOR VIRGIN E-GLASS BELOW 0.05 CM LENGTH

One conclusion from this discussion is that there can be no generalized damage model. A steeper slope, such as those shown in Figure 8, may be caused by:

1. Spacing the flaws closer together without any change of flaw severity (Fig. 14)
2. Increasing flaw severity without changing the separation
3. Reducing the spread of interflaw distances leaving the average separation unchanged (Fig. 15)

Experimental proof of case 1 by artificial damage of fibers is given in Figure 17A. Closer spacing of damage (curve D2) was achieved by a ten-fold increase in particle flow as noted in the figure. No further evaluation of this preliminary study (Ref. 10) was made at that time. Increase of flaw severity (case 2) was not investigated since it is to be expected that more severe flaws would lower the strength and would also increase the declination of the slope because of the nonuniformity of defects, i.e., the variation in stress concentrations. Such a condition appears to be present in Figure 17B for the slopes of artificially damaged and virgin fibers. A narrow mean separation of defects (between 0.1 and 0.2 cm) and a wide dispersion of the distribution existed for the damaged fibers (see insert); a similar flaw distribution is necessary for virgin fibers to account for the shallow strength-length slope (Section 8.1).[1] The "surface flaw-free strength" level in Figure 17B is shown with reference to Figures 14 and 15. Its numerical value of 580,000 psi to 600,000 psi was derived from the high-strength tail of the E-glass probability plots.

One other aspect of the results presented in Figure 17B deserves notice. It has been discussed earlier that the critical gage length, i.e., the location of the slope change, is one-half of the average separation of the more severe flaws, in this case the artificial defects. The average separation is approximately 0.15 cm according to the insert, and the slope change (in this case the intersection with the virgin fiber curve) would have occurred slightly below 0.1 cm were it not for the rather low strength

1. Flaw separation on virgin fibers of 10 μ diameter cannot be measured directly by sodium vapor decoration techniques. Calculation of flaw sizes showed that for a stress concentration factor of 1.1 (as applicable in this case) crack sizes would be in the Angstrom range beyond the resolution of optical microscopes. Most likely, virgin fiber flaws with low stress concentration factors are pits rather than cracks, and pits cannot be detected with vapor decoration, whereas microcracks on larger (200 μ) fibers have been made visible by this method (Ref. 6).

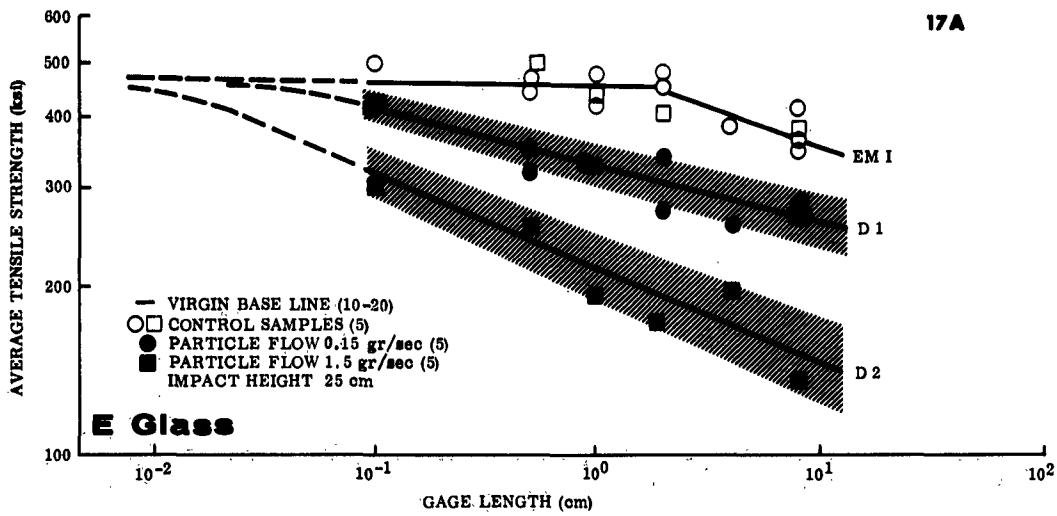

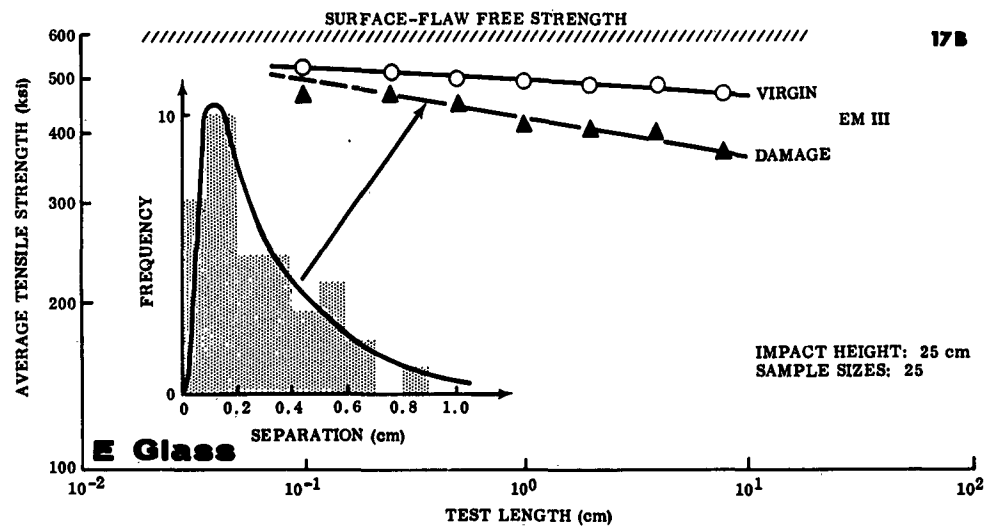

FIGURE 17. EFFECT OF ARTIFICIAL DAMAGE ON VIRGIN E-GLASS FIBER STRENGTH

of the 0.1 cm test point. However, the 0.1 cm probability plot (Appendix B, EM III) shows that more than one-half of the fibers were damaged artificially as evidenced by the departure of the damage strength data from virgin data at approximately 70 percent. An attempt was made to shift the critical gage length experimentally toward higher values (1 cm) in order to have test points on both sides of the slope change, but the damage device could not be controlled sufficiently to obtain reliable separation distributions.

Since this section contains several important aspects concerning fiber strength characteristics, a brief summary may be warranted before discussing further results. First, it has been shown that no generalized damage model exists because the strength depends on both severity and distribution of defects, each of which can assume arbitrary values. However, the processes of fiber drawing and of stranding seem to cause defects or flaws typical for each process, thus giving rise to similar strength-length curves for the two glasses investigated and permiting comparison of stress concentrator effects on the two glasses as will be shown. Secondly, the observed length effect on fiber strength precludes application in the statistical distribution function of a common exponent for all gage lengths. This exponent, for instance Weibull's m, is generally regarded as a descriptive value for "the" strength property, and an erroneous picture evolves unless the length effect is taken into account.

8.3 ANALYSIS OF FAILURE PROBABILITY

8.3.1 Method of Analysis

The failure probability plots in Figures 11 and 12 were shown as a single straight line for a single distribution, and two intersecting straight lines for a mixed distribution. More careful examination shows that this is a simplification for mixed distributions. A typical failure probability plot is shown in Figure 18 with this simple presentation by two straight (dashed) lines through the data. However, a more exact analysis is possible if it is assumed that two populations of flaws control failure and the observed data are the result of failures originating at both types of flaw. The individual flaw population controlling failure at short gage lengths is represented by B, and population A controls failure at long gage lengths. By this it is meant that in the absence of the other type of flaw, the distribution of failure strengths would be as in A or B. As the gage length increases, an increasing percentage of failures originate at the A population of flaws. In Figure 18, the best fit is obtained when 30 percent

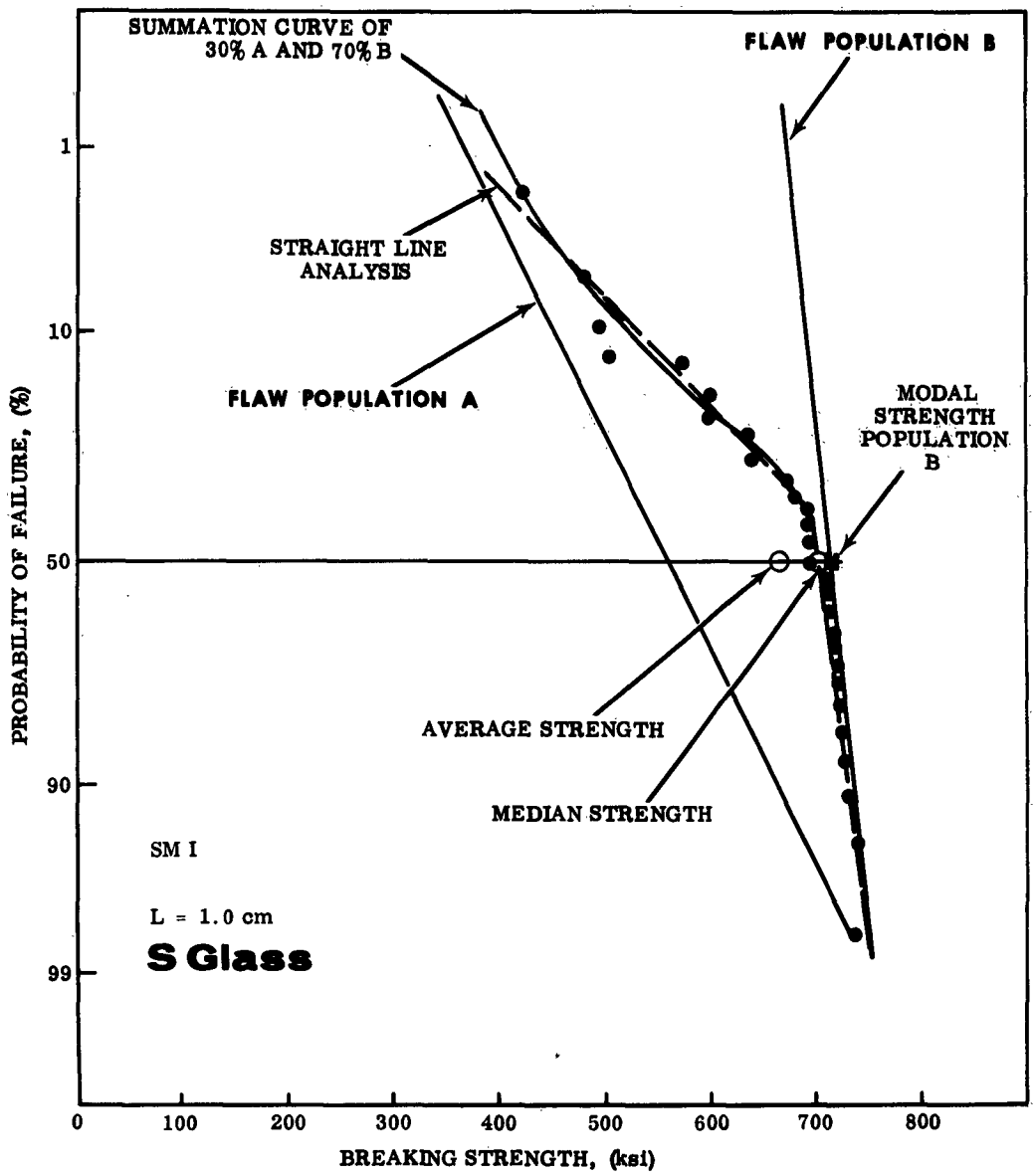

FIGURE 18. GRAPHICAL SEPARATION OF TWO FLAW POPULATIONS ON GAUSSIAN PROBABILITY PAPER

originates at A flaws and 70 percent at B flaws. The summation curve gives a better fit of the data points than the straight line; two more examples with larger sample sizes are shown in Figure 19. Further, it is found that the failure probability curves across the position of the slope change can be calculated by the summation of appropriate percentages of the fixed curves A and B. Better fits are obtained when population A is moved to lower strengths as the gage length increases; this is an inevitable result of multiple A-type flaws in the gage length. Figure 20 illustrates this shift towards lower strength. The most severe A-type flaw in the gage length causes failure so that, as the gage length increases, the higher strength associated with milder flaws decreases progressively.

The designations, population A and B, were introduced to categorize conveniently the effect of different stress concentrators on virgin or stranded fibers. The physical nature of flaw types carrying the same label may be quite different. In fact, defects caused by stranding override statistically the ones existing on virgin fibers as is borne out by the position of the respective strength-length curves below the virgin fiber curves in Figures 8 and 9.[1]

A suggested use of this type of analysis may be for the treatment of experimental strength data. Although no data have been neglected in the present work, there appears to be a widely spread practice to neglect "low" values and ascribe these to accidental damage. The analysis in Figure 18 suggests a systematic method to perform this separation of data. Thus, low-strength values would be neglected only if they depart significantly from the straight-line portion of the total plot that represents the Gaussian distribution.

---

1. Mr. J.A. Kies commented on analysis of failure probability as follows: "The analytical method provided here for detecting different coexisting flaw populations may become a powerful tool in guiding the development of better manufacturing and processing methods for glass. Cornelissen and others (Ref.) have identified an individual flaw population as being introduced by a certain step in a melting process. They also separated two flaw populations, but used a different technique."

   Reference: Cornelissen, J., Meyer, H.W. and Kruithof, A.M., "Statistical Distribution of the Strength Values of Glass Rods," Advances in Glass Technology, Sixth International Congress on Glass, July 1962, Washington, D.C.

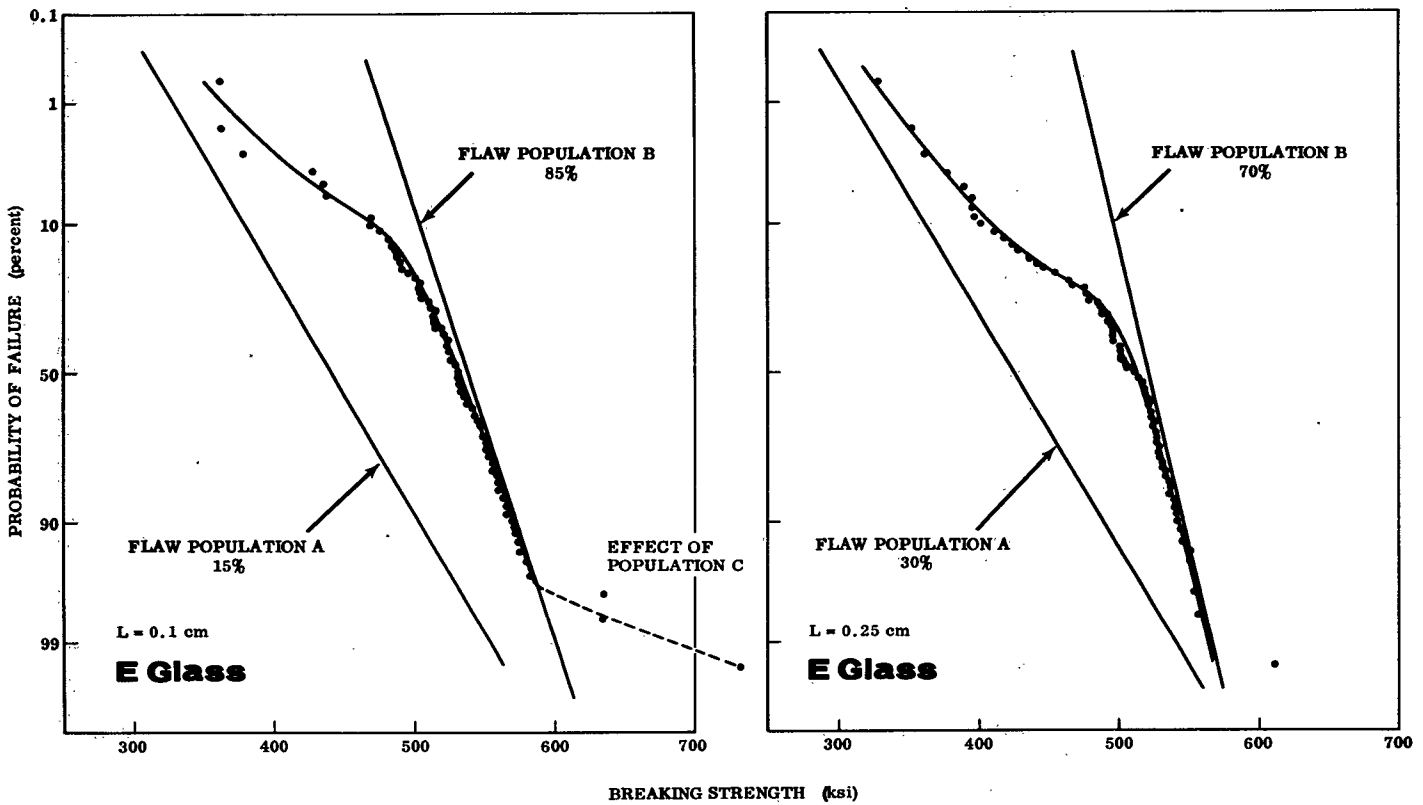

FIGURE 19. BI-MODAL SUMMATION CURVES FOR TWO DIFFERENT TEST LENGTHS OF VIRGIN E-GLASS

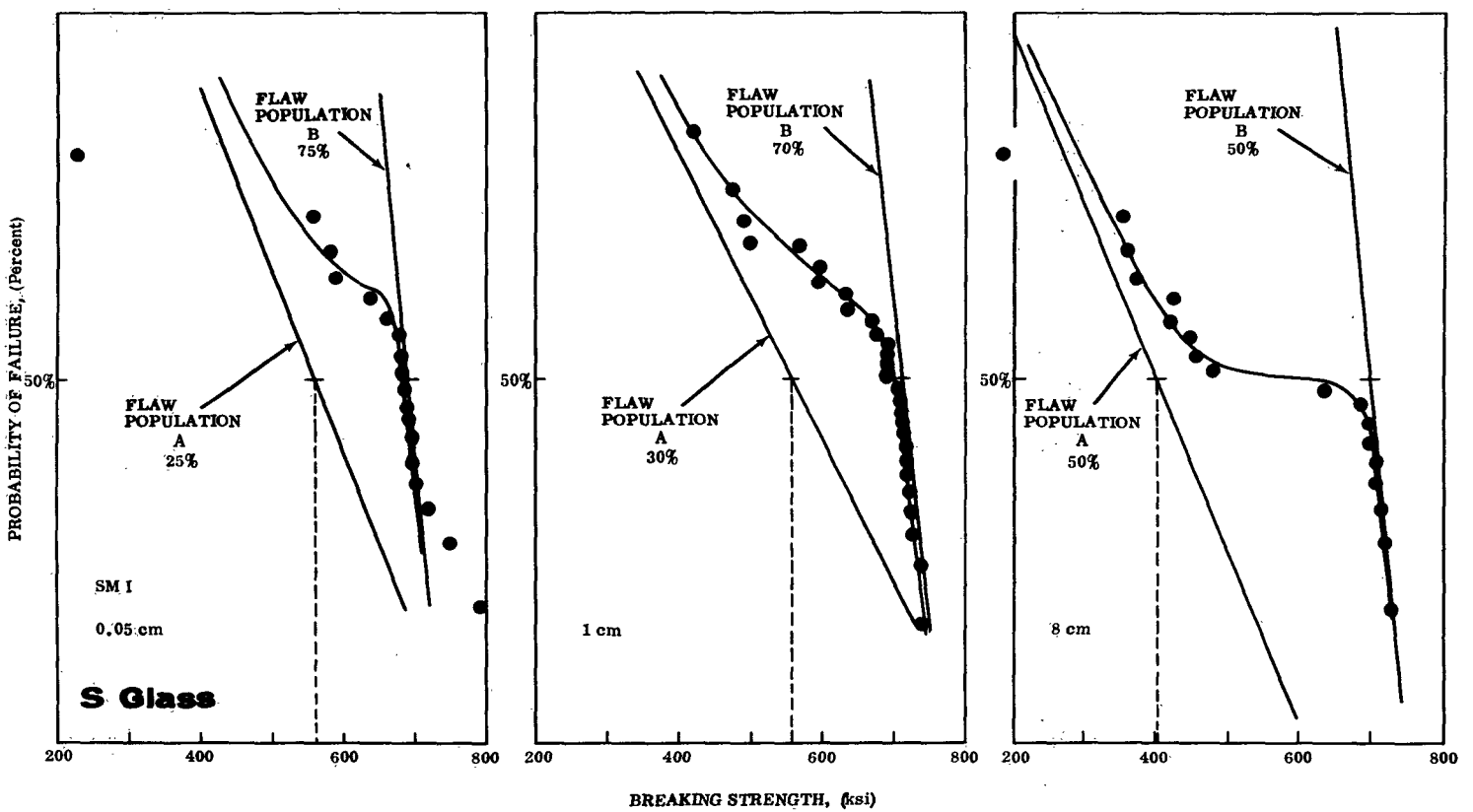

FIGURE 20. SHIFT OF POPULATION A TOWARD LOWER STRENGTH WITH INCREASING GAGE LENGTH

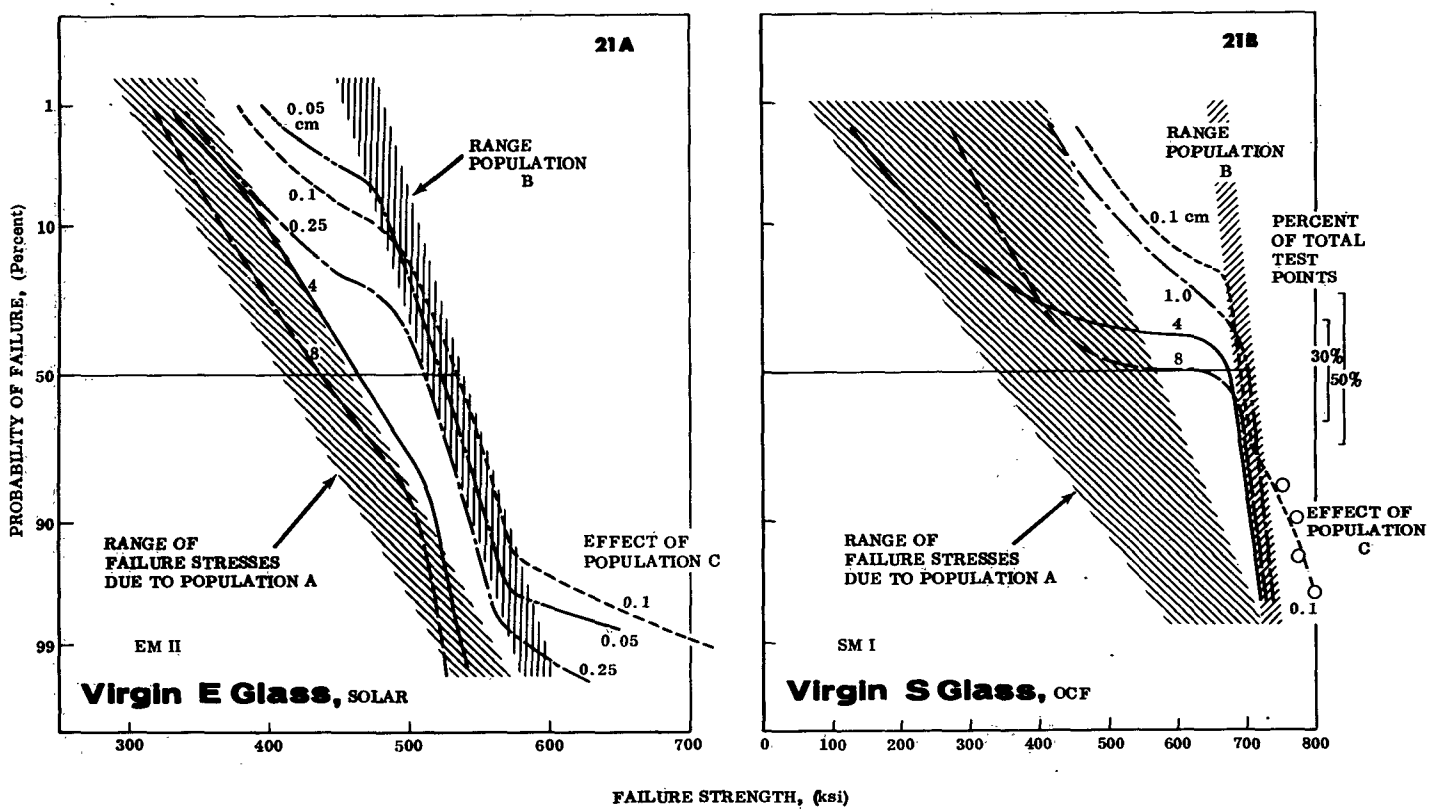

FIGURE 21. PARTIAL SUMMARY OF BI-MODAL SUMMATION CURVES FOR VIRGIN E-GLASS AND S-GLASS; Good Correlation

8.3.2 General Pattern of Probability Curves

The average and the median (50 percent probability) values are both equal to the modal strength for the Gaussian distribution, where the failure probability plot is a straight line. For mixed distributions, this is no longer the case, as shown in Figures 18 through 20. Examining the failure distribution plots from short to long gage length of both E- and S-glass showed that, in general, the median strength first decreases slowly from the modal value of flaw population B (marked x in Fig. 18) to the value shown, until 50 percent failure occurs at flaws of Type A. Then the median strength begins to fall rapidly towards the modal value shown for population A. The median, average, and modal values become equal again for failure controlled by a single Gaussian distribution of A flaws. This trend can readily be observed in Figure 21A, where the distribution curves of several gage lengths are shown for virgin E-glass with data points omitted for clarity; the 0.1 and 0.25 cm curves are those from Figure 19.

A somewhat similar pattern is obtained for S-glass, Figure 21B, with the noticeable difference that the 4 and 8 cm gage lengths contain a considerable amount of high-strength data caused by very mild flaws. This figure demonstrates that omission of low-strength values yield what might be called "potential strength" of the virgin glass while the average strength more realistically presents the "working strength" available in virgin fibers. Presumably, the samples tested have been handled so that the gage length was not touched prior to testing. In the case of E-glass such procedure would be less misleading because of the narrower overall dispersion (from 300 to 600 ksi versus 100 to 750 ksi for S-glass). It may well be that certain glass compositions are more susceptible to flaw formation during drawing than others, in which case a reported average strength based solely on selected higher-strength values (potential strength) would disguise an important characteristic. It appears, therefore, that omission of low values is justified only if either a small number of data are to be rejected, or published strength figures are complemented by description of the method employed.

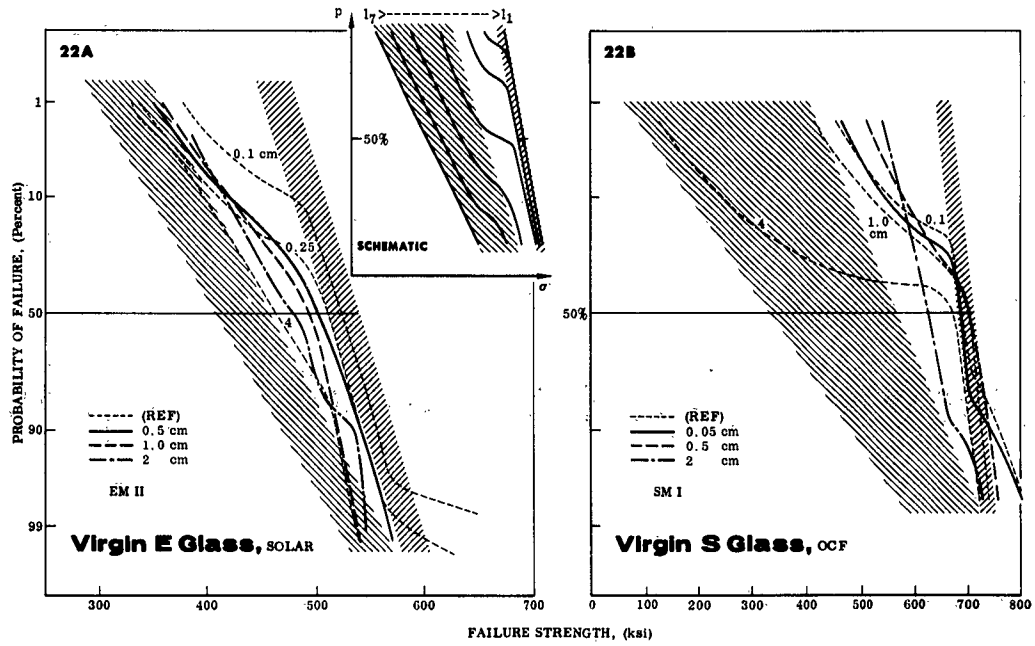

FIGURE 22. PARTIAL SUMMARY OF BI-MODAL SUMMATION CURVES FOR VIRGIN E-GLASS AND S-GLASS; Other Lengths

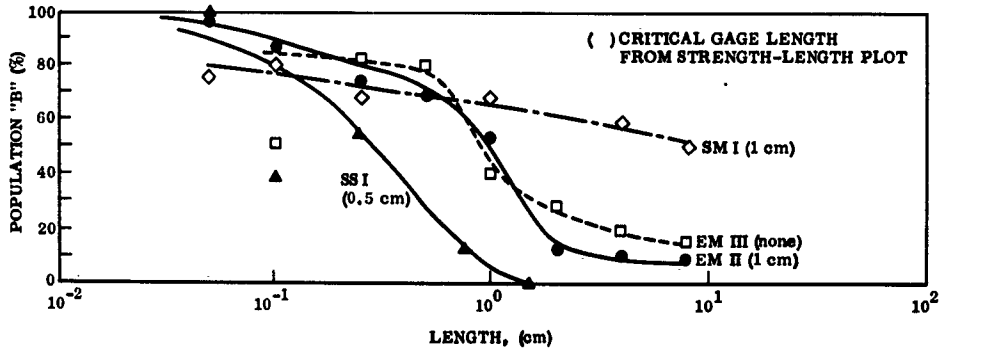

FIGURE 23. PERCENT POPULATION B AS A FUNCTION OF GAGE LENGTH

8.3.3 Deviations From General Pattern

A number of probability curves, not shown in the preceding two summary graphs, exhibited deviations from the general pattern. Such deviations may have several reasons; for instance, variations in drawing conditions, biased sampling, or insufficient sample sizes. Examination of these deviations reveals an interesting relation between probability plots and strength-length curve characteristics.

Figure 22 shows the probability curves in question for both E- and S-glass in the previously shown strength boundaries; some curves from Figure 21 are repeated for reference. It can be seen that the majority of the deviations occur in the lower probability range where the density of data points is relatively low (in some cases only five points), and the shape of the probability curve is most sensitive to irregularities in failure distributions.

The effect of deviations is most noticeable in the ratio of the flaw population A and B which, in turn, is related to the shape of the strength-length curve, specifically near the slope change, as shown in Figure 12.

In order to incorporate such deviating population ratios into the pattern set by more reliable data, a plot of, for instance, percent population B versus gage length is helpful. Figure 23 shows such a plot for several test series. It can be seen that the largest scatter occurs indeed in the higher percent range of population B (or low percent population A), which corresponds to the lower range of the probability of failure scale.

The 50 percent level of the curves should coincide with the critical gage lengths noted in parentheses. Correlation is good for SS I and EM II whereas the EM III curve, although indicating a change in population, does not have a discernable slope change (Fig. 9). The reason becomes clear upon inspection of the EM III probability plots at longer gage lengths, 2, 4, and 8 cm. The population A flaws are rather mild (as are the still existing B flaws compared with EM II) so, that as a net result, the "steeper slope (in the strength-length graph) associated with A-type defects" has become shallow to such a degree as to disappear.

A reversed condition exists for Series SM I. Here little variation of the population ratio exists, yet a marked slope change can be observed in Figure 8 well

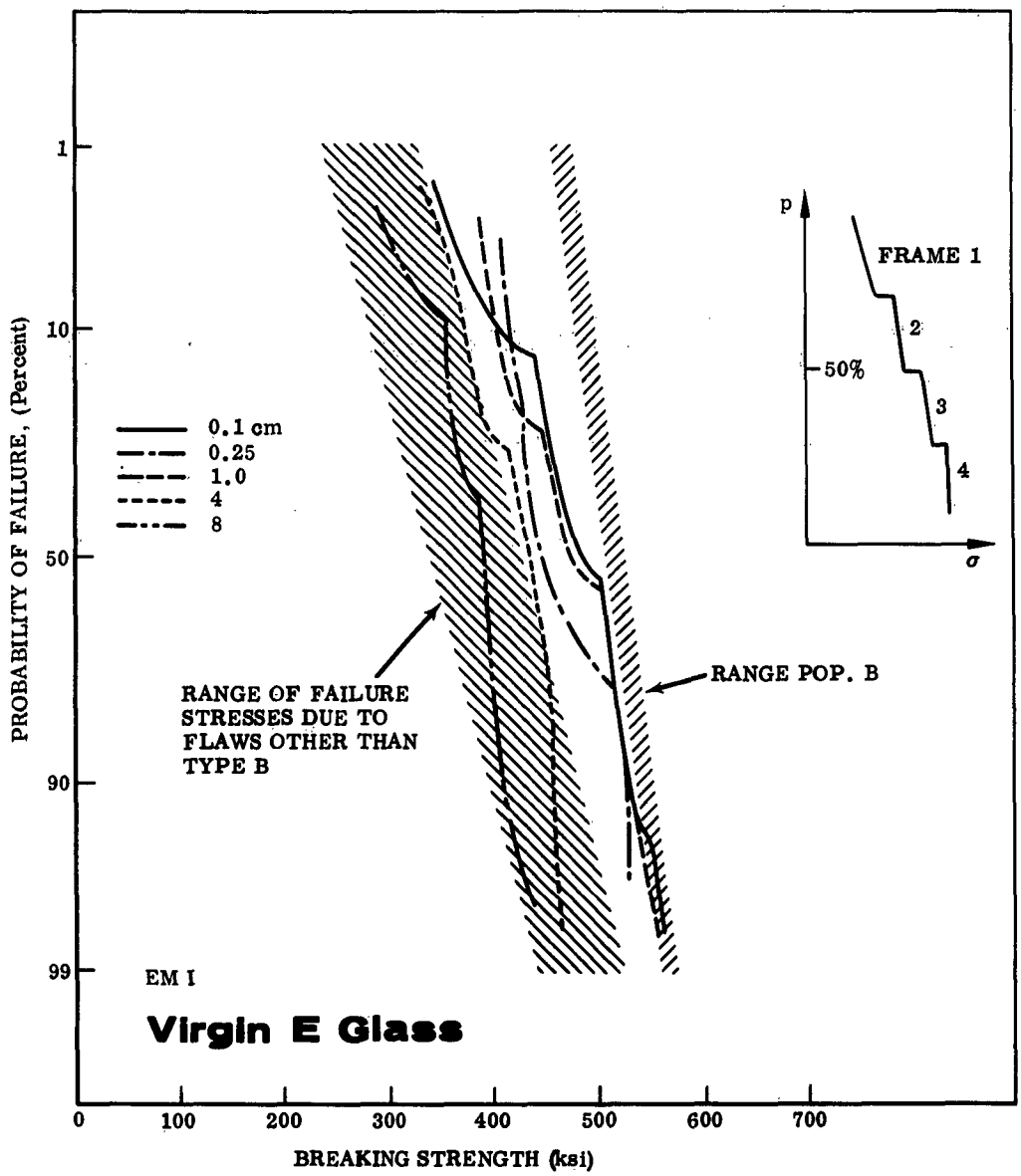

FIGURE 24. PROBABILITY PLOTS OF BIASED SAMPLE POPULATIONS

substantiated by scatter-free average strength data. No immediate explanation can be offered on the basis of previous considerations mainly because the 50:50 ratio occurs at 8 cm, while the slope change occurs at 1 cm. However, a systematic relation exists in as much as the population B curve shows good continuity and the critical gage length falls on the midpoint of the percent increment. This, in conjunction with low population A strength values, appears to be sufficient to account for the observed slope change.

Finally, a typical example of known biased sampling will be discussed. The strength data of test series EM I were obtained from groups of fibers (5 per frame, 3 to 5 frames per gage length) representing samples from various monofilaments of different over-all strength. Figure 24 shows the tracings of the actual probability curves (slightly accentuated)[1] and, in the insert, a simplified pattern for one gage length as obtainable with four frames. The strengths of the fibers of each frame have small dispersion. If this fact were not known from test procedures and original test data, multiple flaw populations would have to be assumed for random sampling. The general trend toward lower strength as the gage length increases, corresponds with the strength-length data in Figure 9.

These findings lead to the conclusion that the relationship between strength-length curves and associated probability plots is somewhat more complex than suggested by the analysis of the classical case, Series SS I. The average strength data appear to be relatively insensitive to certain irregularities in failure distributions (page 25, footnote). A combined analysis of strength-length curves and failure distributions, however, reveals individual characteristics of glasses and thus provides a powerful method for examination of glass fibers.

8.4 RESISTANCE TO DAMAGE

In the experiments with artificial damage, fibers of S- and E-glass were subjected to identical procedures described in Section 6.4.3. The strength loss of the two glasses gives some measure for their relative resistance to damage and data from these controlled experiments can be compared with the strength loss of fibers from strands, provided that the virgin reference strengths are comparable.

---

1. The population ranges are approximated; population B range is fairly accurate.

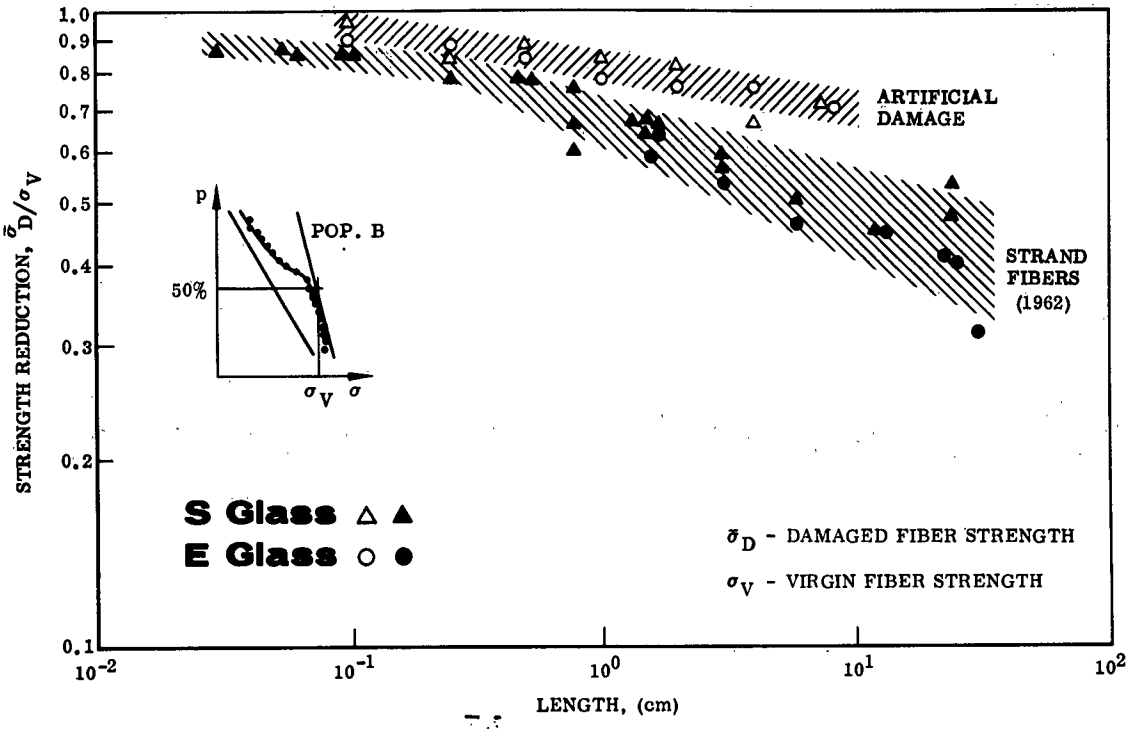

FIGURE 25. STRENGTH REDUCTION OF STRAND FIBERS AND ARTIFICIALLY DAMAGED FIBERS

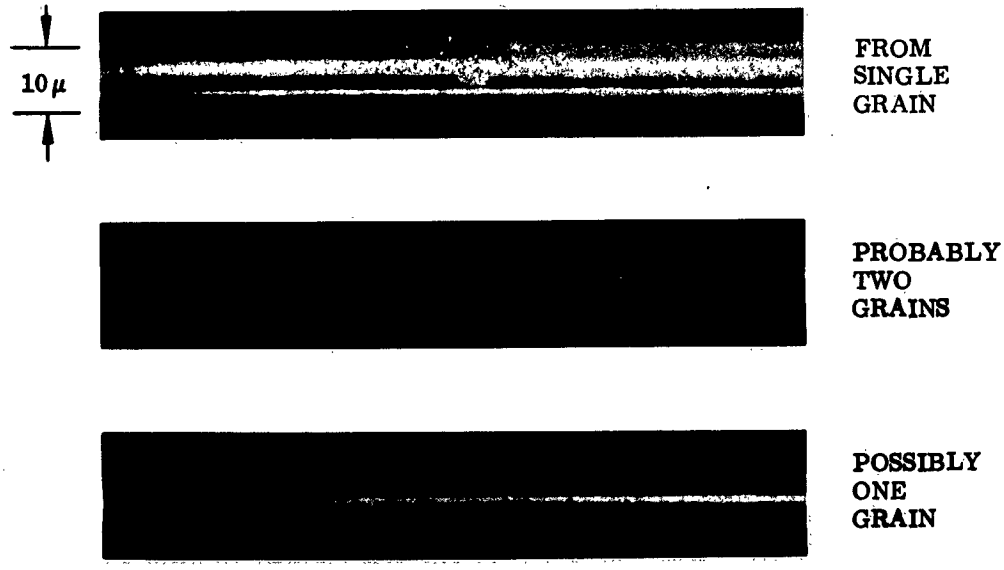

Magnification: 1,000X

FIGURE 26. DAMAGE MARKS FROM GARNET GRAINS ON E-GLASS

The reference strength should be independent of gage length for this purpose of cross reference. Consideration of the probability curves in Figure 21 suggests the usage of the modal strength associated with flaw population B. A simplified method to obtain an approximate, yet close, value is to take the average of the midpoint strengths of the high-strength tail of several probability plots. Evaluation of the available probability plots led to the following virgin reference strengths:

Glass	σ_v (psi)	Remarks
E	525,000	Solar drawn and tested
S	725,000	OCF drawn, Solar tested
994	675,000	High strength data from OCF, to be used for 994 strand fibers.

Strength reductions, expressed by the ratio: $\frac{\text{damaged fiber strength}}{\text{virgin reference strength}}$, were computed on this basis and are shown in Figure 25 for artificially damaged fibers and strand fibers; the extent of surface damage from the particles used for this condition is shown in the microphotographs, Figure 26.

The close proximity of the data points of S- and E-glass for the two damage conditions suggests similar resistance to damage. It can be inferred from the experimental results that the stranding process caused similar distributions of both severity and separation of defects on the two glasses. Recent strand test data presented by OCF at the Polaris meeting, January 1964, substantiated this conclusion. Strength loss was nearly equal for the two glasses, 18 to 19 percent based on 10-inch (25 cm) gage length and virgin control strengths at that length.

Some of the preliminary results with artificial fiber damage were inconclusive, but are reported because of their significance with respect to the susceptibility of the fiber surface to damage.

In one case, fibers were dipped into a fluidized bed of lightweight metal spheres (Solarcel) and of glass spheres. Particle properties are listed below. In another case, damage was attempted by gravity flow of the same glass spheres at three different flow rates, one of which gave inconclusive results.

FIGURE 27. DAMAGE MARKS FROM GLASS SPHERES ON E-GLASS

Particle	Characteristics	Application
SOLARCEL 50 μ	Smooth, glossy surface P = 0.185 gr/cm^3	Fluidized bed, 30-sec dip
Glass Spheres 300 μ	Smooth surface, P = 2.56 gr/cm^3	Fluidized bed, 3-sec dip
Glass Spheres 300 μ	Smooth surface, P = 2.56 gr/cm^3	Gravity flow: 1) 0.15 gr/sec 2) 1.5 gr/sec 3) Controlled single hits, separation as noted.

Solarcel particles in the fluidized-bed application did not cause any strength reduction, in fact, the strength of the exposed specimen was higher than that of the control specimens, 500 and 450 versus 430 ksi. The 450 ksi value is within the expected scatter, whereas 500 ksi appears to be extremely high considering that all specimens (3 groups of 5) were sampled from one monofilament. Fluidized-bed application of glass spheres, on the other hand, caused considerable strength loss (Ref. 10). No microscopic check of the fiber surface was possible at that time.

Glass spheres were applied in three controlled amounts of gravity flow. Satisfactory results from number one and two, shown in Figure 17A, led to the continued usage of glass spheres in the final damage device. However, the flow was reduced considerably to obtain measurable impact separations in the order of 1 hit per cm (Section 6.4.3). The resulting strength data, listed in Table IV, were inconclusive as to the extent of the damage. Typical impact marks from glass spheres are shown in Figure 27. It is difficult to believe that such damage, even a single hit, failed to cause substantial strength loss. The program did not permit further investigation, and sharp-edged irregular garnet grains were used for the comparative damage of E and S-glass as discussed in the preceding paragraphs.

TABLE IV

STRENGTH OF E-GLASS FIBERS DAMAGED BY GLASS SPHERES

	Impact Height (cm)	Control (ksi)	Strength at Fiber Velocities		
			10 cm/sec (ksi)	5 cm/sec (ksi)	2.5 cm/sec (ksi)
L = 2 cm	20 cm	510	520	-	-
		450	465	-	-
		445	475	435	-
		460	-	435,440	-
	40 cm	515	-	440(450,8 cm)	-
		505	-	485,500	-
L = 8 cm	20 cm	420	-	-	470,430
		350	-	-	325,400
	40 cm	445	350	-	-
		400	-	410	-
	20 cm	410	-	-	415
	Approx number of impacts		1 per 2 cm	1 per cm	3-4 per 2 cm

NOTE: Sample sizes: Four per test point. Data across the table are from one monofilament.

Referring to Figure 17A, the hit probability for the 0.15 gr/sec flow rate and 2.5 cm/sec fiber velocity was calculated to approximately 80 hits per cm fiber length, and two sides of the fiber were exposed. The calculation was checked experimentally with four times the fiber velocity, i.e., 10 cm/sec. Calculation: 21 hits per cm length. Experiment: 21, 24, 25 hits per cm. The flow pattern was "frozen" on adhesive tape and spheres were counted along the hairline of a microscopic eyepiece. It is believed that the strength loss at the two flow rates, 0.15 and 1.5 gr/sec, was due mainly to multiple hits, enchanced perhaps by coincidental occurance of severe defects on both sides of the fiber. This would explain the considerable scatter in contrast to the virgin control data.

In summary, no effective damage was observed from fluidized lightweight glossy spheres, whereas severe damage was caused by fluidized glass spheres. Strength data of fibers subjected to single, widely separated hits from glass spheres are inconclusive, while strength loss was large from dense hit distributions, most probably multiple hits. Comparative damage tests with virgin E- and S-glass fibers showed nearly equal resistance to particle-induced damage. These results confirmed the previous conclusion that the process of stranding caused similar damage on the two glasses in terms of both severity and separation of defects.

IX. CONCLUSIONS

The following conclusions can be drawn from this work:

1. Careful control permits tensile tests of glass fibers to be made down to 0.025 cm gage length.

2. The logarithmic strength-length plot is a valuable tool in the study of flaws in glass fibers.

3. Two types of flaws have been identified in virgin fibers of both E- and S-glass. One type is severe, has wide spacing, and governs failure of long fibers. The other type has narrow spacing, is less severe, and determines failure at short gage length. The number of severe flaws depends on drawing conditions.

4. Some strength values approached the theoretical strength of glass and indicate the presence of flaw-free fiber sections in the short length range of freshly drawn fibers.

5. Two types of flaws have been identified on fibers from strands. These flaws originated in the stranding process and are considerably more severe than those of virgin fibers.

6. The stranding processes used for the two type glasses investigated caused similar distributions of both severity and separation of flaws.

7. The single exponent failure probability functions, such as that due to Weibull, are inadequate to describe failure in glass fibers for the conditions investigated. The inadequacy only becomes apparent when the number of flaws in the test volume becomes so small that a second control mechanism begins to assume command.

8. Analysis of failure probability plots allows flaw populations to be separated when mixed control of failure occurs. It also suggests a method to eliminate "low" values (caused by accidental damage) from a test series.

REFERENCES

1. Griffith, A.A., The Phenomena of Rupture and Flow in Solids. Society of London, Philosophical Transactions, Series A, Vol. 221 (1920-21).
   The Theory of Rupture. Procedures of International Congress of Applied Mechanics, 55 (1924).

2. Weibull, W., A Statistical Theory of the Strength of Materials. Handlingar, Royal Swedish Academy of Engineering Sciences, No. 151 (1939).

3. Kies, J.A., The Strength of Glass. NRL Report 5098 (April 1958).

4. Thomas, W.F., An Investigation of Factors Likely to Affect the Strength and Properties of Glass Fibers. Physics and Chemistry of Glasses, Vol. 1 (February 1960).

5. Final Report 1962, Exploration and Evaluation of New Glasses in Fiber Form, NRL Project 62 R05 19A, Technical Memo 215.

6. Gordon, J.E., et al, On The Strength and Structure of Glass, Proc. Roy. Soc. A, Vol 249.

7. Anderegg, F.O., Strength of Glass Fibers. Industrial and Engineering Chemistry, Vol 31 (1939).

8. Sinclair, D., A Bending Method for Measurement of Tensile Strength and Young Modulus of Glass Fibers. Journal of Applied Physics, Vol 21 (1950).

9. Otto, W.H., Private Communication. NARMCO Research & Development, San Diego, California.

10. Bimonthly Progress Report, No. 1, 1963, Exploration and Evaluation of New Glasses in Fiber Form, NRL Project 62 RO5 19A, Technical Memo No. 216.

APPENDIX A

TABULATED TEST DATA

Test Series	Table
EM I	A-I
EM II	A-II
EM III	A-III
SM I	A-IV
SM II	A-V

TABLE A-I

SOLAR E-GLASS, SERIES EM I, VIRGIN AND DAMAGED

Average Test Data Summary

Virgin						Damage 2		Damage 3	
Test Length (cm)	Avg. Diameter (10^{-5} in.)	Avg. Strength (ksi)	Std. Dev. (ksi)	Coeff. of Var. (%)	Sample Size (No.)	Avg. Strength (ksi)	Sample Size (No.)	Avg. Strength (ksi)	Sample Size (No.)
0.1	41.8	478	49.4	10.3	27	420	5 ea	305	9
0.25	42.2	460	42.7	9.3	14	-	-	-	
0.5	40.3	474	32.2	6.8	24	305,350	5 ea	250	10
1.0	41.3	474	48.0	10.1	19	335,335	5 ea	195	5
2	39.6	448	42.2	9.4	26	275,350	5 ea	175	5
4	39.6	419	35.7	8.5	28	260	5 ea	200	5
8	41.0	381	31.9	8.4	20	275,270 295	5 ea	140	5

TABLE A-II

SOLAR E-GLASS, SERIES EM II, VIRGIN

Average Test Data Summary

Test Length (cm)	Average Diameter (10^{-5} in.)	Average Strength (ksi)	Std. Dev. (ksi)	Coeff. of Var. (%)	Sample Size (No.)
0.025	39.2	509	46.8	9.2	49
0.05	38.9	517	59.0	11.4	81
0.1	38.9	526	52.3	10.0	85
0.25	38.4	494	52.2	10.6	92
0.5	38.9	490	47.2	9.6	93
1	38.6	489	40.2	8.2	96
2	38.9	469	57.4	12.3	77
4	38.4	457	50.1	11.0	85
8	39.3	441	49.1	11.1	84

Test Environments: 76 to 80 F and 40 to 50% RH

TABLE A-III

SOLAR E-GLASS, SERIES EM III, VIRGIN AND DAMAGED

Average Test Data Summary

	Test Length (cm)	Average Diameter (10^{-5} in.)	Average Strength (ksi)	Std Dev. (ksi)	Coeff. of Var. (%)	Sample Size (No.)
Virgin Control	0.1	38.3	508	42.9	8.4	22
	0.25	37.9	509	31.6	6.2	23
	0.5	38.6	495	51.6	10.4	23
	1	38.2	490	48.1	9.8	25
	2	38.1	483	56.6	11.7	21
	4	38.4	486	51.1	10.5	25
	8	38.2	470	43.1	9.2	21
Damage 1	0.1	38.4	461	70.2	15.2	25
	0.25	37.9	462	67.3	14.6	25
	0.5	38.4	443	60.7	13.7	24
	1	38.2	406	79.8	19.6	25
	2	38.1	400	66.2	16.6	25
	4	38.3	393	51.2	13.1	25
	8	38.4	366	61.5	16.8	25

Test Environments: 76 to 78 F and 40 to 50% RH

TABLE A-IV

OCF S-GLASS, SERIES SM I, VIRGIN

Average Test Data Summary

Test Length (cm)	Average Diameter (10^{-5} in.)	Average Strength (ksi)	Std. Dev. (ksi)	Coeff. of Var. (%)	Sample Size (No.)	Remarks
0.025	41.8	645	90.7	14.1	31	Low; 14 high values missing
0.05	42.5	648	117.0	18.0	18	Low; 5 high values missing
0.1	42.2	671	85.6	12.7	13	
0.25	39.1	644	77.2	12.0	5	
0.5	41.5	657	106.5	16.2	25	
1.0	42.2	661	83.2	12.6	27	
2	42.1	615	44.4	7.2	24	
4	42.4	549	178.6	32.5	19	
8	41.9	541	168.1	31.1	18	

Test Environments: 78 to 84 F and 45 to 50% RH

TABLE A-V

OCF S-GLASS, SERIES SM II, VIRGIN AND DAMAGED

Average Test Data Summary

	Test Length (cm)	Average Diameter (10^{-5} in.)	Average Strength (ksi)	Std. Dev. (ksi)	Coeff. of Var. (%)	Sample Size (No.)
Virgin Control	0.1	39.7	674	65.2	9.7	10
	0.25	39.5	718	61.8	8.6	10
	0.5	39.8	700	57.4	8.2	20
	1	39.3	632	135.5	21.5	14
	2	39.6	608	145.5	23.9	14
	4	39.2	630	120.7	19.2	17
	8	39.9	557	104.5	18.8	17
Damage 1	0.1	40.3	689	43.6	6.3	12
	0.25	39.5	602	123.0	20.5	17
	0.5	39.5	631	88.2	14.0	20
	1	39.8	608	84.6	13.9	18
	2	39.6	591	53.1	9.0	15
	4	38.6	475	157.9	33.2	12
	8	38.8	508	117.2	23.1	17

Test Environments: 70 to 78 F and 40 to 50% RH

APPENDIX B

GAUSSIAN FAILURE DISTRIBUTIONS

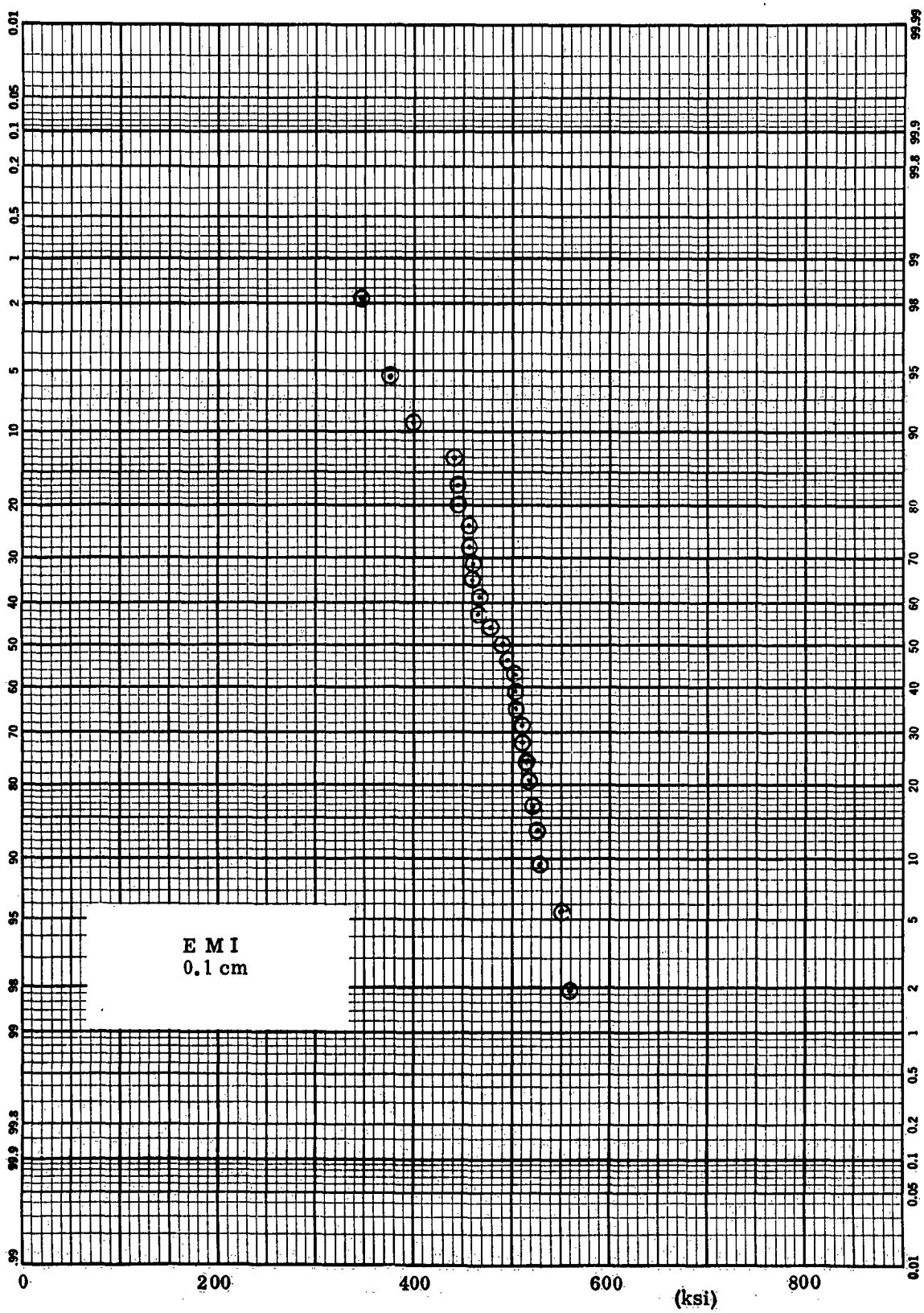
0.01
0.05
0.1
0.2
0.5
1
2
5
10
20
30
40
50
60
70
80
90
95
98
99
99.8
99.9
99.99
E M I
0.1 cm
0
200
400
600
800
(ksi)

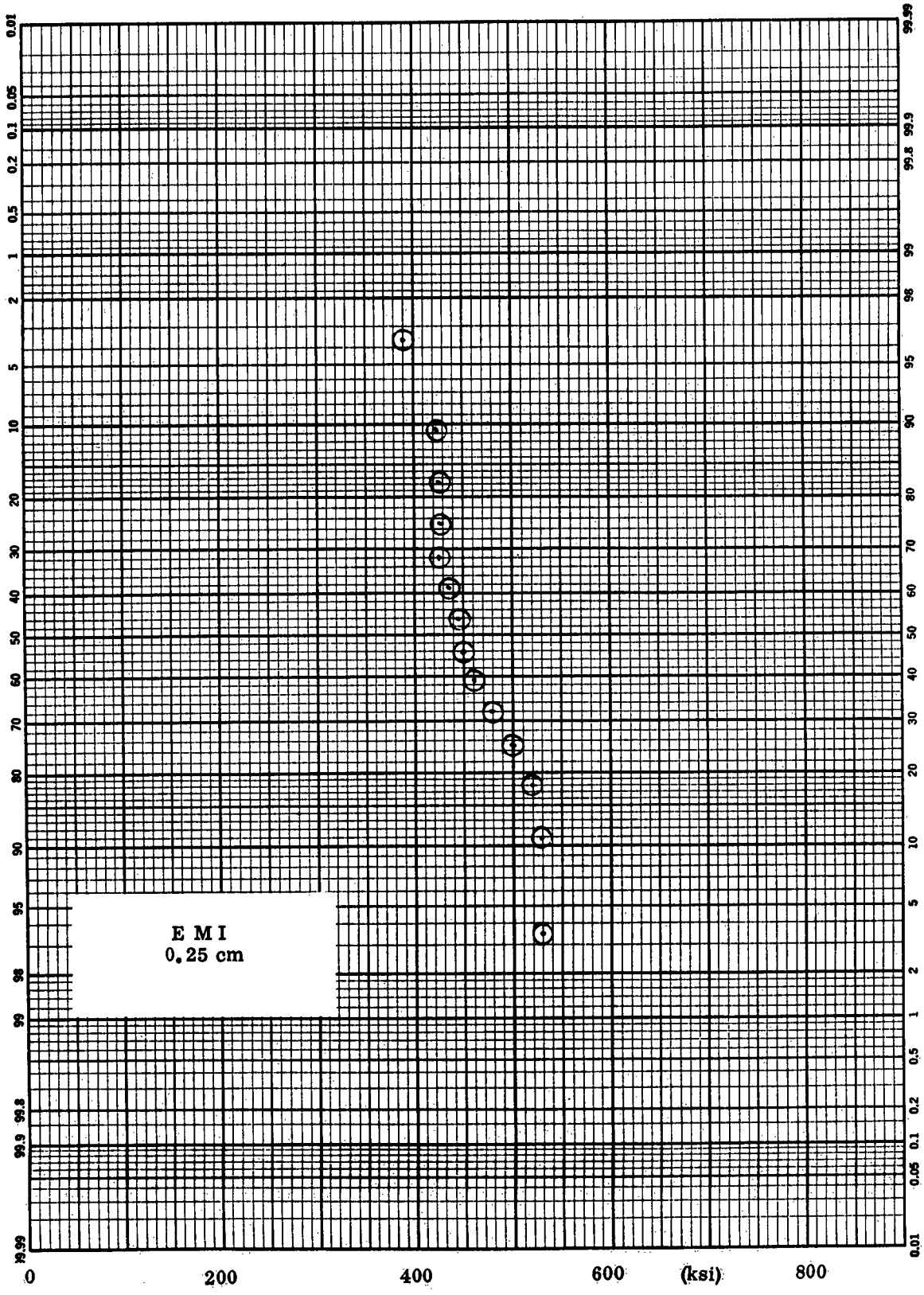
E M I
0.25 cm
0
200
400
600
(ksi)
800

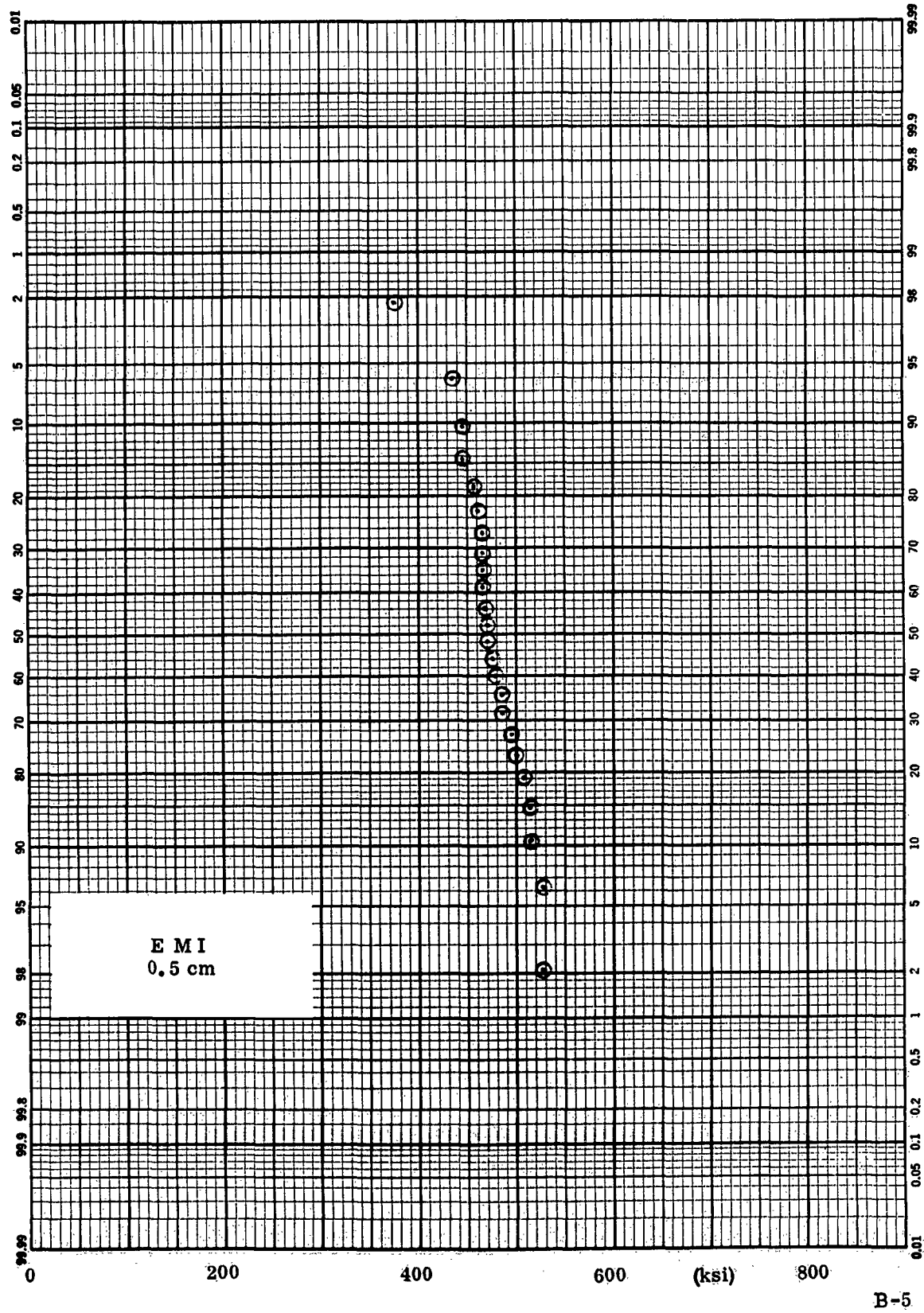
0.01
0.05
0.1
0.2
0.5
1
2
5
10
20
30
40
50
60
70
80
90
95
98
99
99.8
99.9
99.99
E M I
0.5 cm
0
200
400
600
(ksi)
800

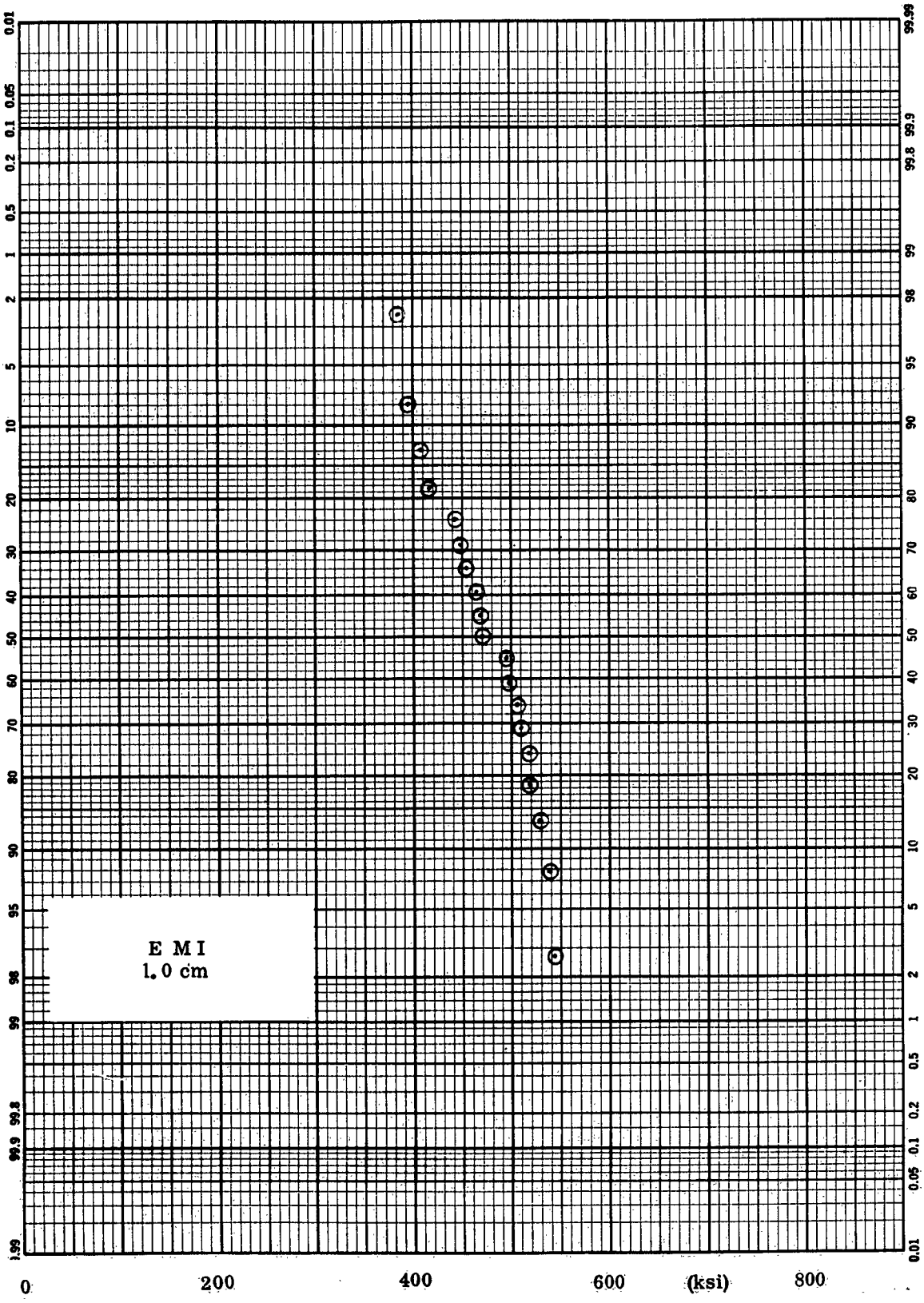
0.01
0.05
0.1
0.2
0.5
1
2
5
10
20
30
40
50
60
70
80
90
95
98
99
99.8
99.9
99.99
E M I
1.0 cm
0
200
400
600
(ksi)
800

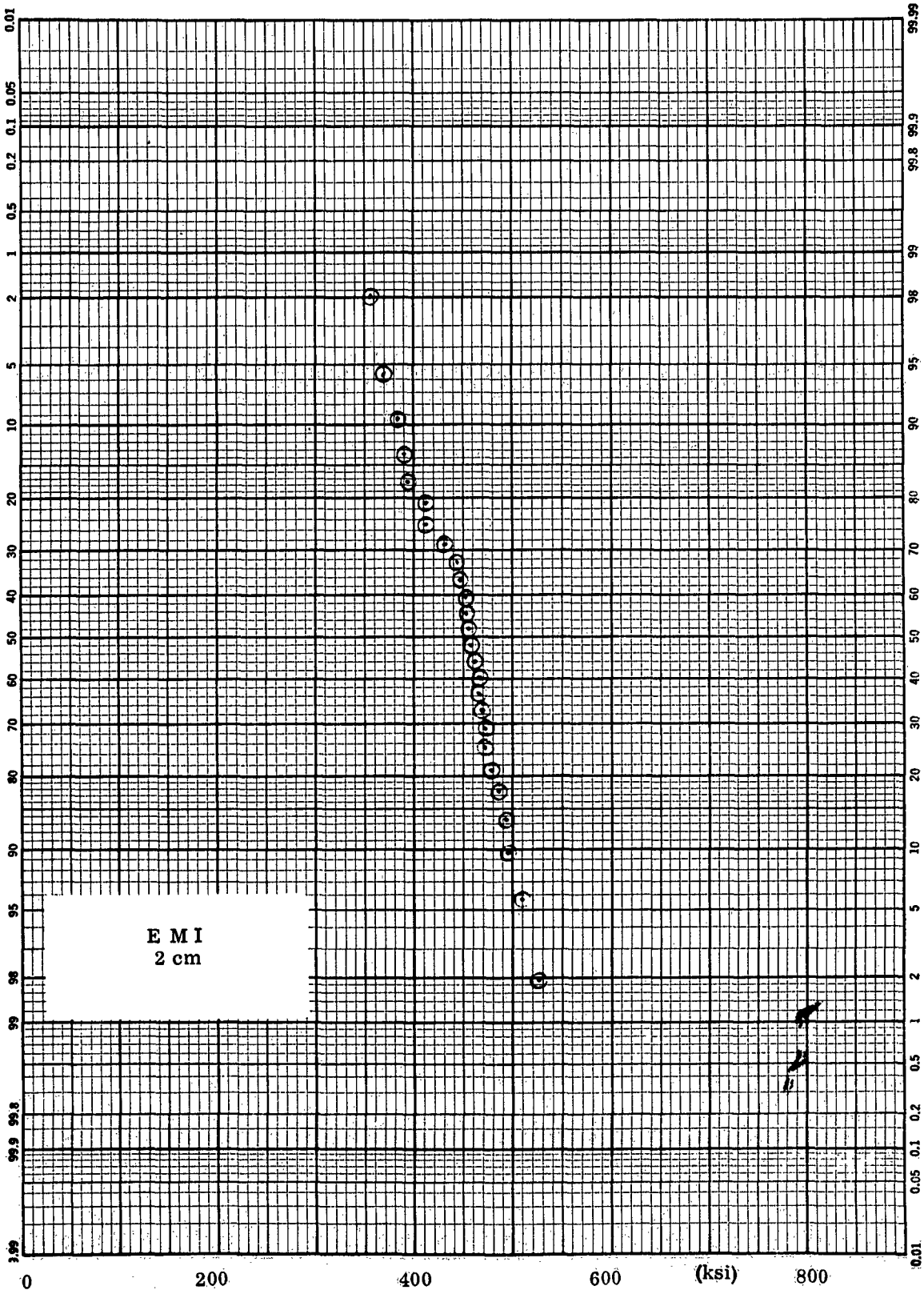
E M I
2 cm
0.01
0.05
0.1
0.2
0.5
1
2
5
10
20
30
40
50
60
70
80
90
95
98
99
99.8
99.9
99.99
0
200
400
600
(ksi)
800

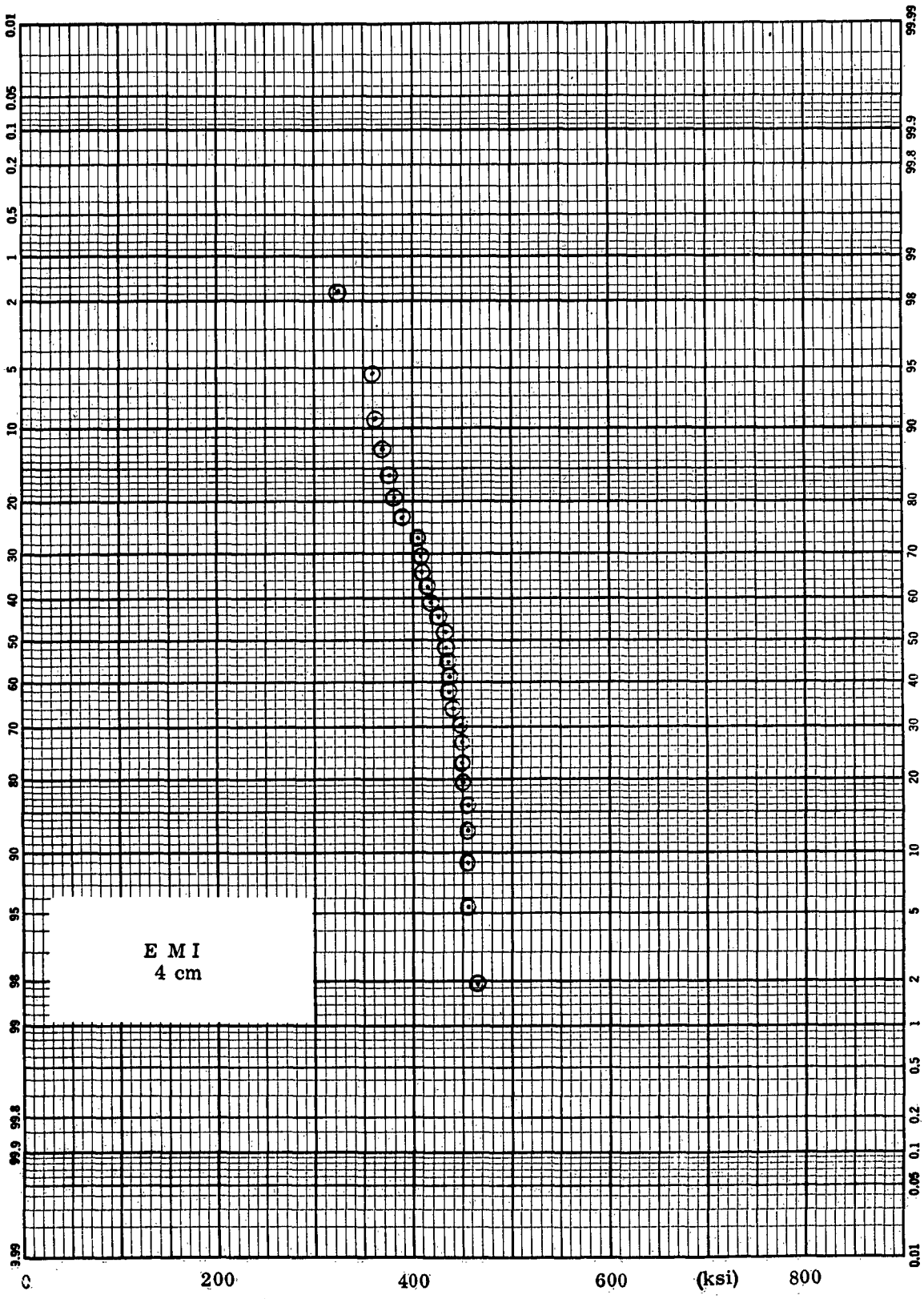
E M I
4 cm
0
200
400
600
(ksi)
800
0.01
0.05
0.1
0.2
0.5
1
2
5
10
20
30
40
50
60
70
80
90
95
98
99
99.8
99.9
99.99

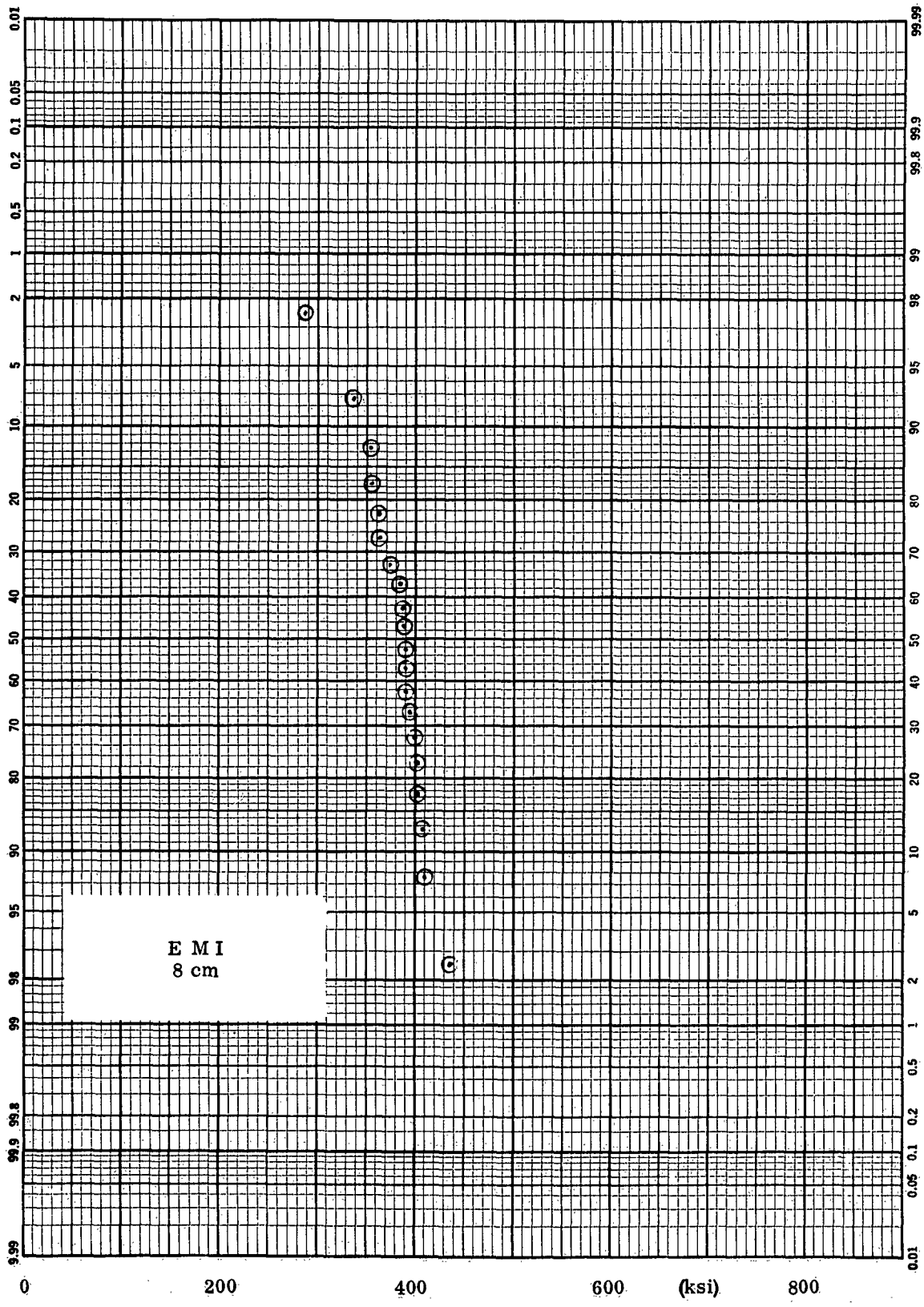
E M I
8 cm
0
200
400
600
(ksi)
800

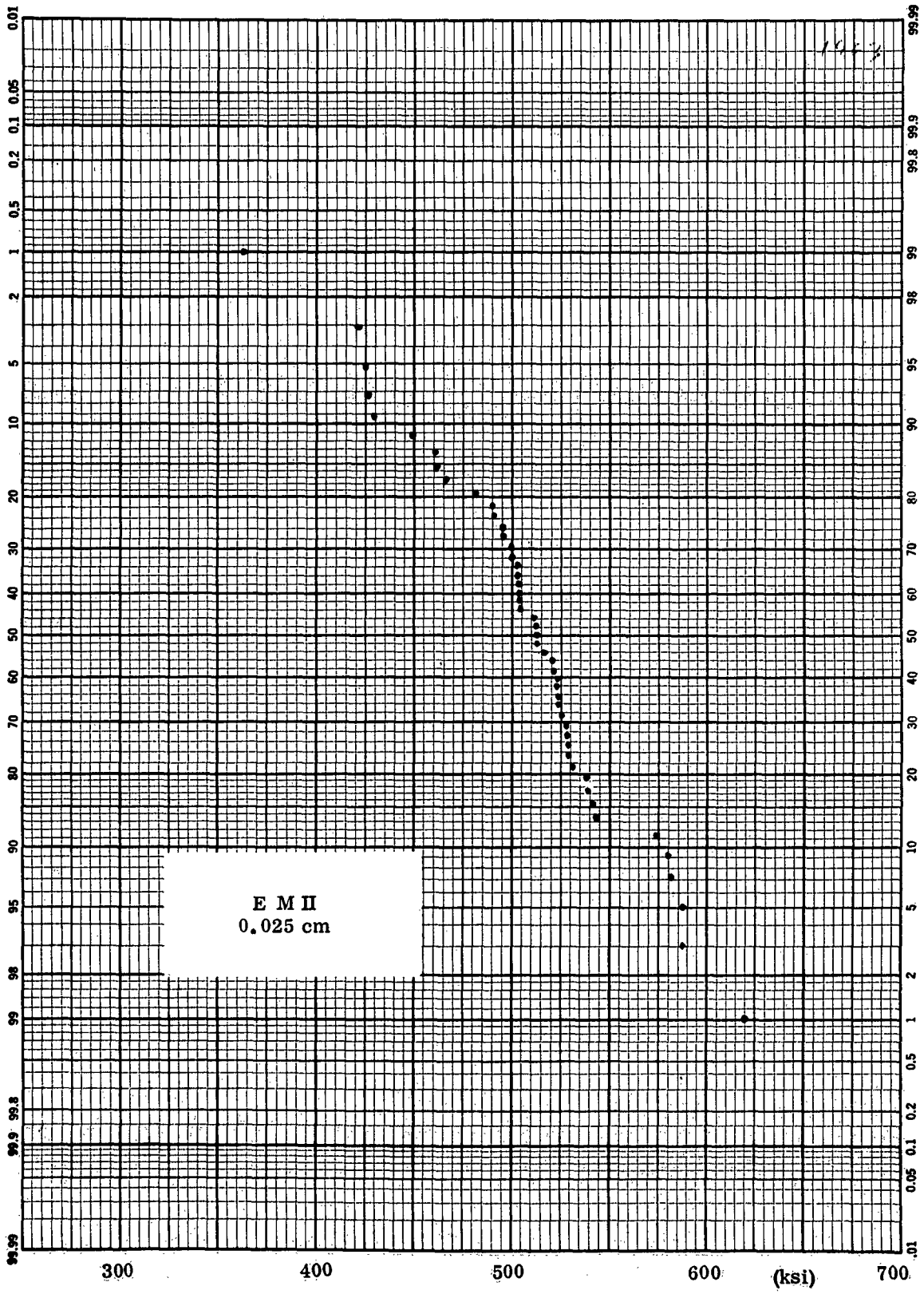
E M II
0.025 cm
0.01
0.05
0.1
0.2
0.5
1
2
5
10
20
30
40
50
60
70
80
90
95
98
99
99.8
99.9
99.99
300
400
500
600
(ksi)
700

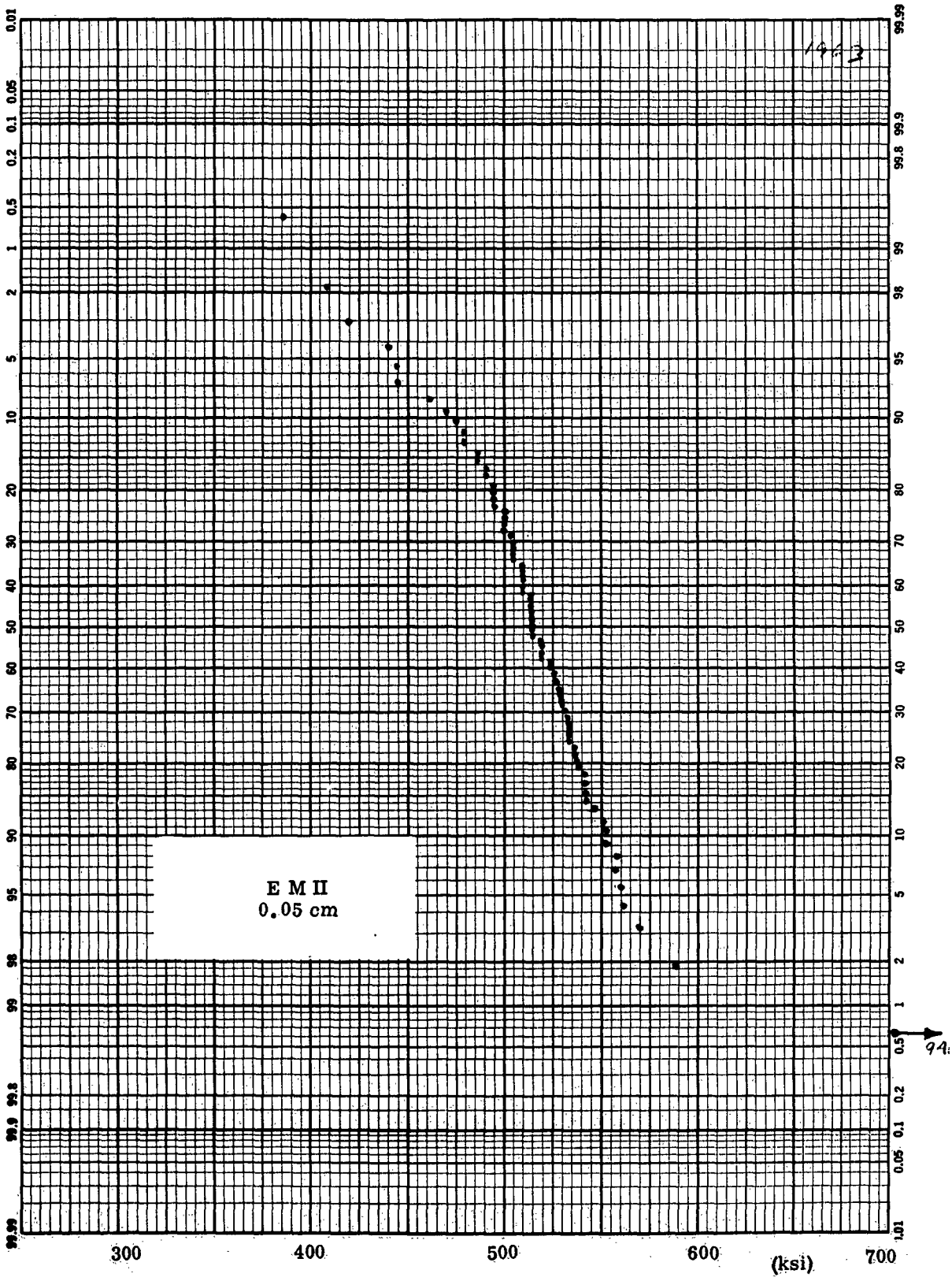
E M II
0.05 cm
300
400
500
600
700
(ksi)
0.01
0.05
0.1
0.2
0.5
1
2
5
10
20
30
40
50
60
70
80
90
95
98
99
99.8
99.9
99.99

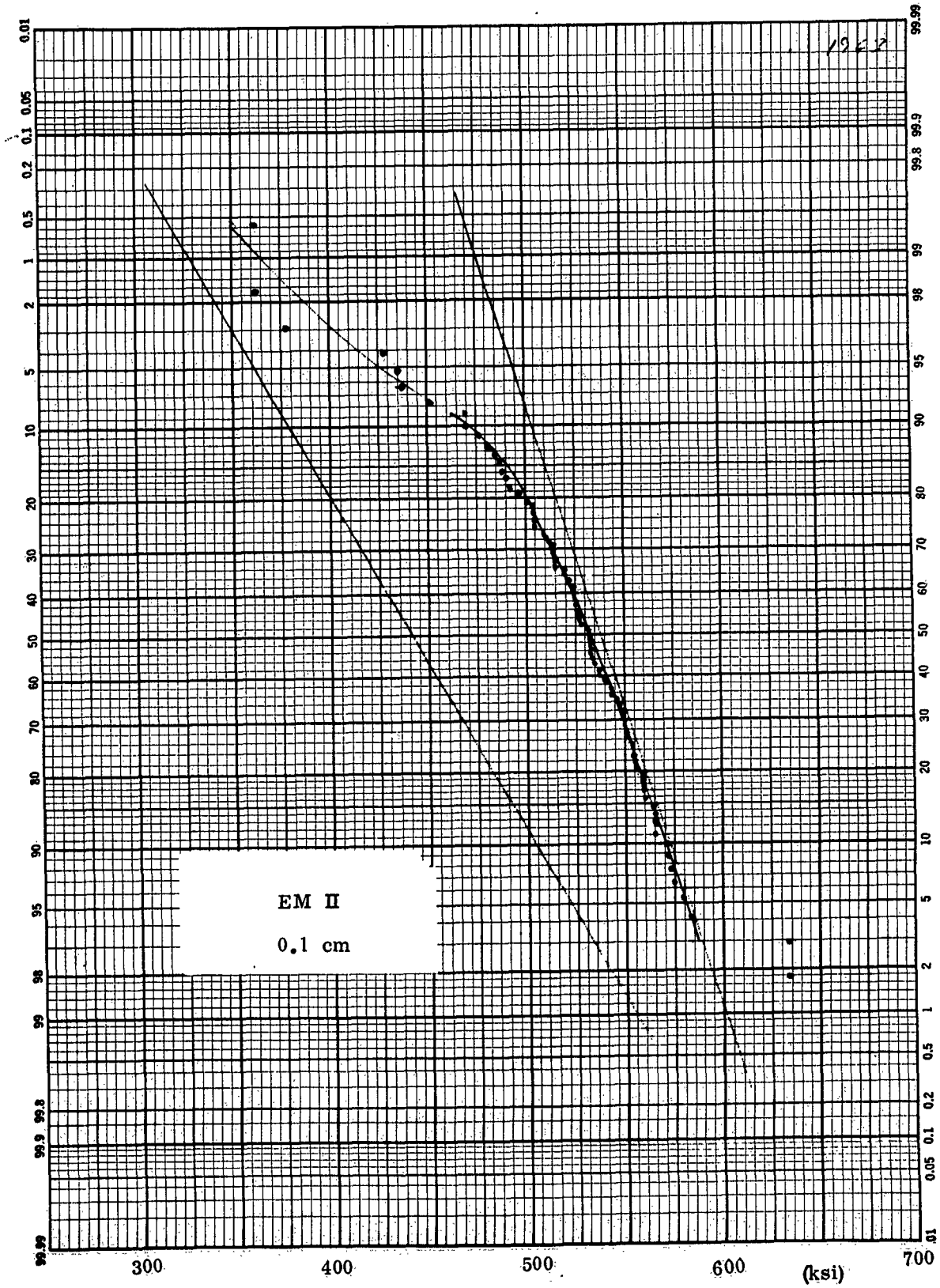
EM II
0.1 cm
300
400
500
600
700
(ksi)

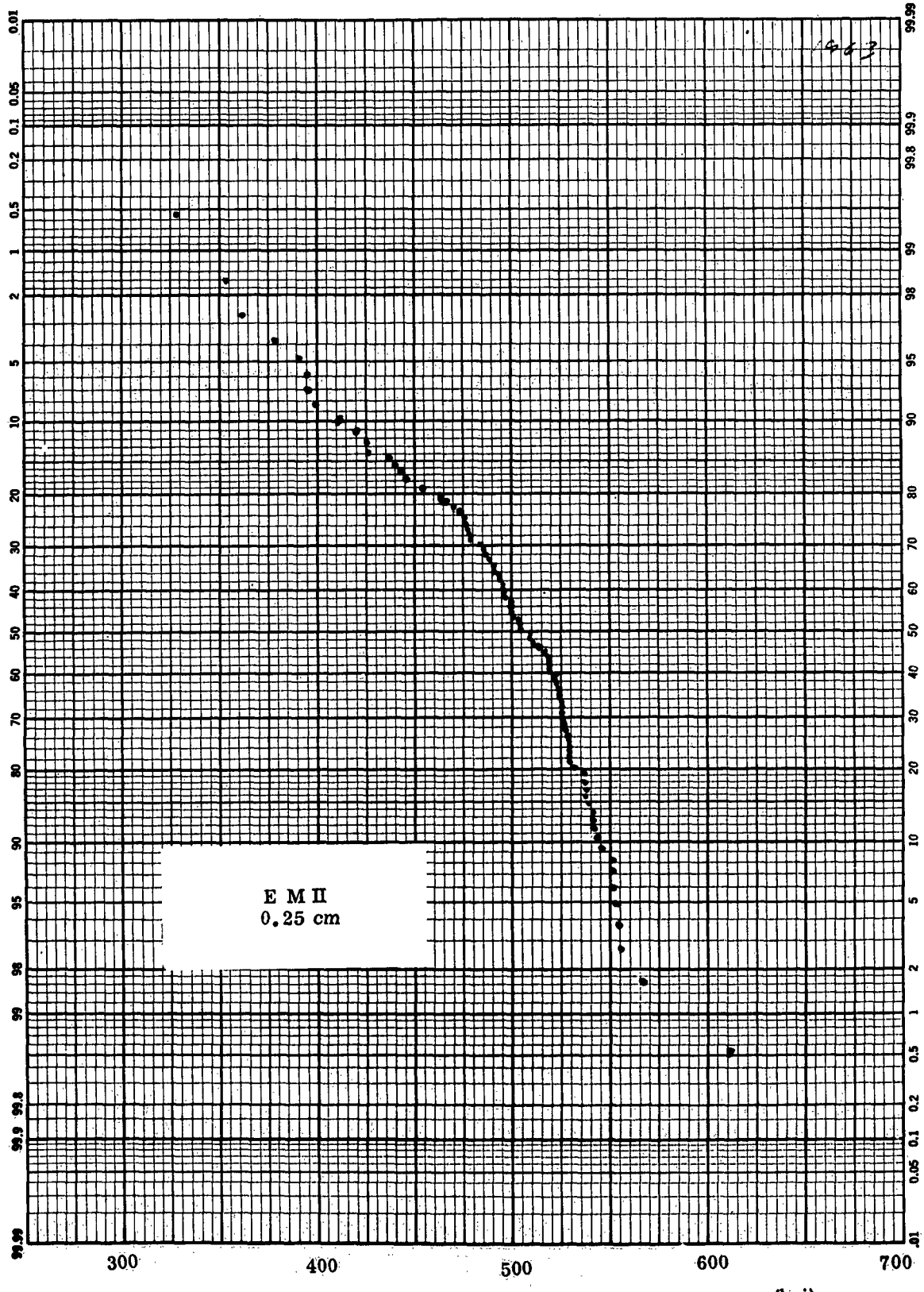
E M II
0.25 cm
300
400
500
600
700
(ksi)

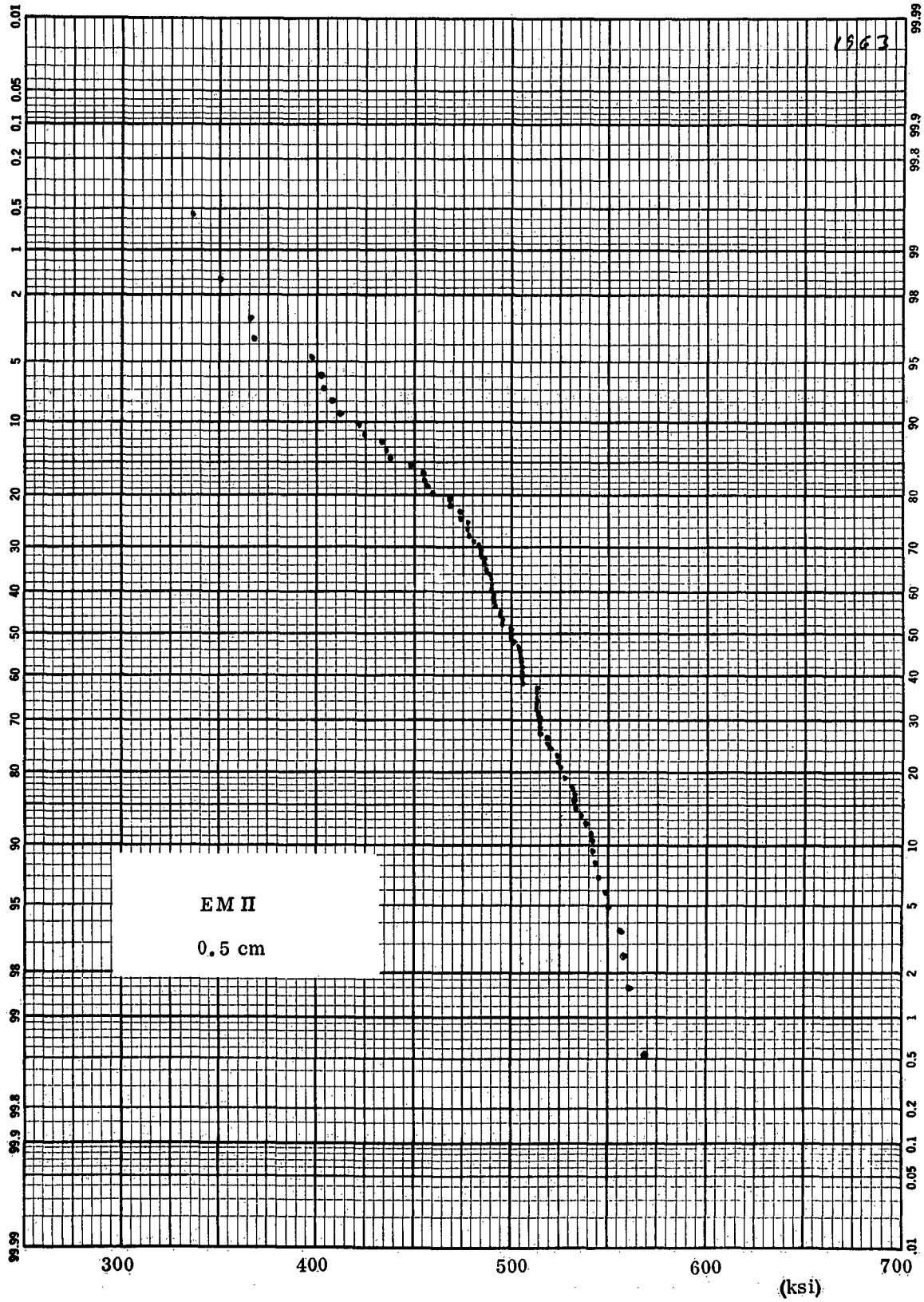
1963
0.01
0.05
0.1
0.2
0.5
1
2
5
10
20
30
40
50
60
70
80
90
95
98
99
99.8
99.9
99.99
ЕМ П
0.5 cm
300
400
500
600
700
(ksi)

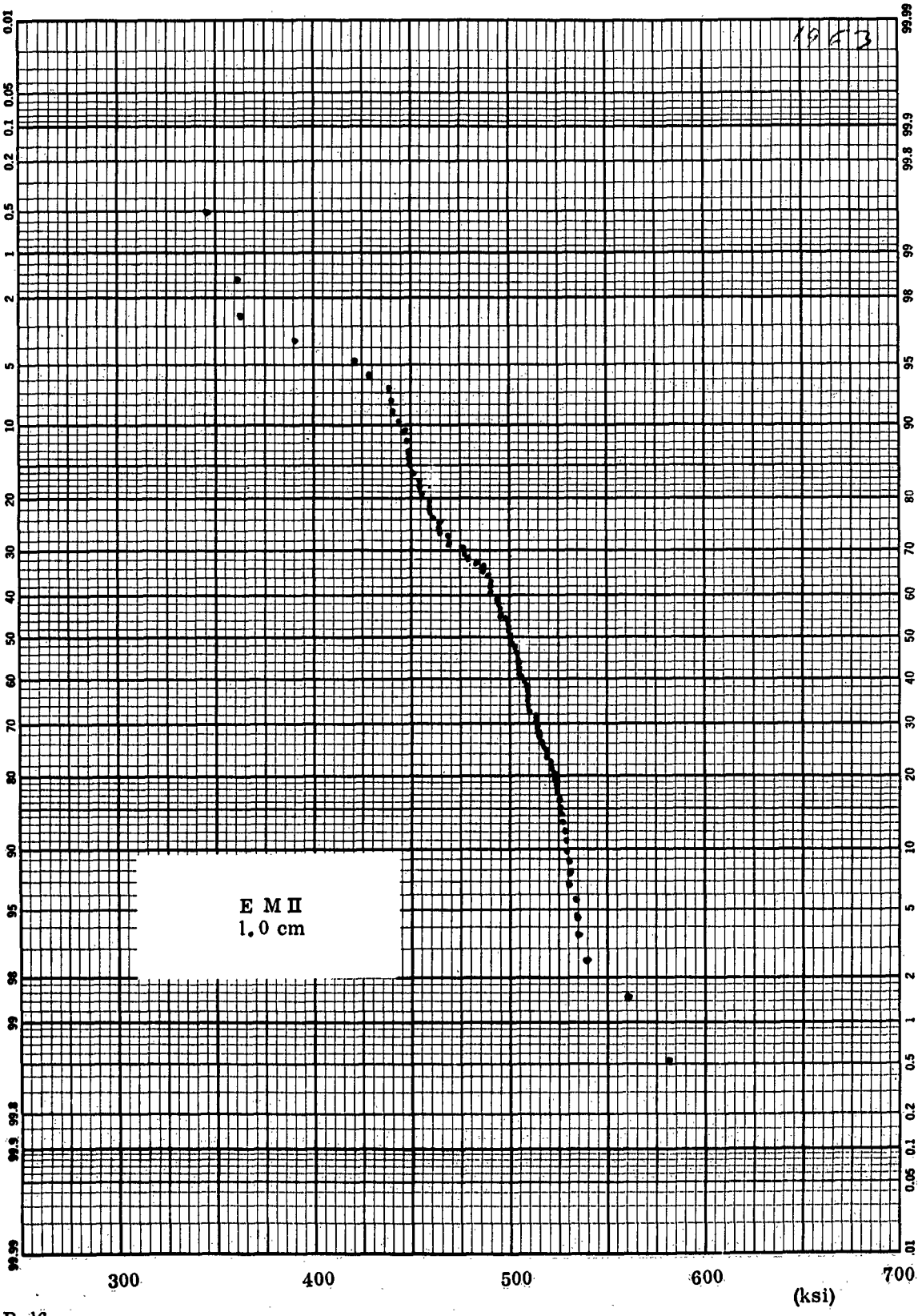
1953
E M II
1.0 cm
0.01
0.05
0.1
0.2
0.5
1
2
5
10
20
30
40
50
60
70
80
90
95
98
99
99.8
99.9
99.99
300
400
500
600
700
(ksi)

B-16

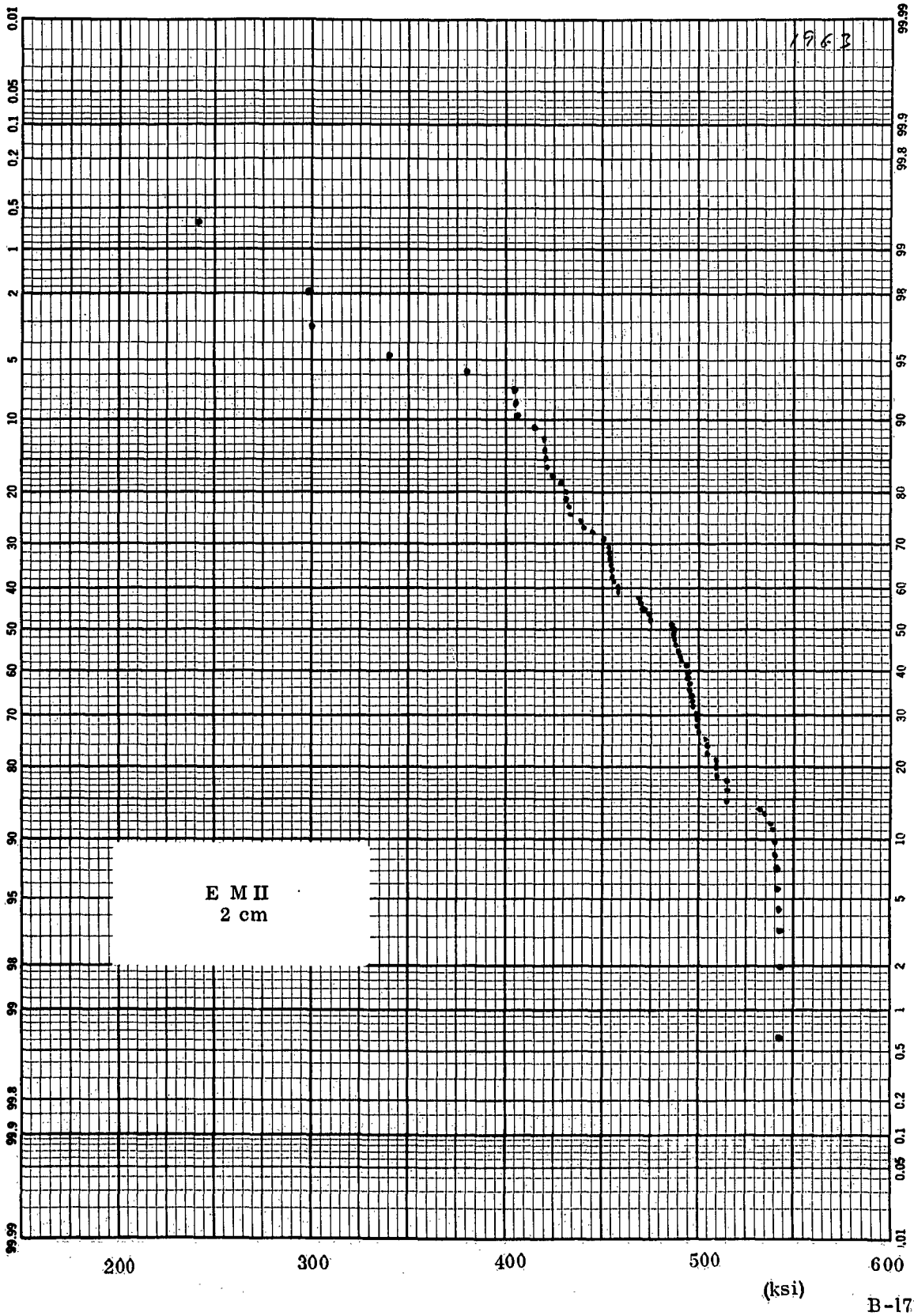
1963
0.01
0.05
0.1
0.2
0.5
1
2
5
10
20
30
40
50
60
70
80
90
95
98
99
99.8
99.9
99.99
E M II
2 cm
200
300
400
500
600
(ksi)

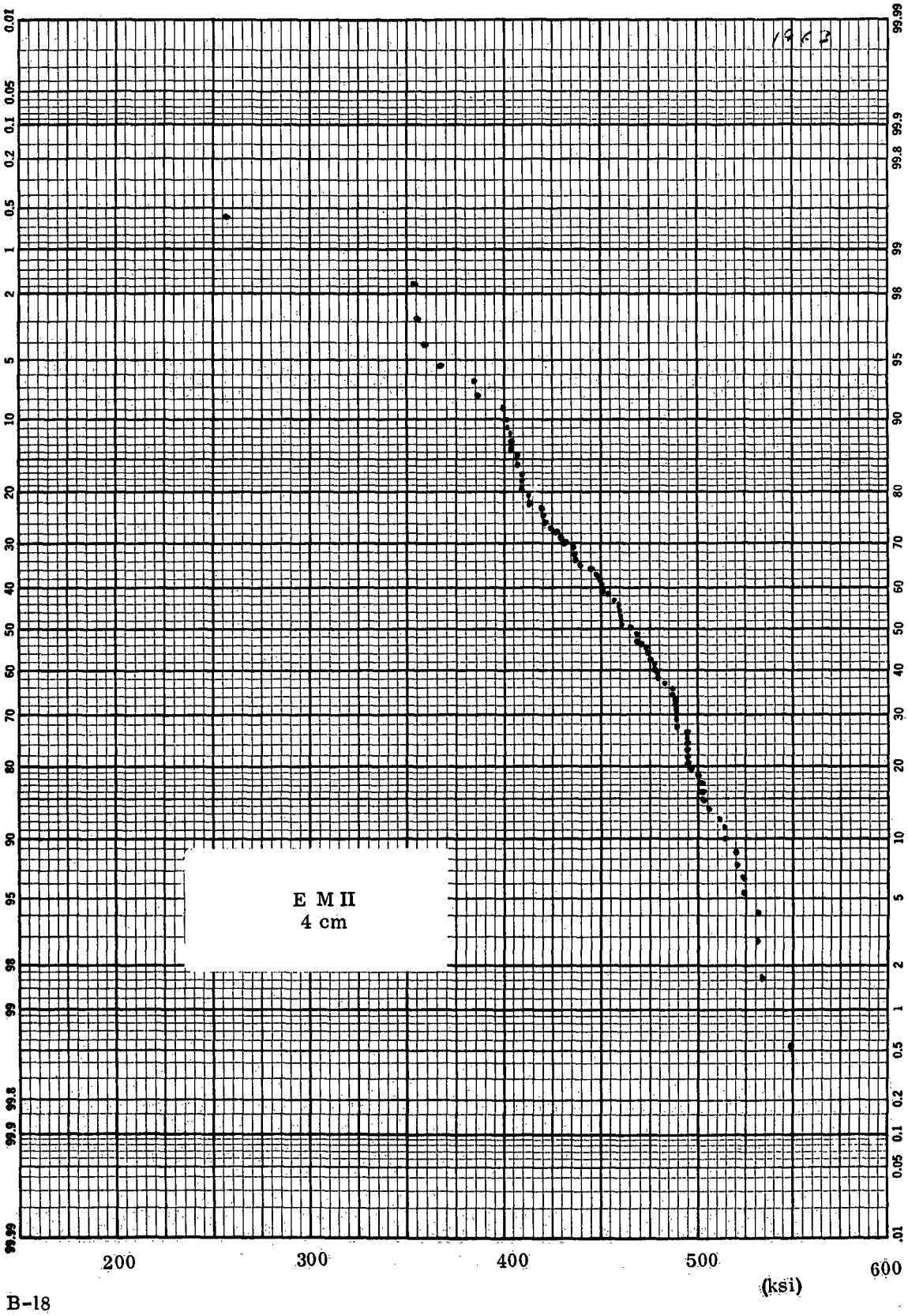
E M II
4 cm
200
300
400
500
600
(ksi)

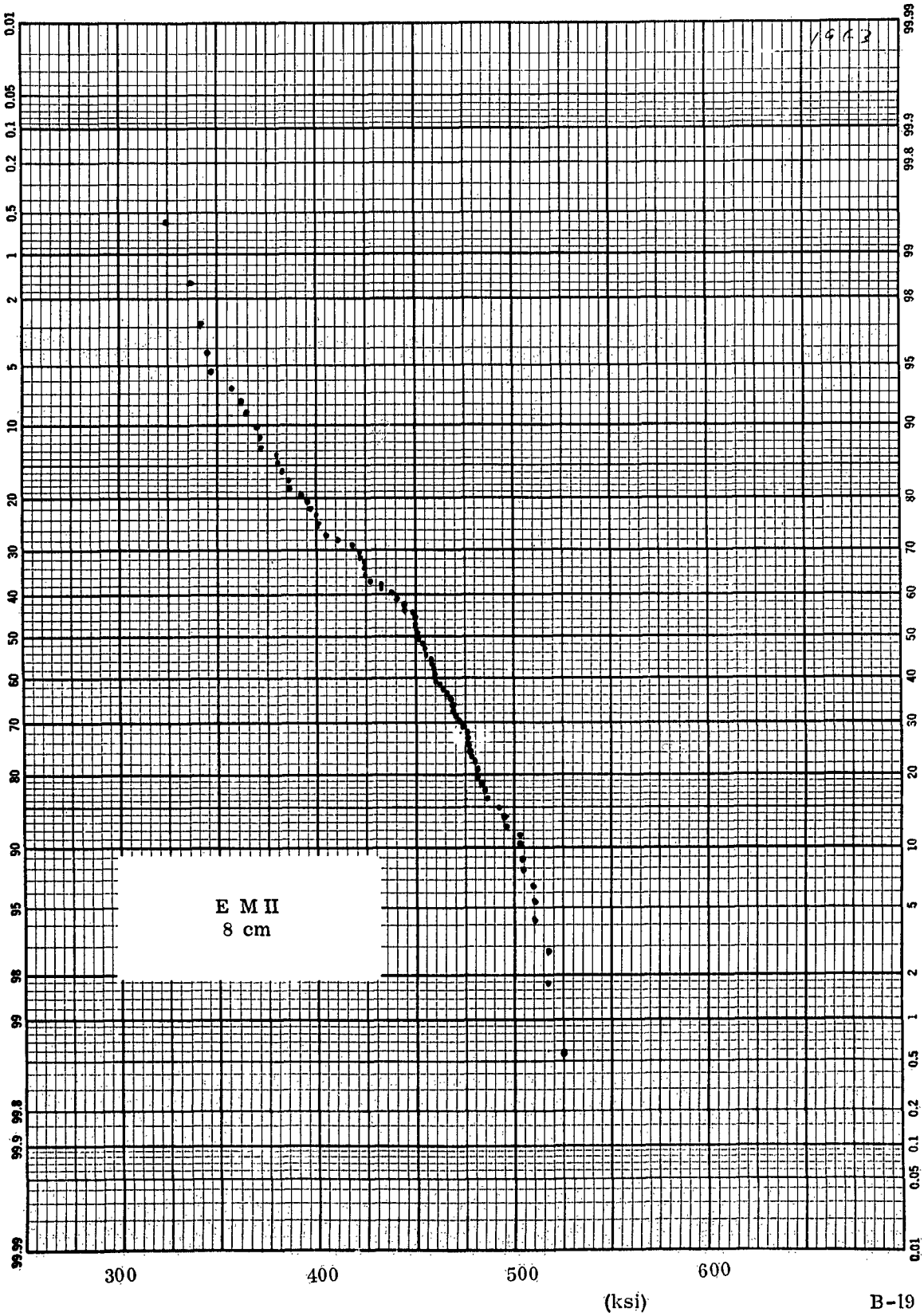
1963
E M II
8 cm
0.01
0.05
0.1
0.2
0.5
1
2
5
10
20
30
40
50
60
70
80
90
95
98
99
99.8
99.9
99.99
300
400
500
600
(ksi)

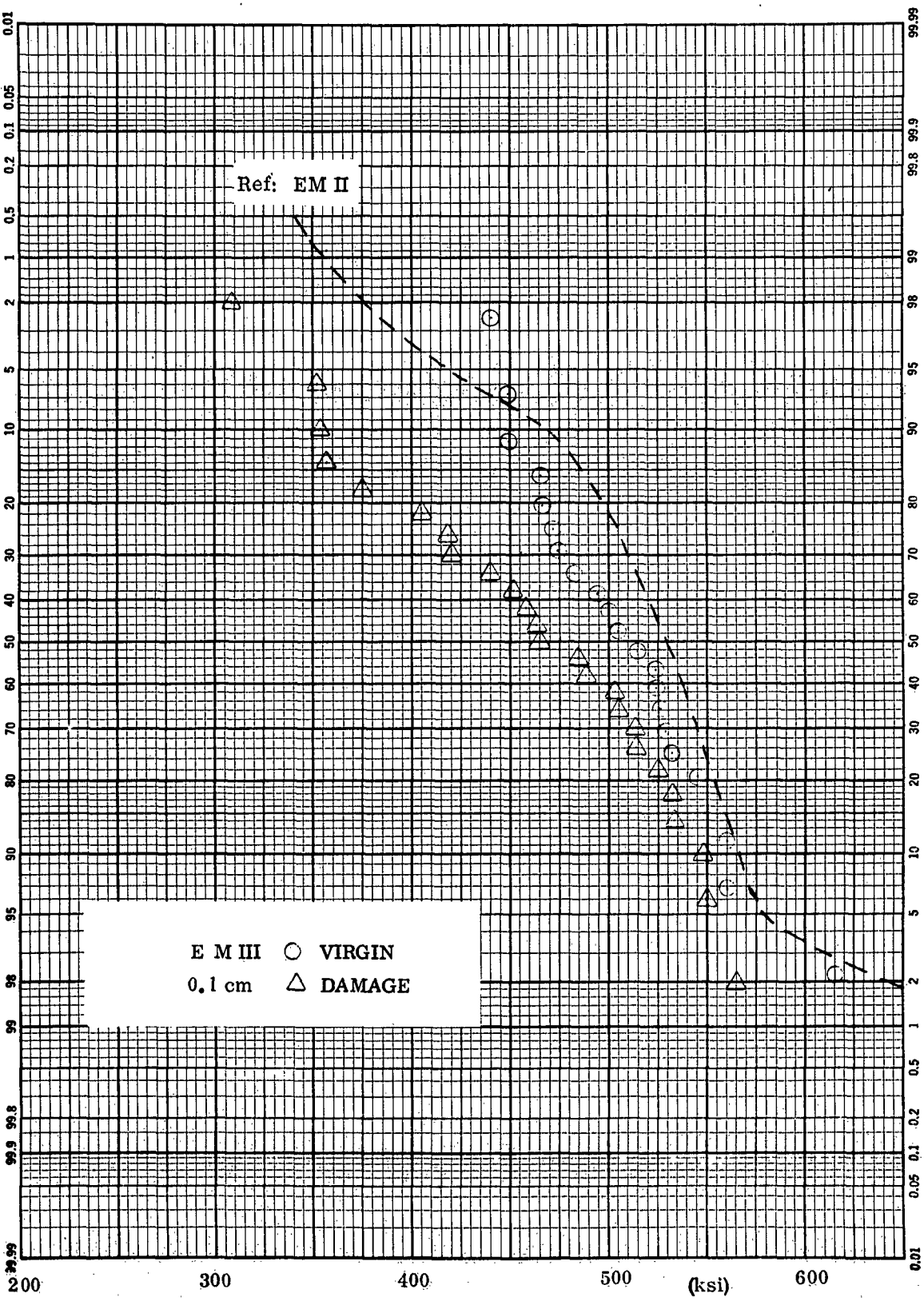
Ref: EM II
E M III ○ VIRGIN
0.1 cm △ DAMAGE
0.01
0.05
0.1
0.2
0.5
1
2
5
10
20
30
40
50
60
70
80
90
95
98
99
99.8
99.9
99.99
200
300
400
500
600
(ksi)

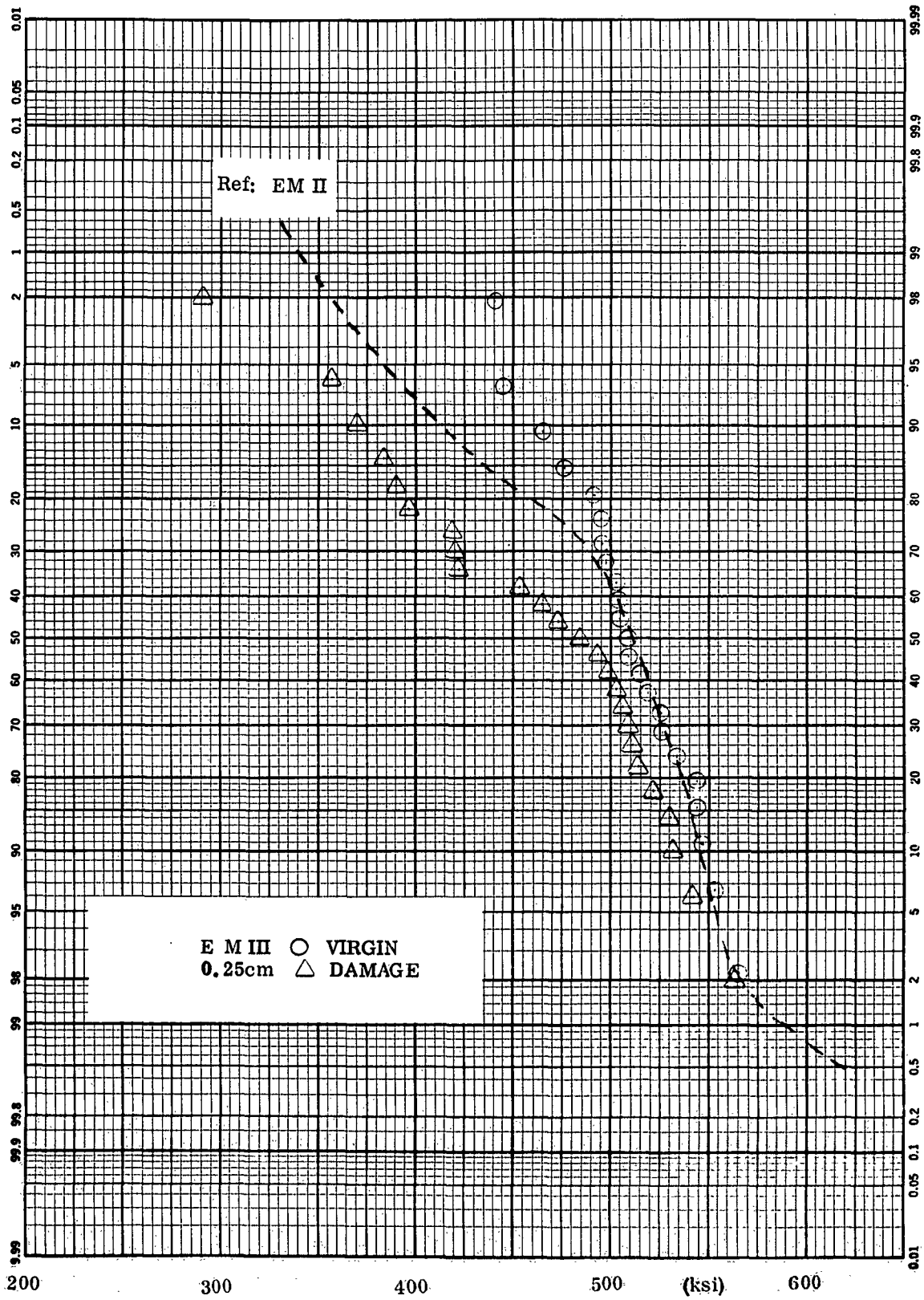
Ref: EM II
E M III ○ VIRGIN
0.25cm △ DAMAGE
0.01
0.05
0.1
0.2
0.5
1
2
5
10
20
30
40
50
60
70
80
90
95
98
99
99.8
99.9
99.99
200
300
400
500
(ksi)
600

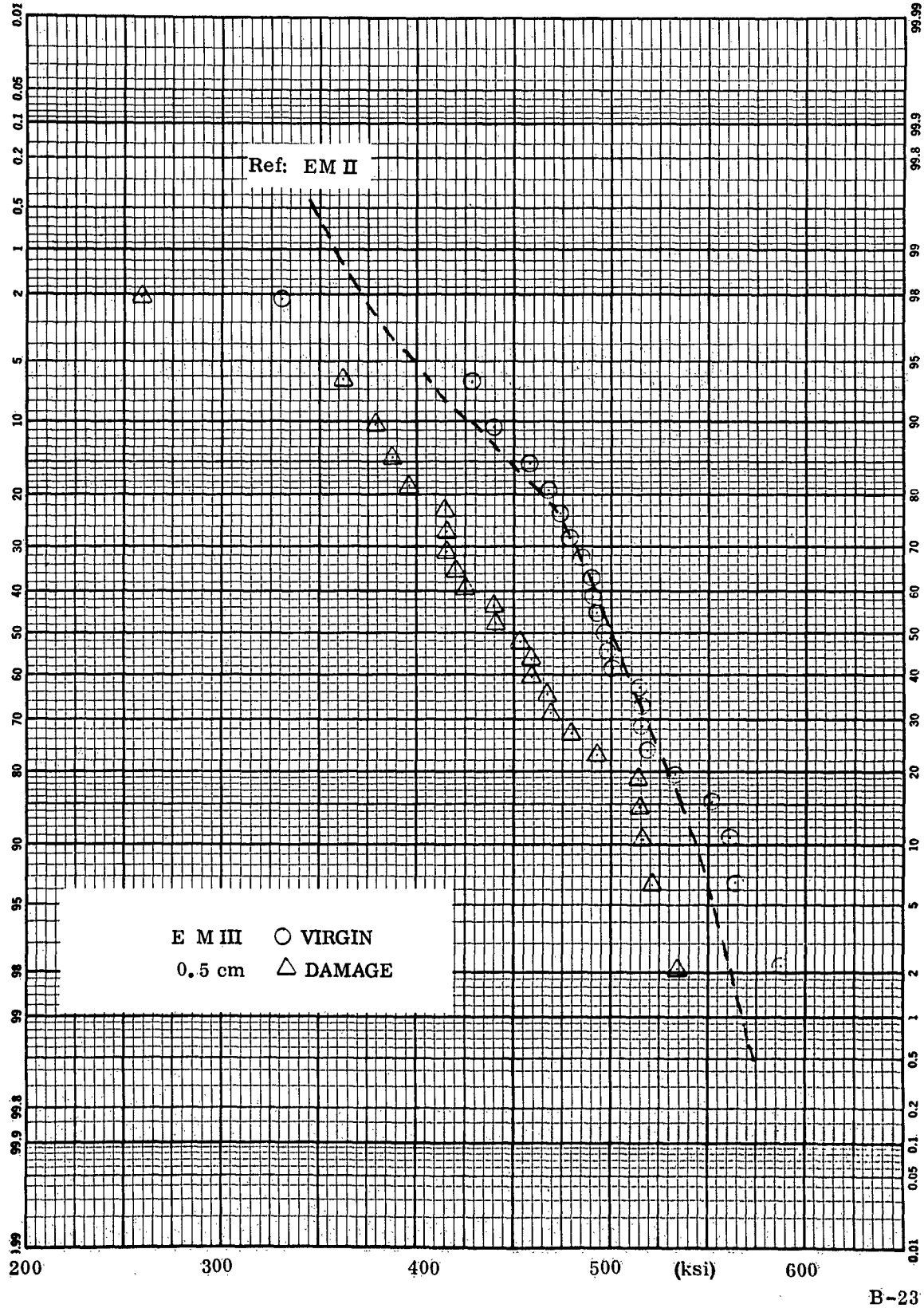
Ref: EM II
E M III
0.5 cm
VIRGIN
DAMAGE
200
300
400
500
(ksi)
600

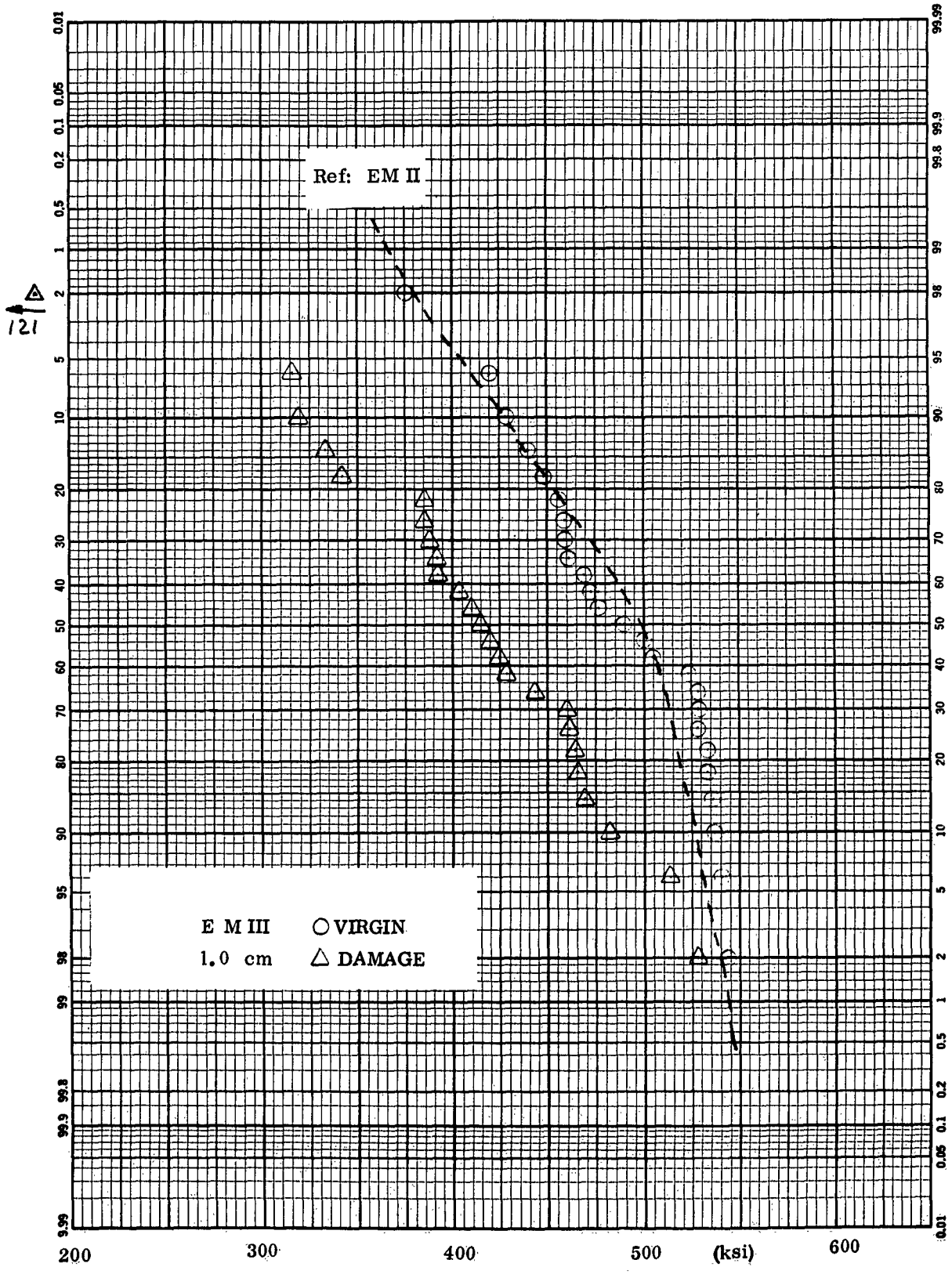
Ref: EM II
121
E M III
1.0 cm
○ VIRGIN
△ DAMAGE
200
300
400
500
(ksi)
600
0.01
0.05
0.1
0.2
0.5
1
2
5
10
20
30
40
50
60
70
80
90
95
98
99
99.8
99.9
99.99

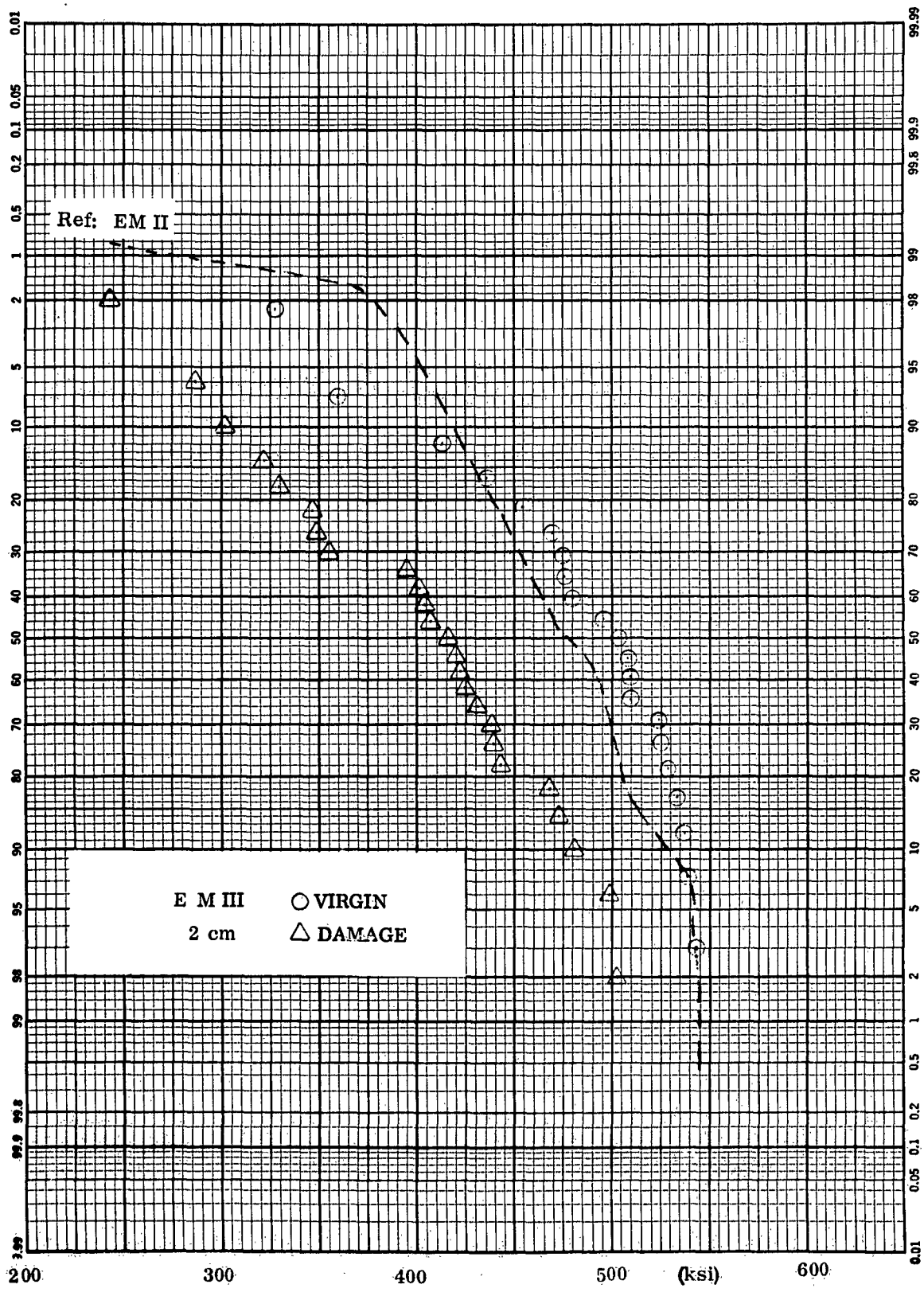
Ref: EM II
E M III
2 cm
VIRGIN
DAMAGE
200
300
400
500
(ksi)
600

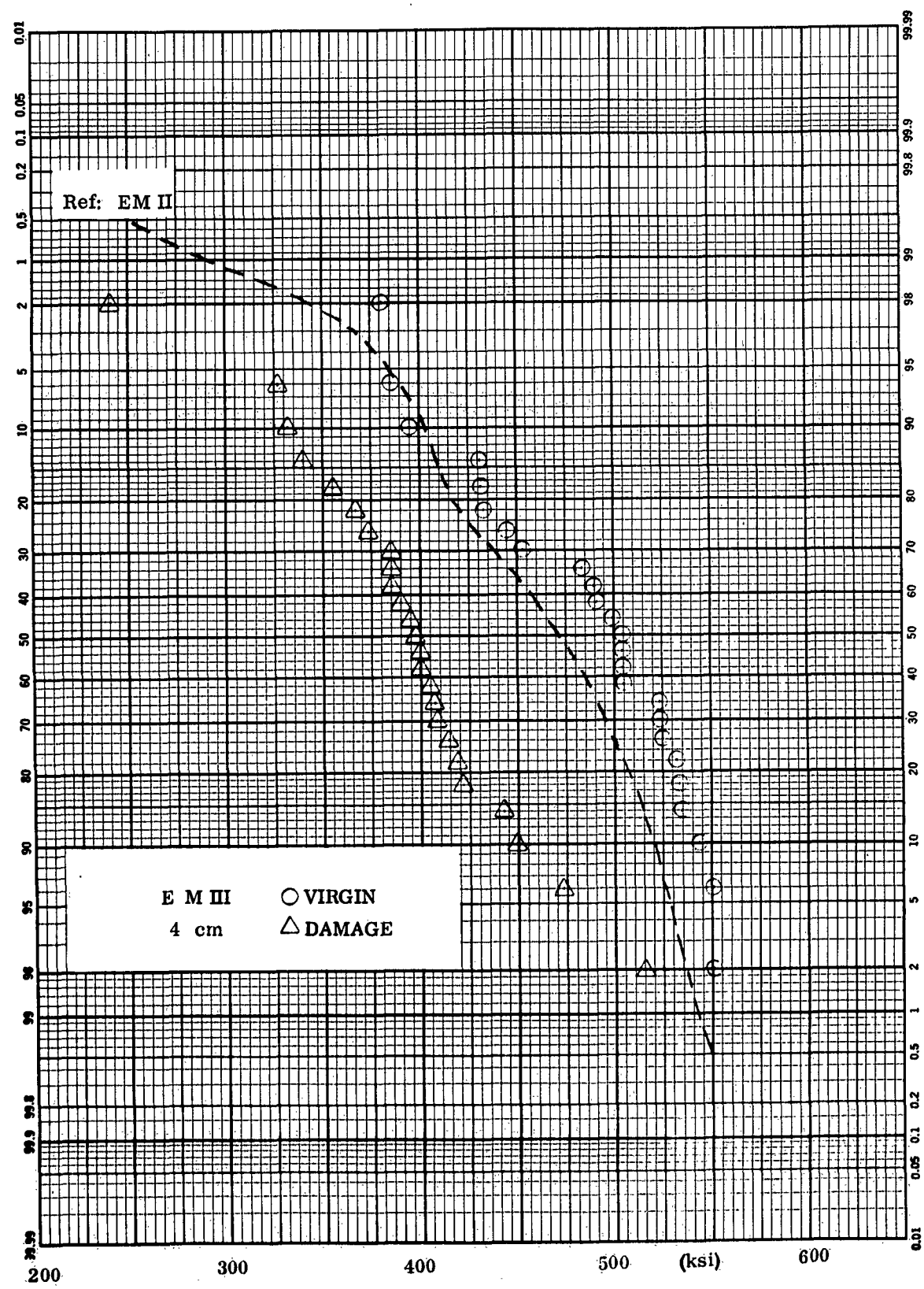
Ref: EM II
E M III
4 cm
VIRGIN
DAMAGE
200
300
400
500
600
(ksi)
0.01
0.05
0.1
0.2
0.5
1
2
5
10
20
30
40
50
60
70
80
90
95
98
99
99.8
99.9
99.99

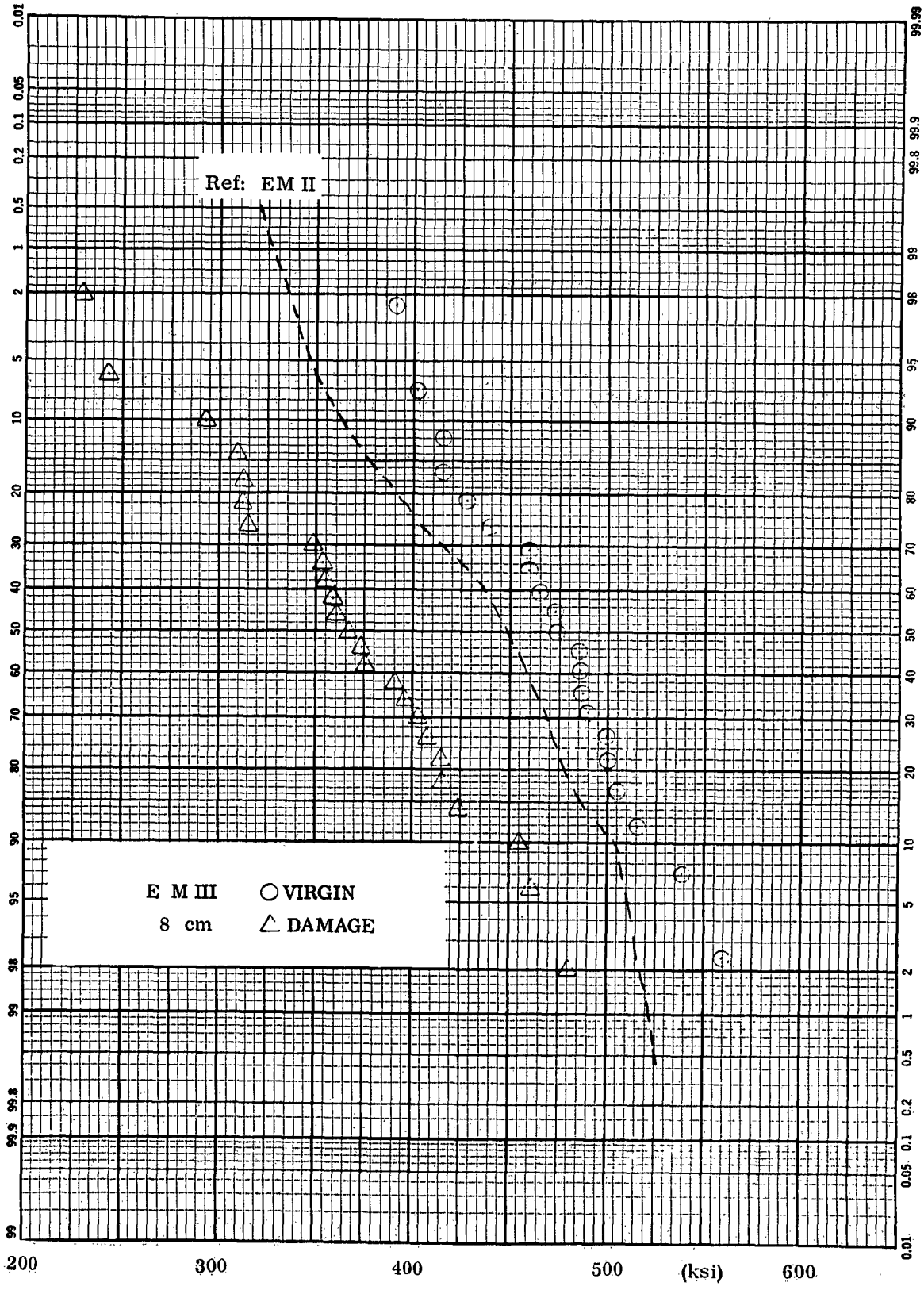
Ref: EM II
E M III
8 cm
VIRGIN
DAMAGE
200
300
400
500
(ksi)
600
0.01
0.05
0.1
0.2
0.5
1
2
5
10
20
30
40
50
60
70
80
90
95
98
99
99.8
99.9
99.99

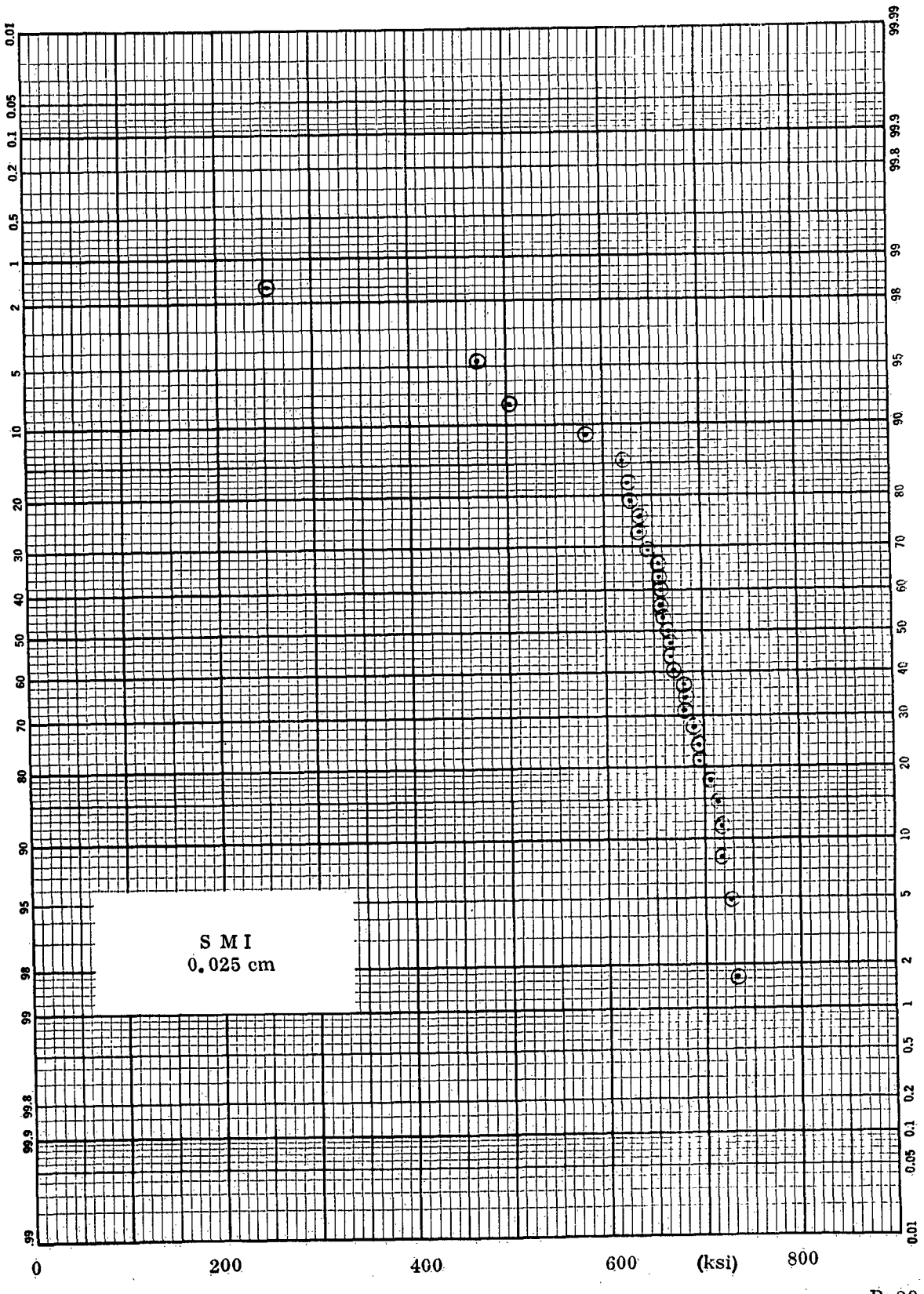
S M I
0.025 cm
0
200
400
600
(ksi)
800

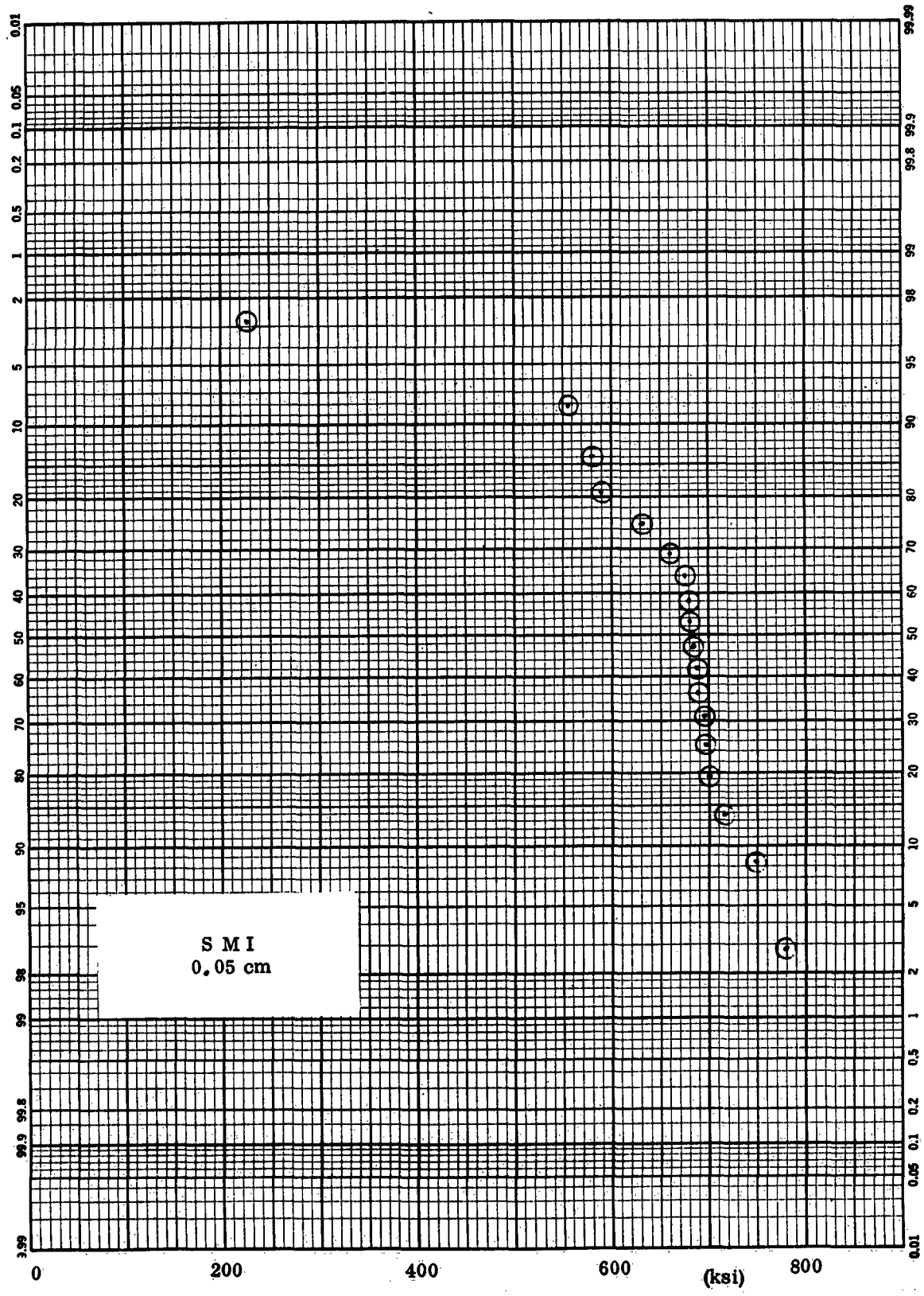
S M I
0.05 cm
0
200
400
600
800
(ksi)

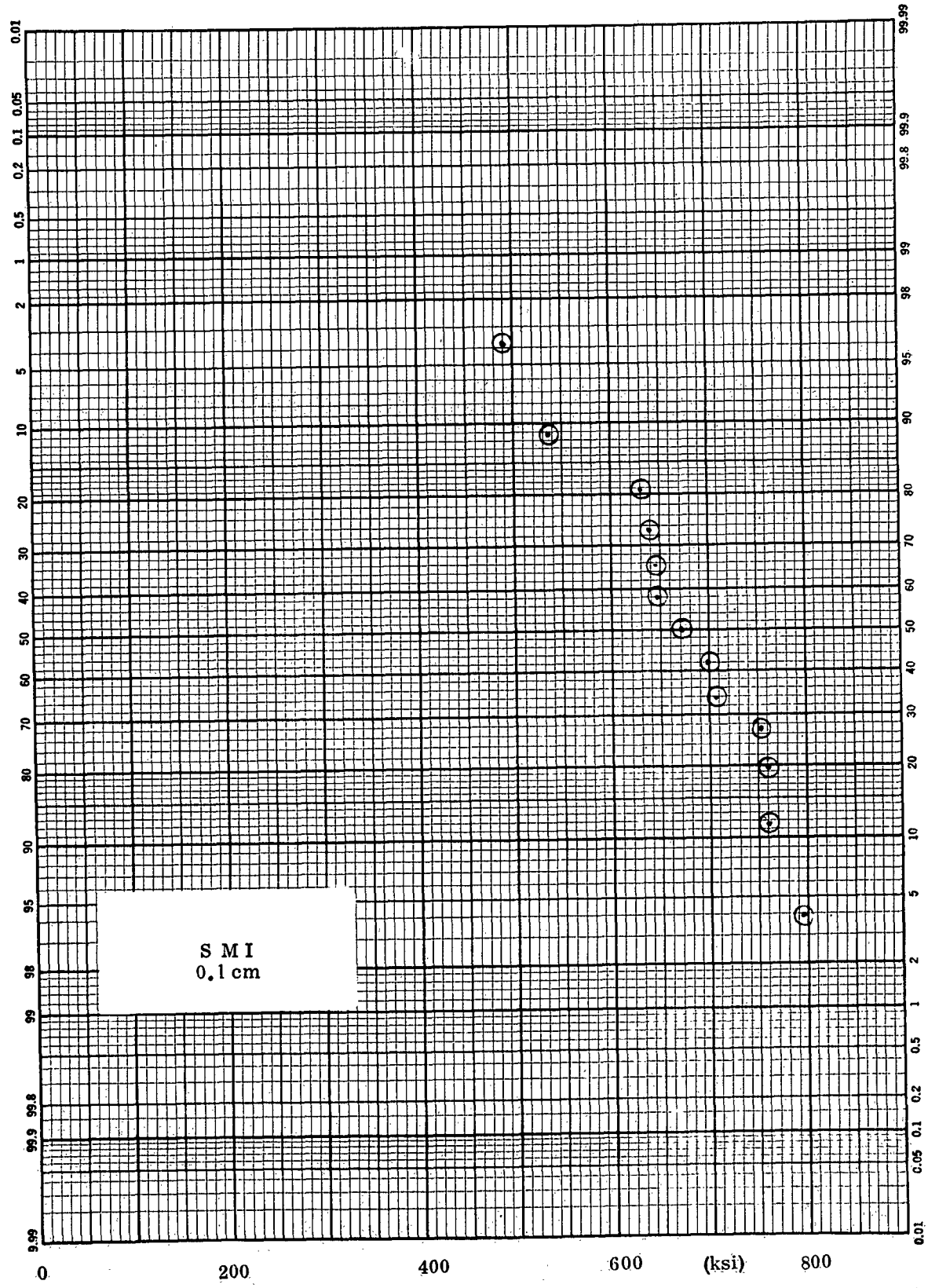
S M I
0.1 cm
0
200
400
600
(ksi)
800

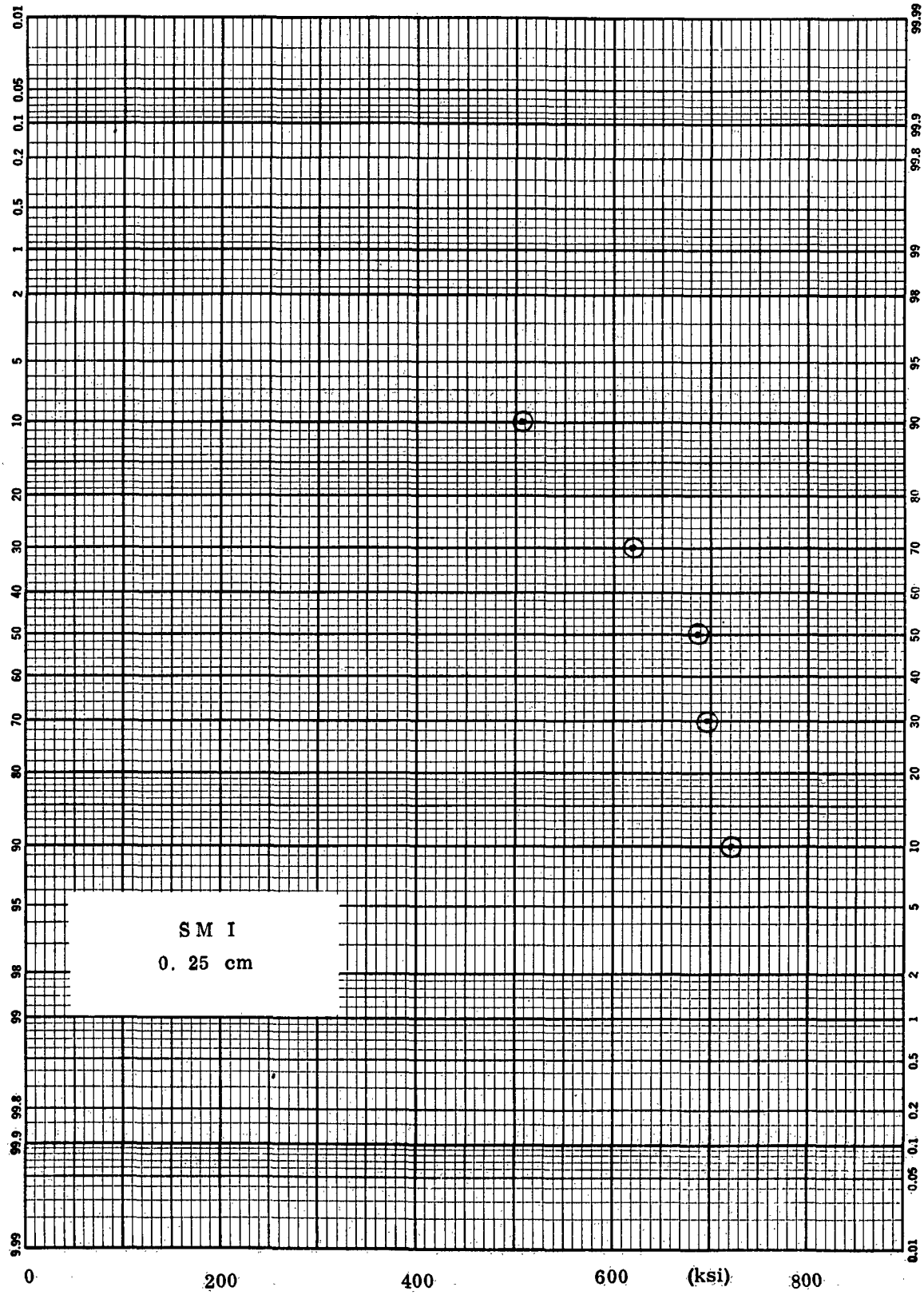
0.01
0.05
0.1
0.2
0.5
1
2
5
10
20
30
40
50
60
70
80
90
95
98
99
99.8
99.9
99.99
SM I
0. 25 cm
0
200
400
600
(ksi)
800

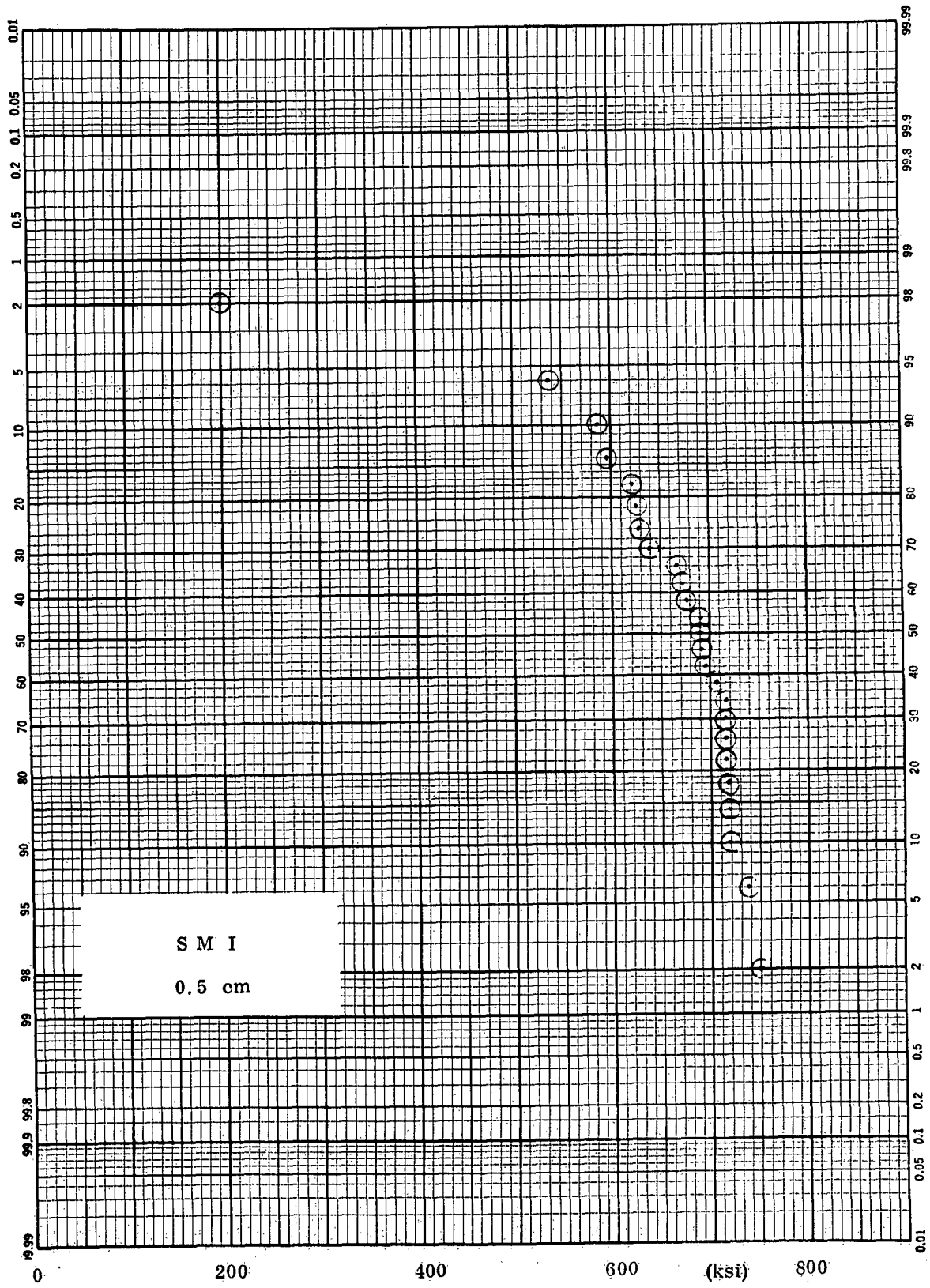
0.01
0.05
0.1
0.2
0.5
1
2
5
10
20
30
40
50
60
70
80
90
95
98
99
99.8
99.9
99.99
S M I
0.5 cm
0
200
400
600
(ksi)
800

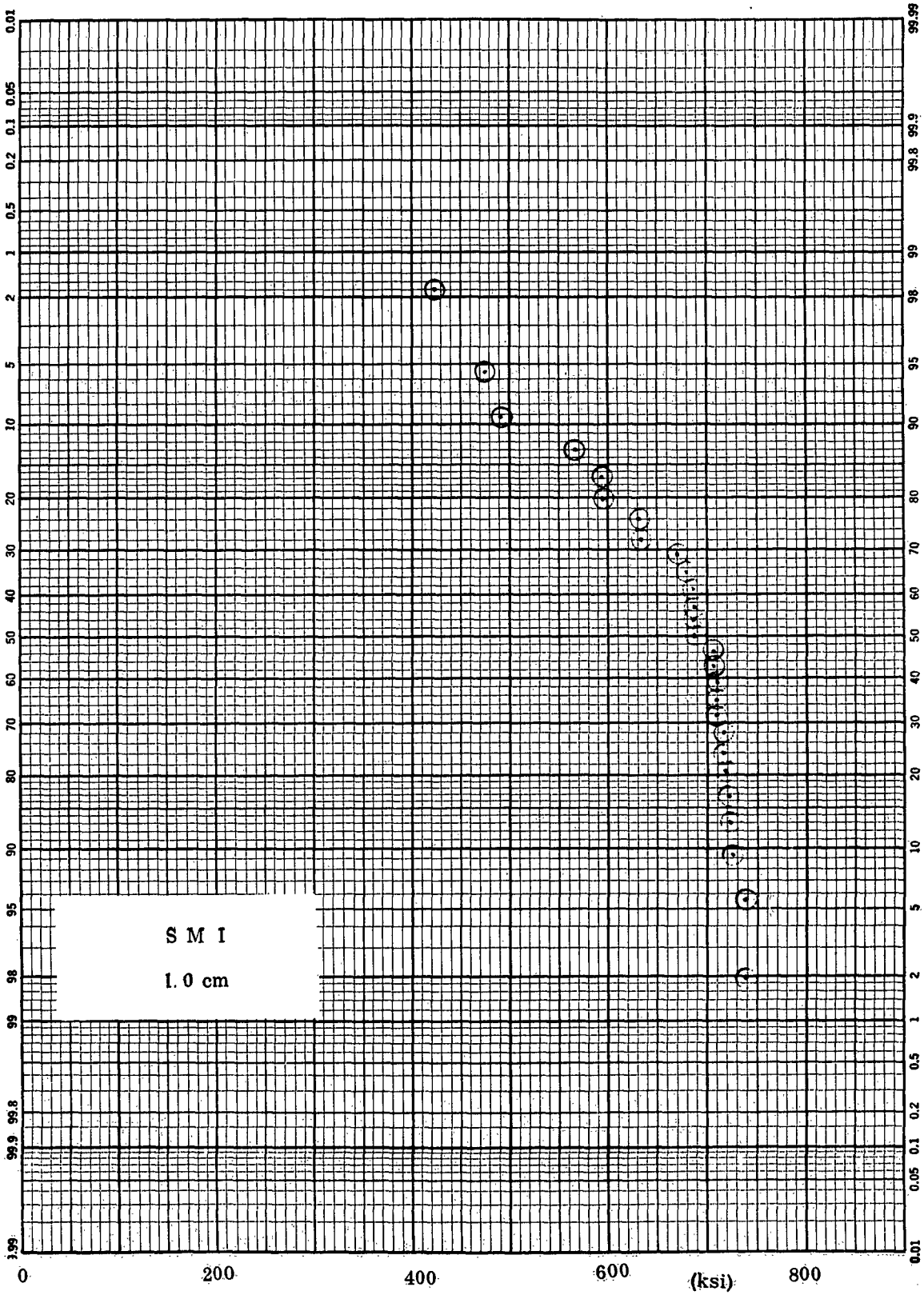
S M I
1.0 cm
0.01
0.05
0.1
0.2
0.5
1
2
5
10
20
30
40
50
60
70
80
90
95
98
99
99.8
99.9
99.99
0
200
400
600
800
(ksi)

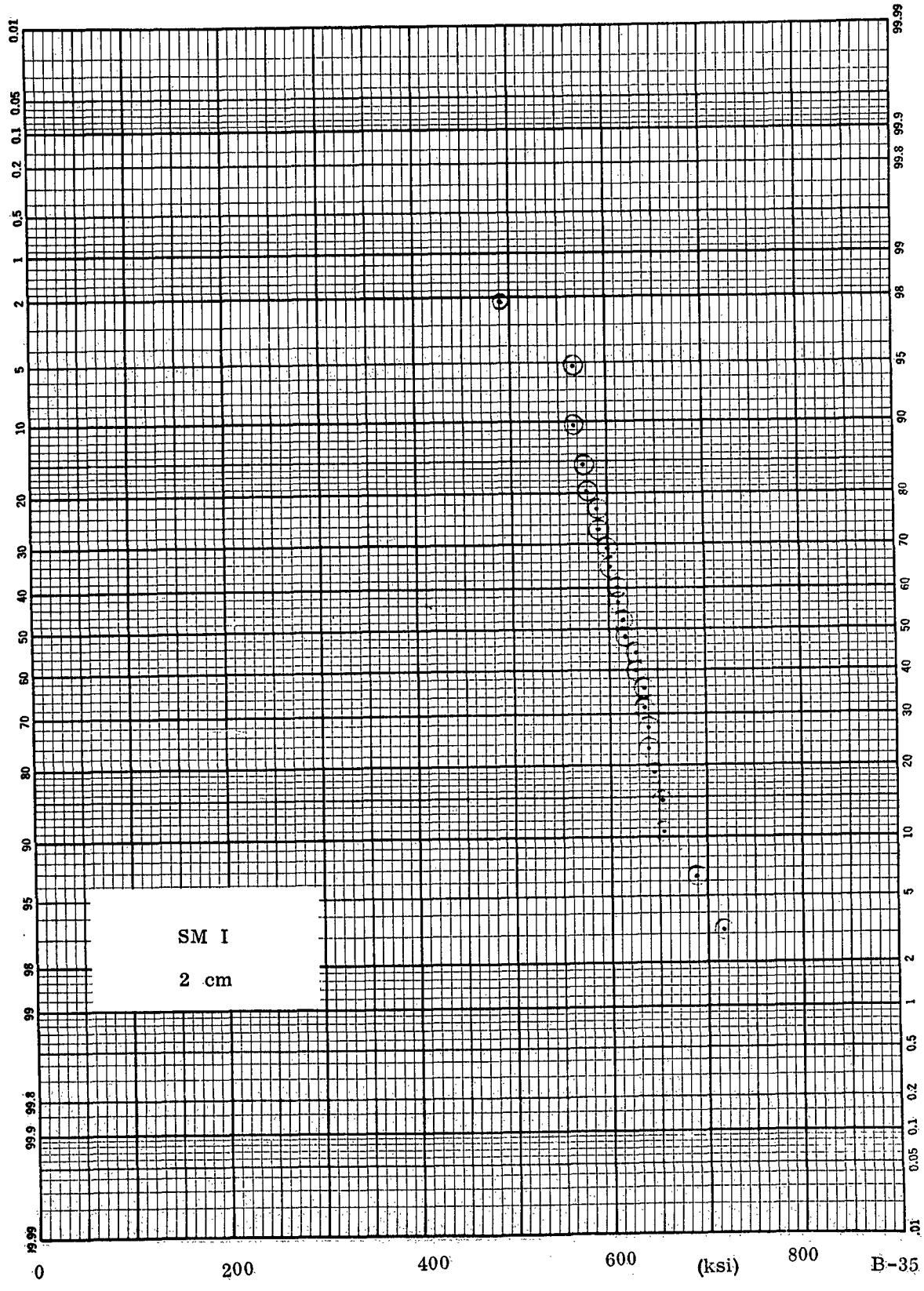
SM I
2 cm
0
200
400
600
(ksi)
800
B-35

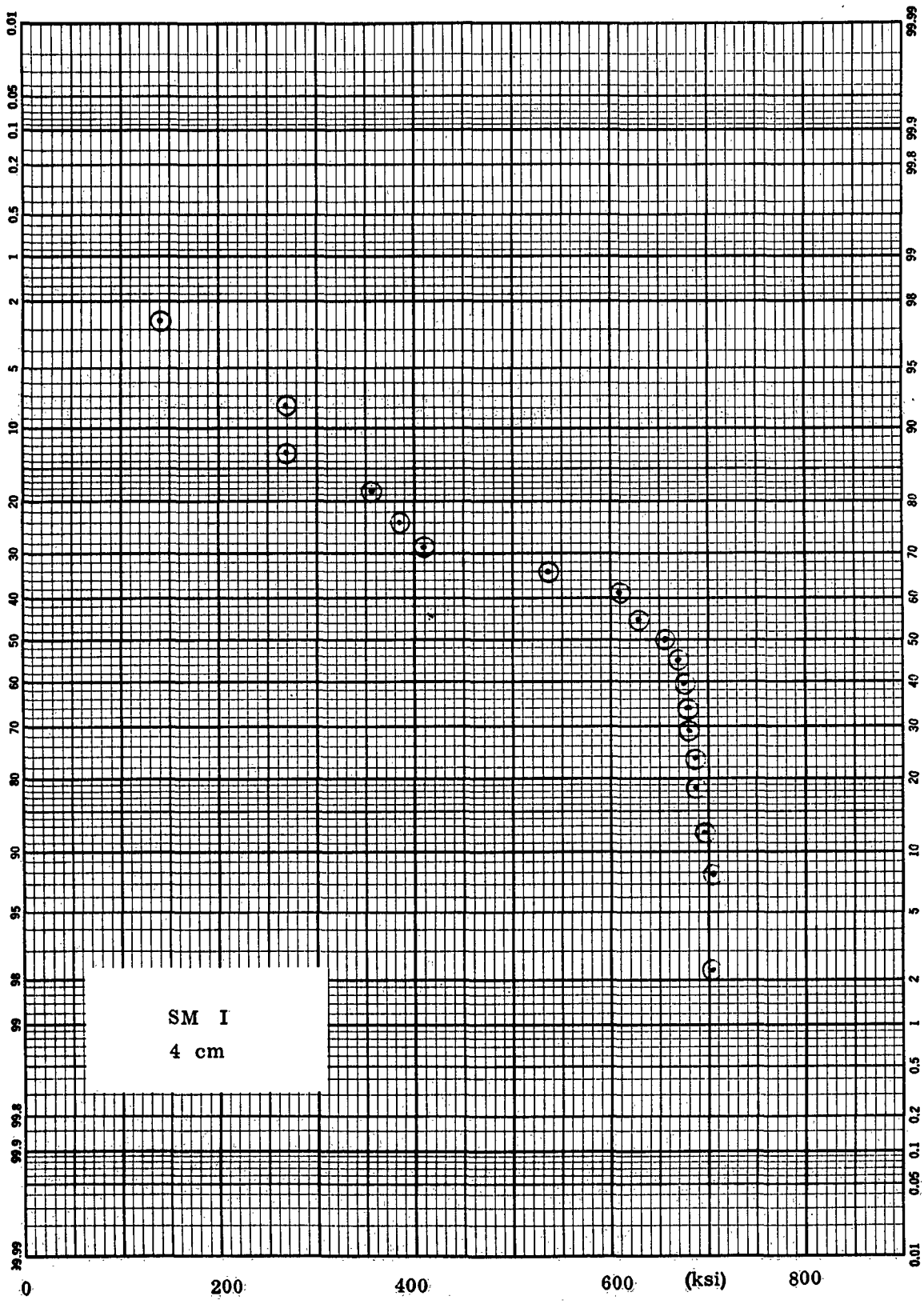
SM I
4 cm
0
200
400
600
(ksi)
800

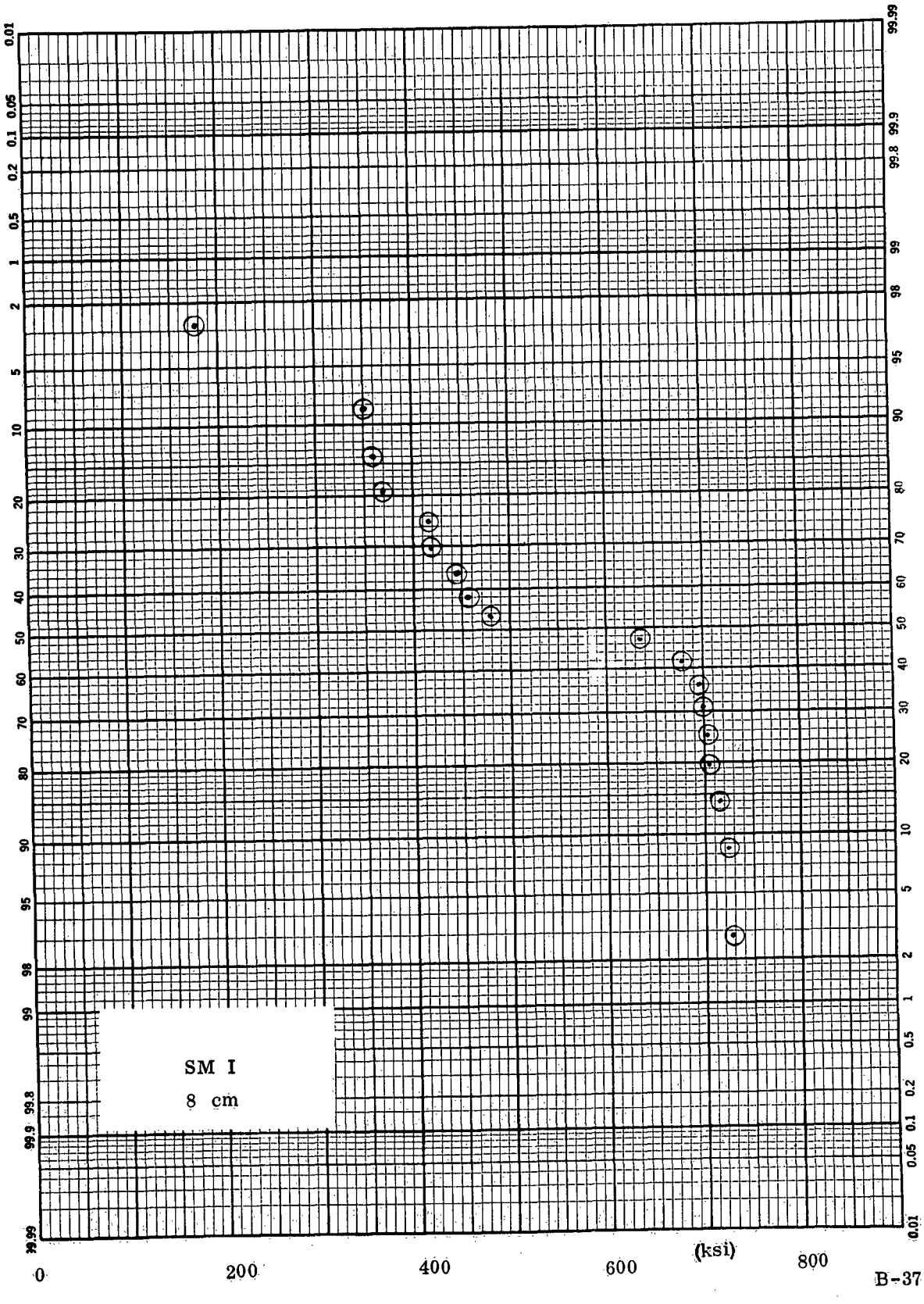
SM I
8 cm
0
200
400
600
800
(ksi)
0.01
0.05
0.1
0.2
0.5
1
2
5
10
20
30
40
50
60
70
80
90
95
98
99
99.8
99.9
99.99

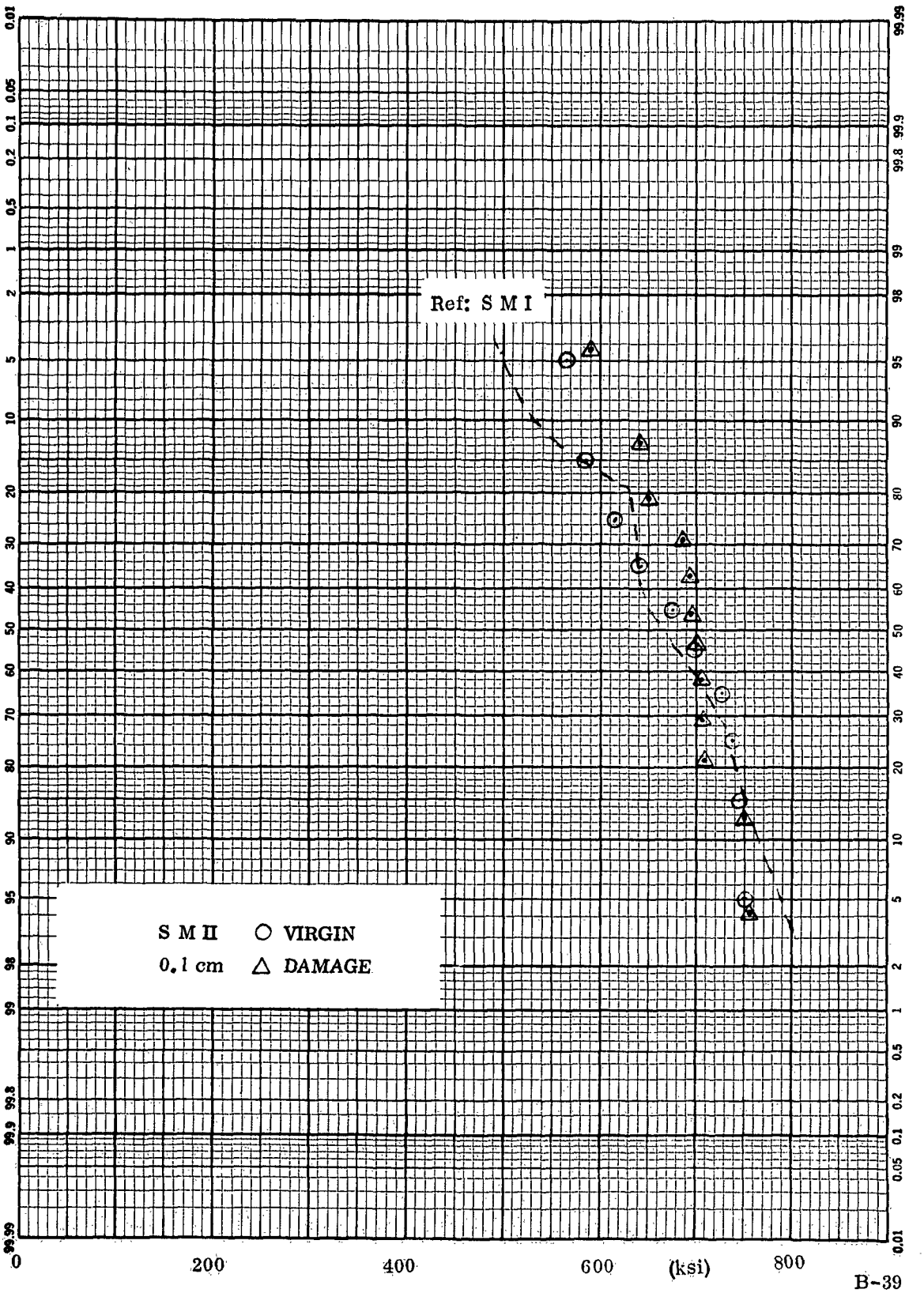
Ref: S M I
S M II ○ VIRGIN
0.1 cm △ DAMAGE
0
200
400
600
(ksi)
800
0.01
0.05
0.1
0.2
0.5
1
2
5
10
20
30
40
50
60
70
80
90
95
98
99
99.8
99.9
99.99

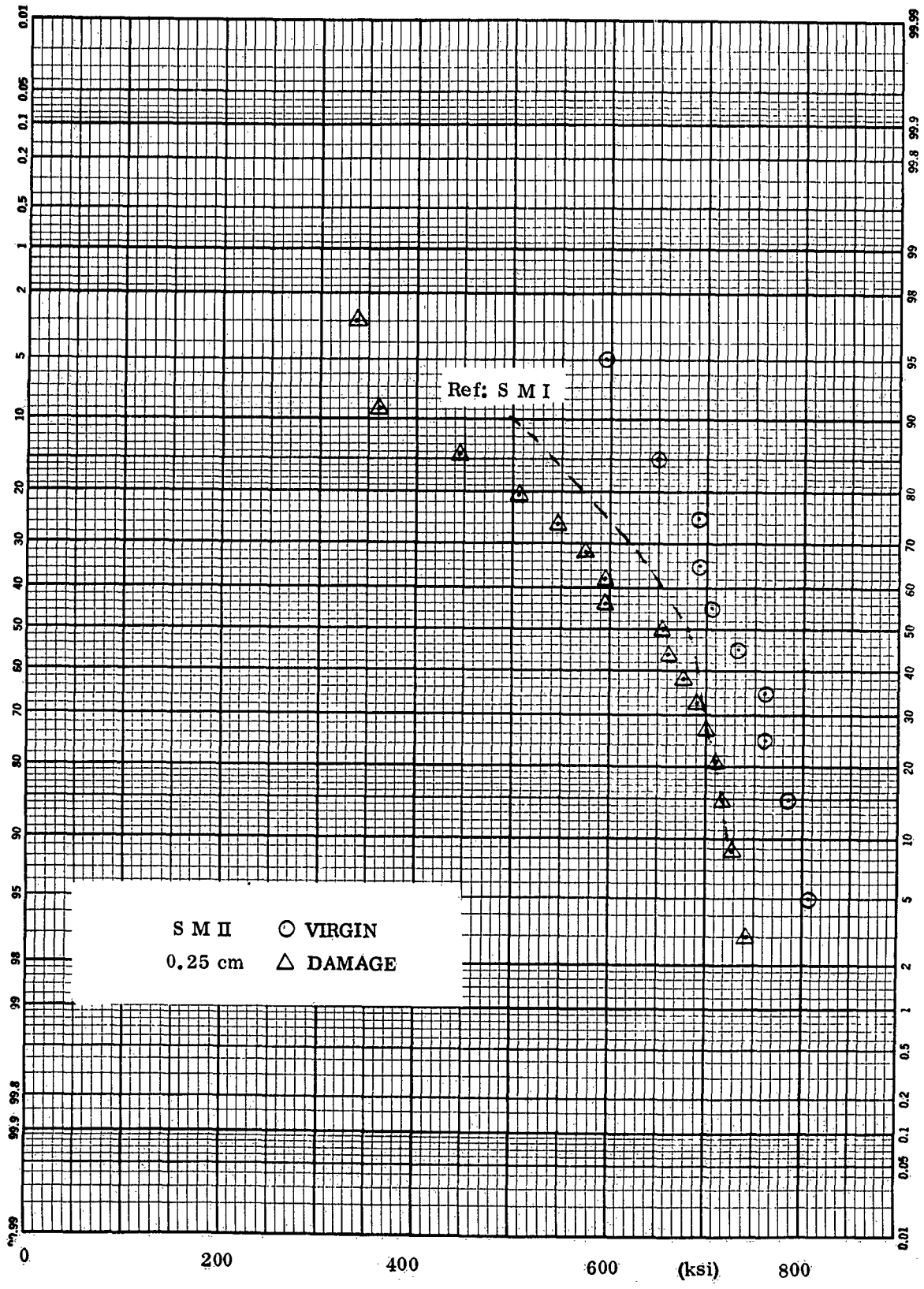
Ref: S M I
S M II ⊙ VIRGIN
0.25 cm △ DAMAGE
0
200
400
600
(ksi)
800
0.01
0.05
0.1
0.2
0.5
1
2
5
10
20
30
40
50
60
70
80
90
95
98
99
99.8
99.9
99.99

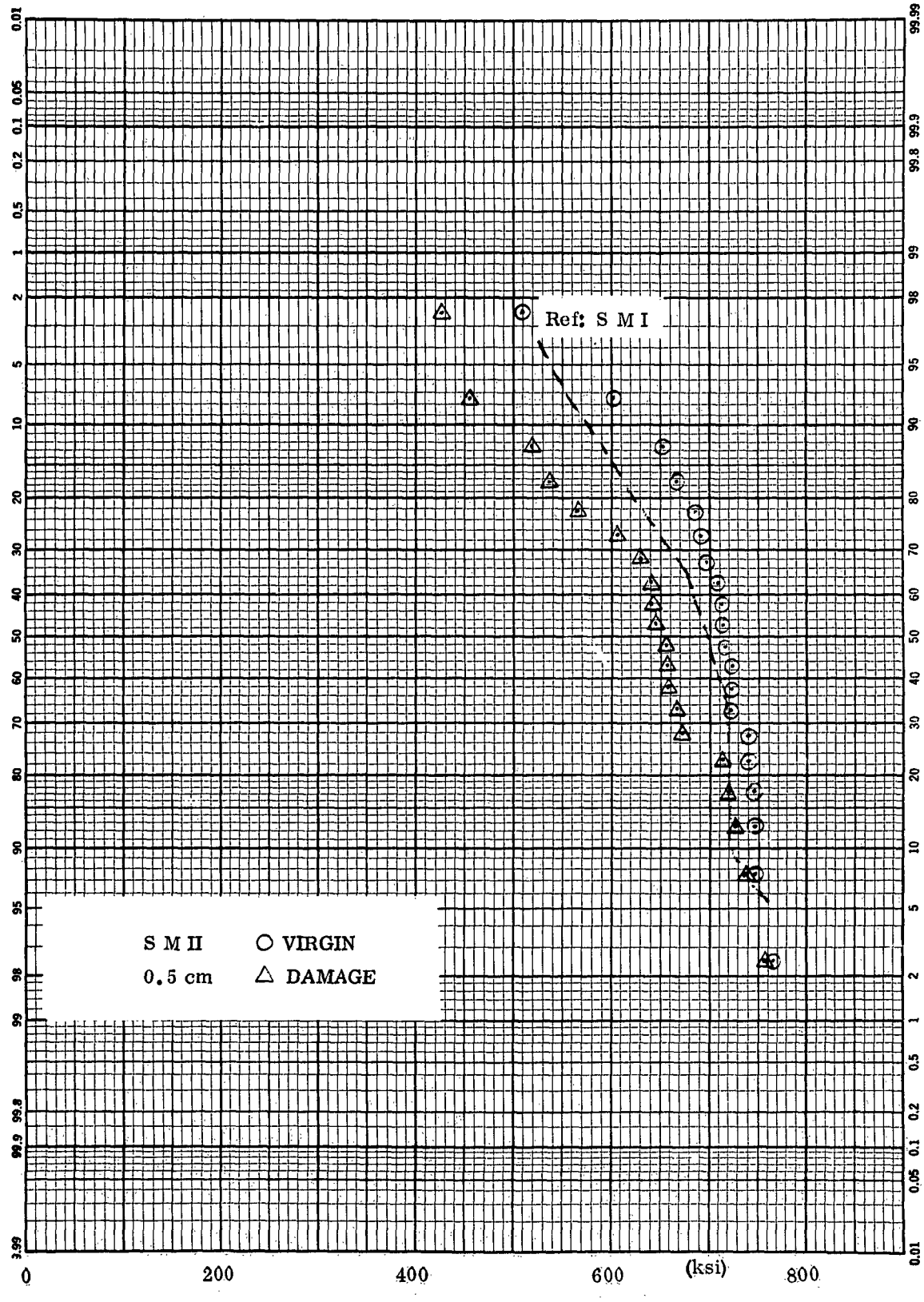
Ref: S M I
S M II
0.5 cm
VIRGIN
DAMAGE
0
200
400
600
(ksi)
800
0.01
0.05
0.1
0.2
0.5
1
2
5
10
20
30
40
50
60
70
80
90
95
98
99
99.8
99.9
99.99

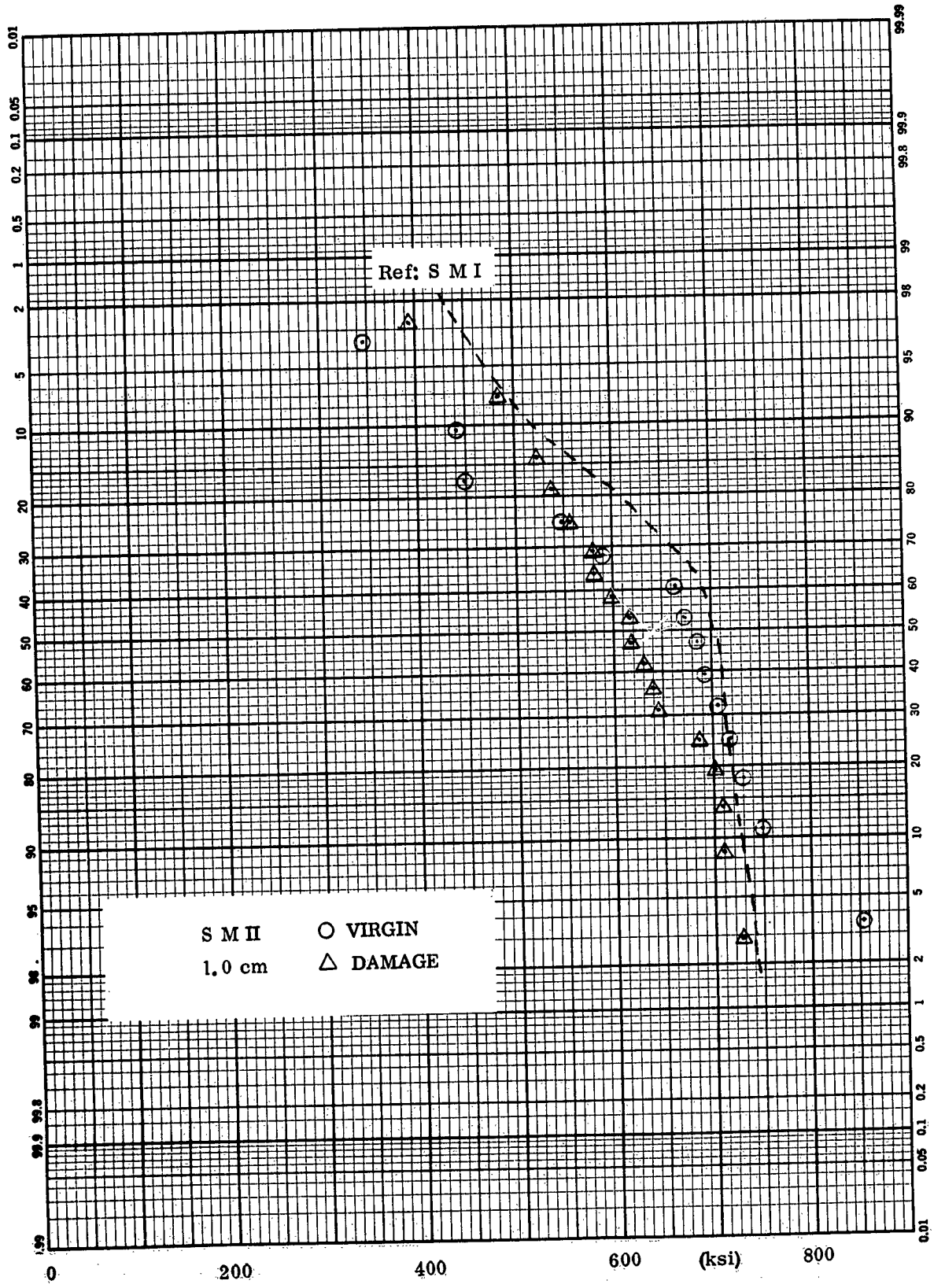
Ref: S M I
S M II
1.0 cm
O VIRGIN
△ DAMAGE
0
200
400
600
(ksi)
800
0.01
0.05
0.1
0.2
0.5
1
2
5
10
20
30
40
50
60
70
80
90
95
98
99
99.8
99.9
99.99

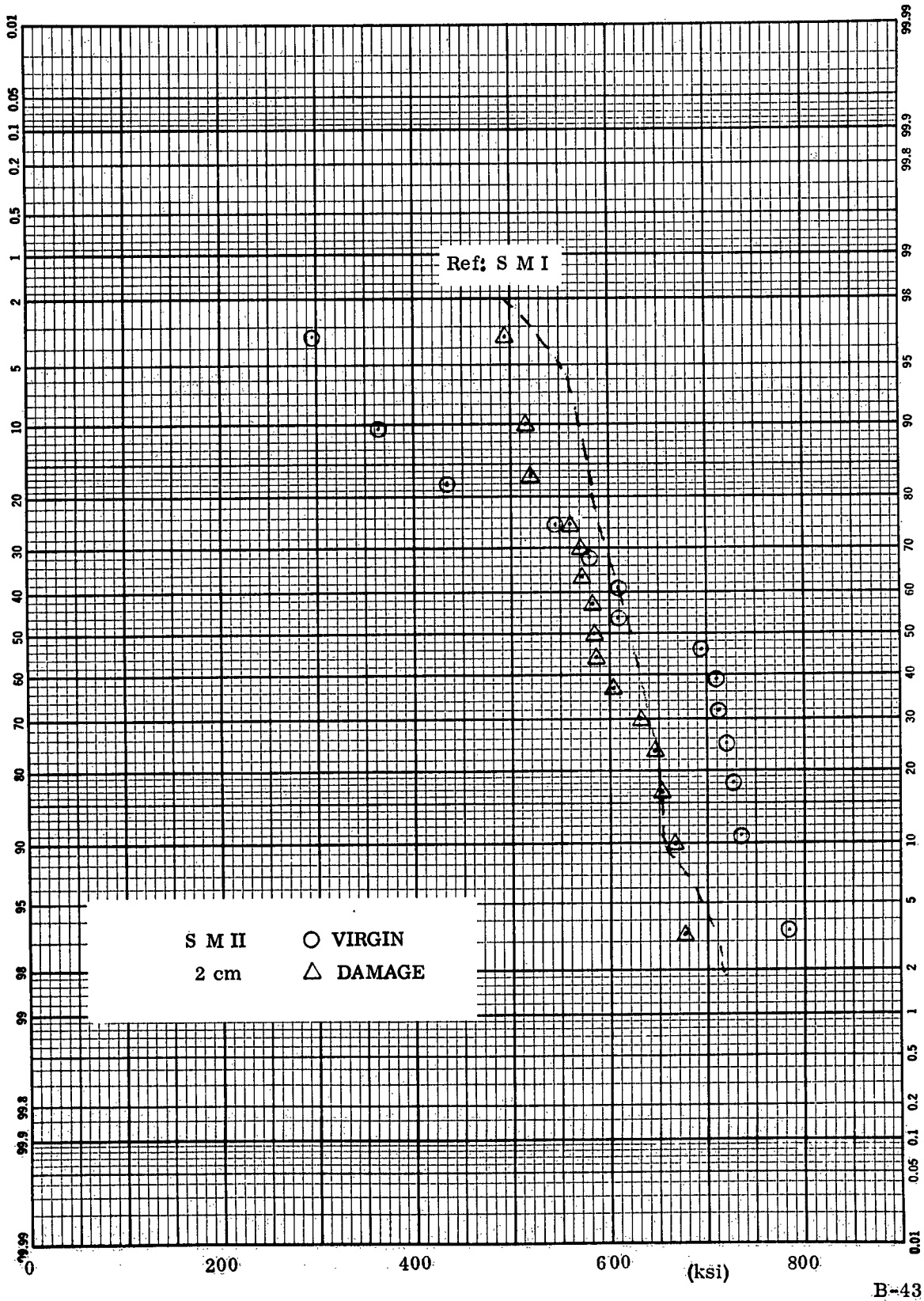
Ref: S M I
S M II
2 cm
VIRGIN
DAMAGE
0
200
400
600
800
(ksi)
0.01
0.05
0.1
0.2
0.5
1
2
5
10
20
30
40
50
60
70
80
90
95
98
99
99.8
99.9
99.99

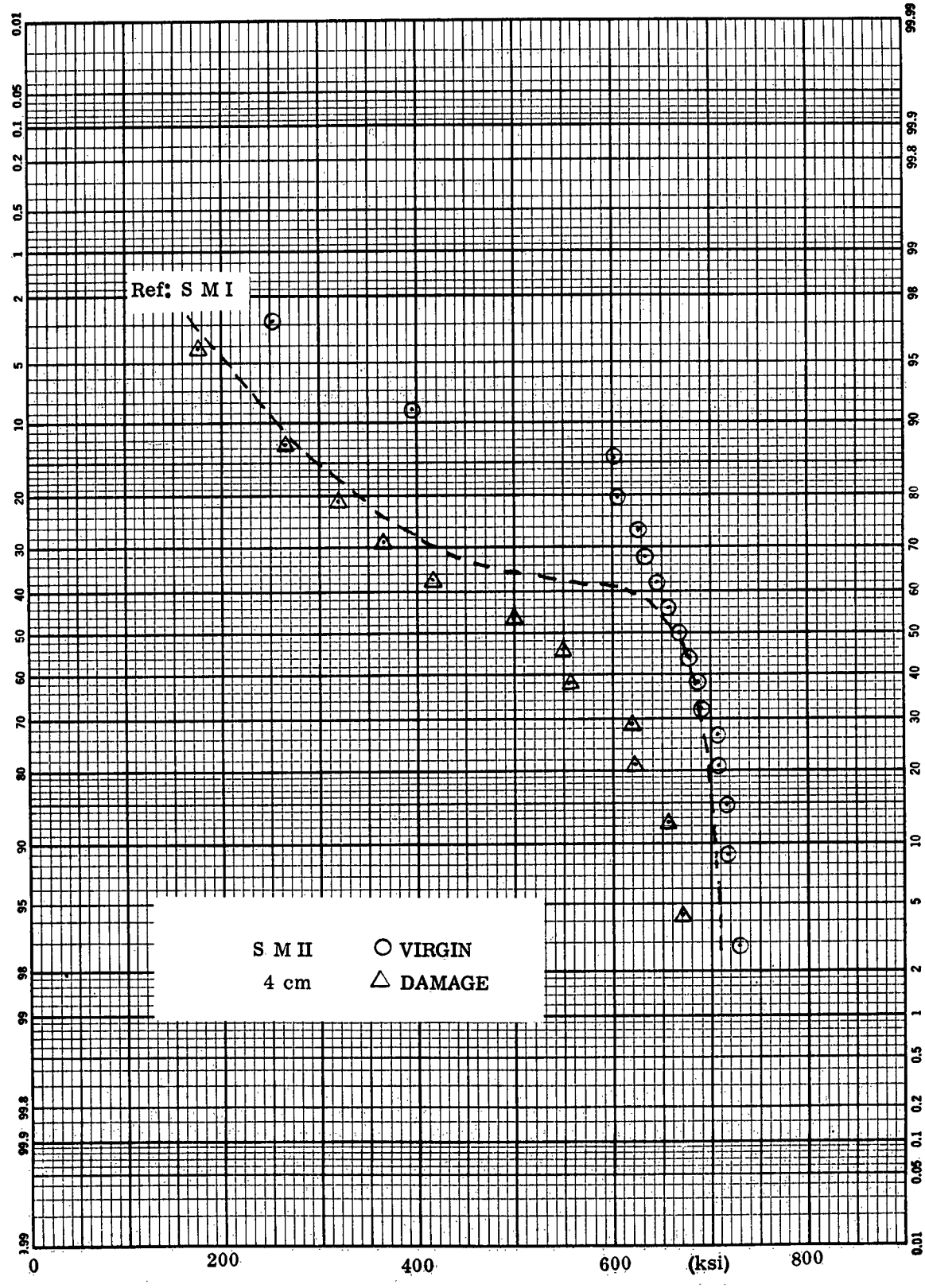
Ref: S M I
S M II
4 cm
VIRGIN
DAMAGE
0
200
400
600
(ksi)
800
0.01
0.05
0.1
0.2
0.5
1
2
5
10
20
30
40
50
60
70
80
90
95
98
99
99.8
99.9
99.99

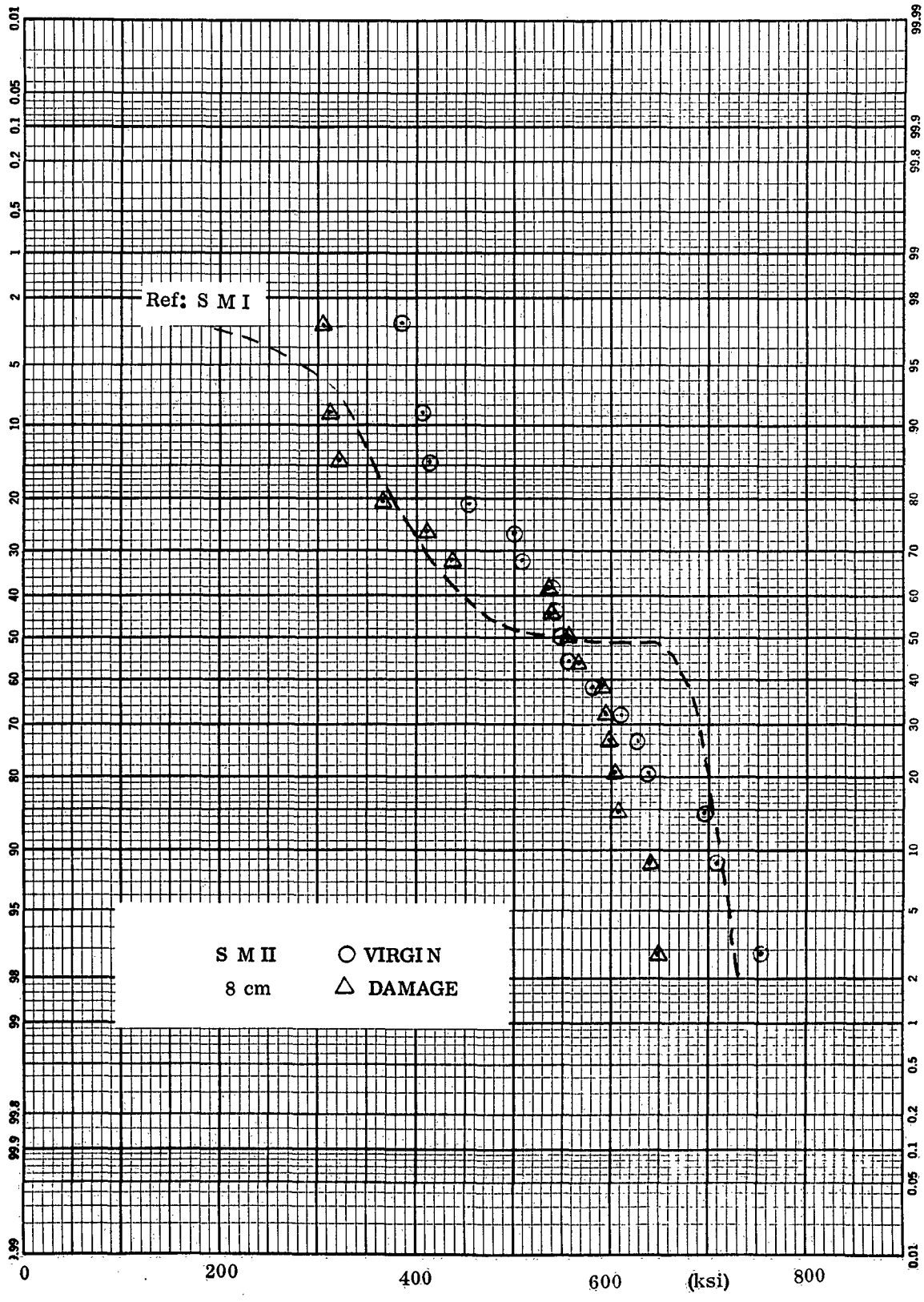
Ref: S M I
S M II
8 cm
VIRGIN
DAMAGE
0
200
400
600
(ksi)
800
0.01
0.05
0.1
0.2
0.5
1
2
5
10
20
30
40
50
60
70
80
90
95
98
99
99.8
99.9
99.99

DISTRIBUTION LIST

Contract NONR -3654(00)(X)

Office of Naval Research (2)
American Embassy
London, England

Commanding Officer
ONR Branch Office
1030 E. Green Street
Pasadena 1, California

Contract Administrator
Southeastern Area
Office of Naval Research
2110 G Street, N. W.
Washington, D. C. 20037

Director, U.S. Naval Res. Lab. (6)
Attn: Technical Information Officer

Office of Technical Services,
Dept of Commerce
Washington, D.C. 20230

Defense Documentation Center, (10)
Cameron Station, Bldg 5
5010 Duke St.
Alexandria, Va

U.S. Naval Research Laboratory
Washington 25, D.C.
Attn: Dr. P. King
Code 6000

U.S. Naval Research Laboratory
Washington 25, D.C.
Attn: Dr. G. R. Irwin
Code 6200

U.S. Naval Research Laboratory
Washington 25, D.C.
Attn: Mr. P. Waterman (2)
Code 5360

U.S. Naval Research Laboratory
Washington 25, D.C.
Attn: Mr. J. A. Kies (10)
Code 6210

U.S. Naval Research Laboratory
Washington 25, D.C.
Attn: Dr. Irvin Wolock
Code 6213

U.S. Naval Research Laboratory
Washington 25, D.C.
Attn: Mrs. Doris Baster
Code 2027

Department of the Navy
Bureau of Naval Weapons
Washington 25, D.C.
Attn: Mr. H. Bernstein (3)
Code SP-2714

Department of the Navy
Bureau of Naval Weapons
Washington 25, D.C.
Attn: Mr. Phillip M. Goodwin
Code RRMA-3

Department of the Navy
Bureau of Naval Weapons (2)
Washington 25, D.C.
Attn: Technical Library

Commander
U.S. Naval Ordnance Laboratory
White Oak, Maryland

Bureau of Naval Weapons Rep.
P.O. Box 504
Sunnyvale, California

Bureau of Naval Weapons Resident Rep.
P.O. Box 1947
Sacramento, California

Bureau of Naval Weapons Branch Rep.
Allegany Ballistics Laboratory
Cumberland, Maryland
Attn: Code 4

Bureau of Naval Weapons Resident Rep.
(Special Projects Office)
c/o Hercules Powder Company
Bacchus Works
Magna, Utah

DISTRIBUTION LIST (Cont.)

Contract NONR -3654(00)(X)

Commander
U.S. Naval Ordnance Test Station
China Lake, California
Attn: Mr. S. Herzog
Code 5557

BuShips Code 634 C 3
Washington 25, D.C.
Attn. W. Graner

Department of the Navy
Bureau of Naval Weapons (2)
Washington 25, D.C.
Attn: RMMP

Mr. W. Cohen, Code LPS
National Aeronautics and Space Adm.
1512 H. Street, N.W.
Washington 25, D.C.

National Aeronautics & Space Adm.
Lewis Research Center
21000 Brookpark Road
Cleveland 35, Ohio
Attn: Chief Librarian

Commander
Air Force Ballistic Missile Division
Hq. Air Res. and Devel. Command
P.O. Box 262
Inglewood, California

Commanding General
Aberdeen Proving Ground
Maryland

Commanding Officer
Picatinny Arsenal
Dover, New Jersey

Commander
Army Ballistic Missile Agency
Redstone Arsenal, Alabama

Commander
Armed Services Technical Info. Agency
Arlington Hall Station (10)
Arlington 12, Virginia

Department of the Army
Office, Chief of Ordnance
Washington 25, D.C.

Commander
Army Rocket and Guided Missile Agency
Redstone Arsenal, Alabama

Commander
Aeronautical Systems Division (2)
ASRCNC-1
Af Systems Command
U.S. Air Force
Wright-Patterson AFB, Ohio

National Bureau of Standards
Washington 25, D.C.
Attn: M. Kerper

Dr. N. LeBlanc
Allegany Ballistics Laboratory (2)
Cumberland, Maryland

Mr. E. Rucks
Aerojet-General Corporation (2)
Azusa, California

Dr. F.J. Climent
Aerojet-General Corporation (2)
P.O. Box 1947
Sacramento, California

Mr. George Moe
Lockheed Aircraft Company
LMSD Headquarters
P.O. Box 504
Sunnyvale, California

Solar
A Division of International Harvester
San Diego 12, California
Attn: John V. Long

Professor John Outwater
University of Vermont
Burlington, Vermont

Professor H.T. Corten
University of Illinois
Urbana, Illinois

DISTRIBUTION LIST (Cont.)

Contract NONR-3654(00)(X)

Professor H. H. Johnson
Department of Eng. Mechanics & Mat'ls
Thurston Hall
Cornell University
Ithaca, New York

University of Dayton
Research Institute
Dayton 9, Ohio
Attn: Miss Barbara Henn
Librarian

Scientific & Tech. Info. Facility
P. O. Box 5700
Bethesda, Maryland
Attn: NASA Rep. (S-AK/DL)

Aerojet-General Corporation
P.O. Box 296
Azusa, California
Attn Librarian

Jet Propulsion Laboratory
4800 Oak Grove Drive
Pasadena 3, California
Attn: I.E. Newlan
Chief, Reports Group

Allegany Ballistics Laboratory
Hercules Powder Company (2)
Cumberland, Maryland
Attn: Tech. Library

Solid Propellant Information Agency
Applied Physics Laboratory (3)
The Johns Hopkins University
Silver Spring, Maryland
Attn: G. McMurray

Hercules Powder Company
Bacchus Works
Magna, Utah
Attn: Librarian

Lockheed Missiles and Space Company
A Div. of Lockheed Aircraft Corp.
1122 Jagels Road
Sunnyvale, California
Attn: Tech. Library

Aerojet-General Corporation
P.O. Box 1947 (5)
Sacramento, California
Attn: Dr. W.O. Wetmore

Aerospace Corporation
P.O. Box 95085
Los Angeles 45, Calif.
Attn: Library-Tech-Documents Group

Defense Metals Information Center
Battelle Memorial Institute
505 King Avenue
Columbus 1, Ohio

Black, Sivalls and Bryson
Oklahoma City, Oklahoma
Attn: Manager of Engineering

B. F. Goodrich Company
500 S. Main
Akron, Ohio
Attn: Mr. H.W. Stevenson

Goodyear Aircraft Corporation
Akron 15, Ohio
Attn: Mr. R. Burkley

Narmco Industries, Inc.
Research and Development Division
8125 Aero Drive
San Diego, California
Attn: Mr. W. Otto

General Electric Company
Schenectady, New York
Attn Mr. T. Jordan

Hercules Powder Company
P.O. Box A
Rocky Hill, New Jersey

Rocketdyne Engineering
A Div. of North American Aviation, Inc.
6633 Canoga Park Blvd
Canoga Park, California
Attn: Mr. E. Hawkinson

Lockheed Missiles and Space Company
A Division of Lockheed Aircraft Corp.
3251 Hanover Street
Palo Alto, California
Attn: Mr. M. Steinberg

Plastic Evaluation Center
Picatinny Arsenal
Dover, New Jersey
Attn: ORD-BB

Owens-Corning Fiberglass Corp.
Wash. Rep. R.J. Weber (2)
806 Connecticut Ave., N.W.
Washington, D.C.

Syracuse University
Wood Products Eng. Dept
Syracuse 10, New York
Attn: E.A. Anderson, Chairman

H.I. Thompson Fiberglass Co.
1602 West 135th Street
Gardena, California